Western Graduate&PostdoctoralStudies

Western University
Scholarship@Western

Electronic Thesis and Dissertation Repository

8-24-2021 10:30 AM

Coevolution of Hosts and Pathogens in the Presence of Multiple Types of Hosts

Evan J. Mitchell, *The University of Western Ontario*

Supervisor: Wild, Geoff, *The University of Western Ontario*
A thesis submitted in partial fulfillment of the requirements for the Doctor of Philosophy degree in Applied Mathematics
© Evan J. Mitchell 2021

Follow this and additional works at: https://ir.lib.uwo.ca/etd

Part of the Ecology and Evolutionary Biology Commons, and the Ordinary Differential Equations and Applied Dynamics Commons

Recommended Citation

Mitchell, Evan J., "Coevolution of Hosts and Pathogens in the Presence of Multiple Types of Hosts" (2021). *Electronic Thesis and Dissertation Repository*. 8075.
https://ir.lib.uwo.ca/etd/8075

This Dissertation/Thesis is brought to you for free and open access by Scholarship@Western. It has been accepted for inclusion in Electronic Thesis and Dissertation Repository by an authorized administrator of Scholarship@Western. For more information, please contact wlswadmin@uwo.ca.

Abstract

How will hosts and pathogens coevolve in response to multiple types of hosts? I study this question from three different perspectives. First, I model a scenario in which hosts are categorized as female or male. Hosts invest resources in maintaining their immune system at a cost to their reproductive success, while pathogens face a trade-off between transmission and duration of infection. Importantly, female hosts are also able to vertically transmit an infection to their newborn offspring. The main result is that as the rate of vertical transmission increases, female hosts will have a greater incentive to pay the cost to invest in their immune system, while the pathogen will evolve a lower rate of disease-induced mortality in female hosts relative to male hosts. Second, I study a model where hosts can change their type. Hosts are classified according to whether they engage or do not engage in prophylactic behaviours that reduce the transmission rate of an infectious disease and may freely start or stop these behaviours. I study the evolution of the degree to which the pathogen exploits its host's resources. The main result is that, when hosts engage in prophylaxis, I expect pathogens to evolve a lower level of host exploitation than would otherwise be predicted in the absence of prophylactic behaviours. Finally, I consider the possibility of multiple pathogen strains in addition to multiple types of hosts. I develop a general theoretical framework to link ideas from evolutionary epidemiology to those from kin selection theory to study the evolution of coinfecting pathogen strains. The main result is that pathogens will evolve to balance both the direct and indirect benefits of increased transmission with the associated direct and indirect costs of decreased duration of infection within each type of host. The more genetically related is a pathogen strain to its coinfecting group, the more it will reduce its own disease-induced mortality rate for the benefit of the whole group. Overall, this work shows how standard results from evolutionary epidemiology change when considering the coevolution of hosts and pathogens in the presence of multiple types of hosts.

Keywords: disease dynamics, epidemiology, evolution, game theory, inclusive fitness, kin selection, mathematical model, natural selection, Price equation, sexual selection

Summary for Lay Audience

Pathogens and their hosts evolve over time. Researchers build mathematical models to study this evolution and make predictions about the long-term behaviour of host-pathogen systems. A great deal of work has been done to understand the forces that shape the evolution of pathogens and the degree to which they harm their hosts. Other researchers have studied how hosts and pathogens evolve together, as changes in one group will affect the other group. They have shown that considering the evolution of both groups simultaneously allows us to make new and different predictions than if we consider only the evolution of one group. An area of interest which has received less attention is how hosts and pathogens evolve together when the host population is subdivided into different types. Host populations often have defining characteristics, such as sex or age, that can be used to distinguish subgroups within that population. Empirical evidence has shown that pathogens faced with these different types of hosts can evolve to behave differently in one type of host than in the other, and that this will, in turn, affect the evolution of the hosts themselves. This thesis addresses this area of research by building mathematical models and drawing predictions on how we expect hosts and pathogens to evolve when hosts are grouped into different types. I show that the evolution of hosts and pathogens together and the existence of different types of hosts are important features that can generate new evolutionary predictions, which can be used to help explain some of the trends observed in real host-pathogen systems.

Co-Authorship Statement

I, Evan James Mitchell, declare that this thesis titled, “Coevolution of hosts and pathogens in the presence of multiple types of hosts”, has been written by me under the supervision of Dr. Geoff Wild.

Chapter 2: This chapter is a paper co-authored by G. Wild and F. Úbeda, and is currently being prepared for submission for publication. EM developed the model with input from GW and FÚ. EM performed analysis of the model, and drafted the manuscript with input from GW and FÚ.

Chapter 3: This chapter is a paper co-authored by G. Wild and published as “Prophylactic host behaviour discourages pathogen exploitation” in the Journal of Theoretical Biology, volume 503, October 2020. It is included here under the “Author Rights” set out by Elsevier Ltd. in the publishing agreement signed by EM and GW. In particular, these rights allow the author to “include [the paper] in a thesis or dissertation (provided this is not published commercially)”. EM developed and performed analysis of the model, and drafted and finalized the manuscript, with supervisory input from GW.

Chapter 4: This chapter is a paper co-authored by G. Wild, and is currently being prepared for submission for publication. EM developed the framework, performed analysis of the illustrative examples, and drafted the manuscript with supervisory input from GW.

Acknowledgements

I would first like to thank my supervisor, Geoff Wild, for his guidance, feedback, and critiques of my work. His mentorship has allowed me to grow as a scientist, as a mathematician, and as a writer. I would also like to thank all those in the Applied Mathematics department, from the administrative staff to the faculty, for all of their help and instruction over my time here. In particular, I would like to thank Lindi Wahl for her countless helpful comments and questions on my papers, all of which helped to add new dimensions to those projects. Finally, I would like to thank all of my family and friends, especially my parents Gary and Denise and my sister Emma, for their constant support throughout this process. None of this work would have been possible without all of you. Thank you.

Contents

Abstract i

Summary for Lay Audience ii

Co-Authorship Statement iii

Acknowledgements iv

List of Figures viii

List of Tables ix

List of Appendices x

1 Introduction 1

1.1 Mathematical Models of Infectious Diseases 1

1.2 Evolution of Pathogens 5

1.3 Evolution of Hosts 9

1.4 Host-Pathogen Coevolution 12

1.5 Multiple Pathogen Strains 13

1.6 Multiple Types of Hosts 15

1.7 Contributions of this Thesis 16

2 Female Reproduction and the Evolution of Sex-specific Differences in Immunity **19**

2.1 Introduction 19

2.2 Model 21
   2.2.1 Epidemiological Dynamics 21
   2.2.2 Evolutionary Dynamics 24
   2.2.3 Methods of Analysis 28
2.3 Results 29
   2.3.1 No Sex-Specific Differences 29
   2.3.2 General Case 33
2.4 Discussion 37

3 Prophylactic Host Behaviour Discourages Pathogen Exploitation 40

3.1 Introduction 40
3.2 Model 42
   3.2.1 Disease Dynamics 42
   3.2.2 Evolutionary Dynamics 48
3.3 Results 51
   3.3.1 Simple Cases 51
   3.3.2 Evolution Near the Critical Cost 52
   3.3.3 Evolution for Arbitrary Cost 53
3.4 Discussion 57

4 Cooperation between Related Coinfecting Pathogen Strains in Multiple Types of Hosts 62

4.1 Introduction 62
4.2 Theoretical Framework 64
4.3 Illustrative Examples 70
   4.3.1 Example 1: Infections in Age-structured Host Populations 70
   4.3.2 Example 2: Sexually Transmitted Infections 77
4.4 Discussion 83

5 Conclusion **86**

5.1 Summary 86

5.2 Future Directions 88

Bibliography **91**

Appendix A Chapter 2 - Evolutionary Analysis for Simple Cases **104**

Appendix B Chapter 3 - Details of the Replicator Dynamics **109**

Appendix C Chapter 3 - Linear Stability Analysis **111**

Appendix D Chapter 3 - Evolutionary Analysis of Simple Cases **113**

Appendix E Chapter 3 - Evolutionary Analysis in the Case of Arbitrary Cost **115**

Appendix F Chapter 3 - Perturbation Analysis **118**

Appendix G Chapter 3 - Maple Code **121**

Curriculum Vitae **127**

List of Figures

1.1 Example solutions to the SI model 3

2.1 Schematic diagram of the sex-specific model 23
2.2 Results from numerical simulation of the sex-specific model 32
2.3 Evolutionary trends within each sex 34
2.4 Results on public health measures from the sex-specific model 36

3.1 Sample trajectories from the resident system 47
3.2 Results from the perturbation analysis 54
3.3 Numerical results for pathogen evolution in response to host prophylactic behaviour 56

4.1 Graphical depiction of the effect of increasing relatedness between the focal pathogen and its coinfecting group 75

List of Tables

2.1 Ranges of parameter values tested in the sex-specific model 33

List of Appendices

Appendix A Chapter 2 - Evolutionary Analysis for Simple Cases 104
Appendix B Chapter 3 - Details of the Replicator Dynamics 109
Appendix C Chapter 3 - Linear Stability Analysis 111
Appendix D Chapter 3 - Evolutionary Analysis of Simple Cases 113
Appendix E Chapter 3 - Evolutionary Analysis in the Case of Arbitrary Cost 115
Appendix F Chapter 3 - Perturbation Analysis 118
Appendix G Chapter 3 - Maple Code 121

Chapter 1

Introduction

1.1 Mathematical Models of Infectious Diseases

Some of the earliest models of epidemics are those of Ross [1] and Kermack and McKendrick [2]. Both used systems of differential equations to describe the progression of an infectious disease through a population of individuals. One of their main goals was to estimate the number of individuals who would contract the disease by the end of the epidemic. An important quantity in the study of such models is the basic reproductive number of the pathogen, which is defined as the expected number of new infections created by a single infected individual over the duration of an infection, in an entirely susceptible population [3]. This quantity can be used to predict if a disease will spread within a population ($\mathcal{R}_0 > 1$) or die out ($\mathcal{R}_0 < 1$) [4].

Later models expanded on this to consider diseases which are persistent in a population. A simple model of such endemic diseases compartmentalizes a population of N individuals into those who are infected with the disease and those who are not infected but are susceptible to infection [4]. At any time t, there will be $S = S(t)$ individuals susceptible to infection and $I = I(t)$ individuals infected with the disease. All infected individuals are also infective. New individuals will be born at a per-capita rate b and all newborns are assumed to be susceptible to infection. Susceptible and infected individuals will die at a per-capita rate μ due to causes unrelated to the disease.

Transmission of the disease will occur at a per-capita rate βS when an infected individual comes into contact with a susceptible individual. Infected individuals may clear their infection at a per-capita rate γ and become susceptible to reinfection. Infected individuals will also experience an additional per-capita disease-induced mortality rate α.

This description can be summarized by the following system of ordinary differential equations:

$$\frac{dS}{dt} = bN + \gamma I - \beta S I - \mu S \tag{1.1a}$$

$$\frac{dI}{dt} = \beta S I - (\gamma + \mu + \alpha) I, \tag{1.1b}$$

where $N = S + I$. Numerical iteration can be used to approximate solutions to system (1.1) and estimate the numbers of susceptible and infected individuals at any given time. Figure 1.1 shows numerical solutions to (1.1) for a given set of parameter values. After a short period of oscillation, the numbers of susceptible and infected individuals settle to a steady state. This steady state, or equilibrium, is important from a biological perspective because it tells us how much of the population we expect to eventually be infected with the disease [4].

In more complicated models, we will only be able to approximate the equilibria. However, model (1.1) is simple enough that we can derive analytical expressions for all possible equilibria. An equilibrium of (1.1) is defined as a point at which the numbers of susceptible and infected individuals are not changing; individuals will still move between compartments, but as one individual leaves a given compartment it is immediately replaced by another individual [4]. Mathematically, this is equivalent to simultaneously solving $dS/dt = 0$ and $dI/dt = 0$. Assuming $b \neq \mu$, solving these equations yields two possible equilibrium states of (1.1): a disease-free equilibrium (DFE), where there are no individuals infected with the disease, given by $(\bar{S}_{\text{DFE}}, \bar{I}_{\text{DFE}}) = (0, 0)$; and an endemic equilibrium (EE), where there are some number of individuals infected with the disease, given by $(\bar{S}_{\text{EE}}, \bar{I}_{\text{EE}}) = (\frac{\gamma+\mu+\alpha}{\beta}, \frac{b-\mu}{\mu+\alpha-b}\frac{\gamma+\mu+\alpha}{\beta})$. In

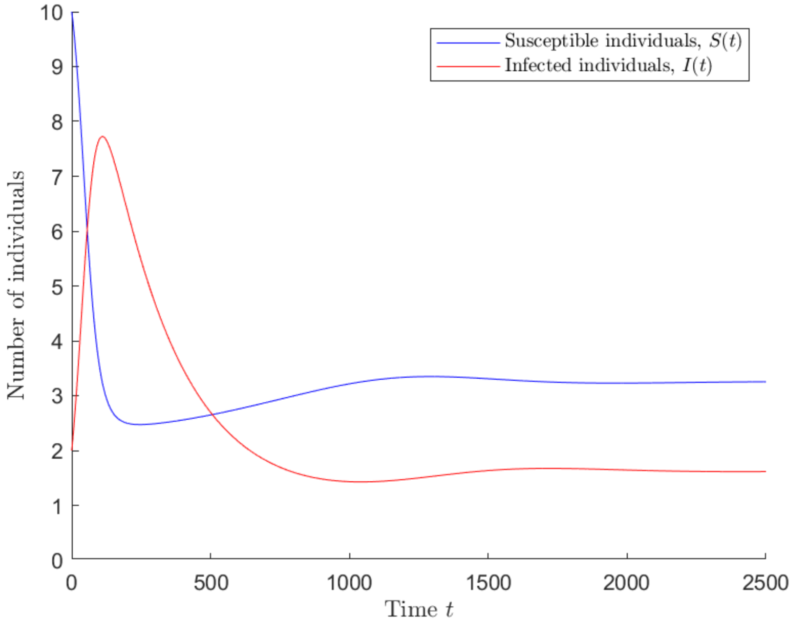

Figure 1.1: Example solutions to system (1.1). After a transient period, the numbers of susceptible and infected individuals settle at a steady state. Model parameters: $b = 4$, $\gamma = 5$, $\beta = 4$, $\mu = 2$.

the case where $b = \mu$, the DFE no longer coincides with the trivial or extinction equilibrium $(\bar{S}_{\mathrm{DFE}}, \bar{I}_{\mathrm{DFE}}) = (0, 0)$. Instead, there is an infinite number of disease-free equilibria of the form $(\bar{S}_{\mathrm{DFE}}, \bar{I}_{\mathrm{DFE}}) = (\bar{S}, 0)$, for any non-negative real number $\bar{S}$. However, none of these equilibria are stable since any small perturbation in $\bar{S}$ will result in a new equilibrium point. Throughout the remainder of this thesis, it is assumed that parameters are chosen so that there is a unique DFE which coincides with the trivial or extinction equilibrium $(\bar{S}_{\mathrm{DFE}}, \bar{I}_{\mathrm{DFE}}) = (0, 0)$, as well as a unique EE $(\bar{S}_{\mathrm{EE}}, \bar{I}_{\mathrm{EE}}) = (\frac{\gamma+\mu+\alpha}{\beta}, \frac{b-\mu}{\mu+\alpha-b}\frac{\gamma+\mu+\alpha}{\beta})$.

Of these two possible equilibria, which one will system (1.1) actually move towards? To answer this, we study the stability of both the DFE and the EE. The stability of a particular equilibrium is determined by first constructing the Jacobian matrix, the matrix of first partial derivatives, of (1.1) and evaluating it at the equilibrium. If the eigenvalues of the resulting matrix are all negative or have negative real parts, then we conclude that the equilibrium is stable and that solutions of (1.1) will converge towards it over time; otherwise, the equilibrium is unstable and solutions of (1.1) will move away from it [4]. The Jacobian matrix J of (1.1) is given by

$$J = \begin{bmatrix} \frac{\partial(dS/dt)}{\partial S} & \frac{\partial(dS/dt)}{\partial I} \\ \frac{\partial(dI/dt)}{\partial S} & \frac{\partial(dI/dt)}{\partial I} \end{bmatrix} = \begin{bmatrix} b-\mu-\beta I & b+\gamma-\beta S \\ \beta I & \beta S-\gamma-\mu-\alpha \end{bmatrix}. \tag{1.2}$$

First, we will determine the stability of the DFE. Evaluating (1.2) at the DFE gives

$$J_{\text{DFE}} = \begin{bmatrix} b-\mu & b+\gamma \\ 0 & -\gamma-\mu-\alpha \end{bmatrix}. \tag{1.3}$$

Since (1.3) is an upper triangular matrix, the eigenvalues are the entries on the main diagonal. In particular, the eigenvalues are $\lambda_1 = b-\mu$ and $\lambda_2 = -\gamma-\mu-\alpha$. Since all of the model parameters are assumed to be positive, we have that $\lambda_2 < 0$. The stability of the DFE then rests on the sign of λ_1. If $\lambda_1 < 0$, i.e., $b < \mu$, then both eigenvalues are negative and the DFE is stable. If $\lambda_1 > 0$, i.e., $b > \mu$, then the DFE is unstable.

To determine the stability of the EE, we start by evaluating (1.2) at this equilibrium:

$$J_{\text{EE}} = \begin{bmatrix} (b-\mu)\left(1-\frac{\gamma+\mu+\alpha}{\mu+\alpha-b}\right) & b-\mu-\alpha \\ \left(\frac{b-\mu}{\mu+\alpha-b}\right)(\gamma+\mu+\alpha) & 0 \end{bmatrix}. \tag{1.4}$$

We could proceed as before and find the eigenvalues of (1.4), but the expressions for the eigenvalues will be more mathematically complicated than in the case of the DFE. Alternatively, we can use the Routh-Hurwitz criteria to determine the stability of the EE. The Routh-Hurwitz criteria for a 2×2 matrix A state that all eigenvalues of A are negative or have negative real parts if and only if $\operatorname{tr}(A) < 0$ and $\det(A) > 0$ [4]. In this case, the trace and determinant of (1.4) will be easier to compute and analyze than the eigenvalues. First, the determinant of (1.4) is given by $\det(J_{\text{EE}}) = (b-\mu)(\gamma+\mu+\alpha)$. This quantity is positive whenever $b > \mu$, which is also what must be true in order for the DFE to be unstable. Second, the trace of (1.4) is given by $\operatorname{tr}(J_{\text{EE}}) = (b-\mu)\left(1-\frac{\gamma+\mu+\alpha}{\mu+\alpha-b}\right)$. Since we already know we must have $b > \mu$, this quantity will be negative whenever $\frac{\gamma+\mu+\alpha}{\mu+\alpha-b} > 1$. Due to the fact that all model parameters are positive, we must have that $\left|\frac{\gamma+\mu+\alpha}{\mu+\alpha-b}\right| > 1$ so it only remains to establish that $\frac{\gamma+\mu+\alpha}{\mu+\alpha-b} > 0$. This is true as long as $b < \mu+\alpha$. So, in summary, the EE is stable whenever $\mu < b < \mu+\alpha$, and is unstable otherwise.

1.2 Evolution of Pathogens

One limitation of the above model is that it assumes that pathogen traits (e.g., disease-induced mortality) are fixed. Realistically, pathogens evolve over time. How do we mathematically study this evolution and make predictions about where natural selection will push pathogen traits?

The theory of adaptive dynamics [5, 6, 7] was developed to answer questions like this. Carrying on with the example model developed in the previous section, we start by supposing that we have some resident population governed by (1.1) and that this resident system has settled at its EE. We then assume that a rare mutant strain of the pathogen, with a disease-induced mortality rate $\tilde{\alpha}$ and a transmission rate $\tilde{\beta}$, is introduced into the equilibrium resident population. If we use $\tilde{I} = \tilde{I}(t)$ to denote the number of hosts infected with the mutant strain, then we can model its dynamics with

$$\frac{d\tilde{I}}{dt} = \tilde{\beta}\bar{S}\tilde{I} - (\gamma + \mu + \tilde{\alpha})\tilde{I}, \tag{1.5}$$

where $\bar{S}$ represents the number of susceptible hosts at the resident EE. Will this mutant pathogen strain die out, or will it grow and establish itself in the population?

To answer this, we first need to establish the effects that will cause the pathogen to change its disease-induced mortality rate. In particular, we must define the benefit gained and the cost incurred for increased disease-induced mortality. One of the most common approaches is to assume that the pathogen faces a trade-off between the rate at which it can transmit itself between hosts and its duration of infection within a host [8]. Biologically, a pathogen will exploit its host's resources in order to reproduce. Greater exploitation will result in an increased number of replicates, making it more likely that the pathogen will transmit itself to another host but also making it more likely that the host is killed by the infection [9]. Such a trade-off was shown by Anderson and May [10] in relation to HIV data, and by Ewald [11] in relation to vector-transmitted diseases. Mathematically, this means that we treat the transmission rate β (resp. $\tilde{\beta}$) as a function of the disease-induced mortality rate α (resp. $\tilde{\alpha}$) of the pathogen and write $\beta = \beta(\alpha)$. As discussed by Alizon and Michalakis [12], data suggests that this relationship between transmission and disease-induced mortality should be represented by a saturating function. Increased disease-induced mortality will then confer a benefit of increased transmission rate, but will come at the cost of a shorter duration of infection $\frac{1}{\gamma+\mu+\alpha}$. Other authors have assumed trade-offs between the pathogen and the host clearance rate γ, mediated by disease-induced mortality [10, 11, 13], viral load [14], the degree to which a pathogen exploits its host's resources [15], or the pathogen growth rate [16].

We next need to define a measure of the fitness $W = W(\tilde{\alpha}, \alpha)$ of the mutant pathogen strain in order to determine how well the mutant strain performs against the established resident strain. Two common measures of fitness are the instantaneous growth rate [7, 17] and the basic reproductive number [12] of the mutant pathogen strain. The instantaneous growth rate can be found from equation (1.5) to be $\tilde{\beta}\bar{S} - \gamma - \mu - \tilde{\alpha}$, and when this quantity is positive (resp. negative) the mutant pathogen population is growing (resp. shrinking). The basic reproductive number, denoted $\mathcal{R}_0$, is defined as the expected number of new infections created by a single infected individual in an entirely susceptible population [3] and is given in our example by $\mathcal{R}_0 = \frac{\beta S}{\gamma+\mu+\alpha}$; the basic reproductive number for the mutant pathogen strain is then given by $\tilde{\mathcal{R}}_0 = \frac{\tilde{\beta}\bar{S}}{\gamma+\mu+\tilde{\alpha}}$. The mutant pathogen population will grow (resp. shrink) if $\tilde{\mathcal{R}}_0 > 1$ (resp. $\tilde{\mathcal{R}}_0 < 1$).

Either of these quantities can be used as a measure of fitness and will yield the same evolutionary results [18]. For our example model here, we will define fitness as the basic reproductive number and write $W(\tilde{\alpha}, \alpha) = \frac{\tilde{\beta}\bar{S}}{\gamma+\mu+\tilde{\alpha}}$, where $\tilde{\beta}$ depends on the mutant disease-induced mortality rate $\tilde{\alpha}$ and $\bar{S}$ depends on the resident disease-induced mortality rate α. We then look for an evolutionary equilibrium α^* by solving the equation

$$\left.\frac{\partial W}{\partial \tilde{\alpha}}\right|_{\tilde{\alpha}=\alpha=\alpha^*} = 0, \tag{1.6}$$

[5, 6, 7]. This condition is equivalent to

$$\frac{\tilde{\beta}'(\alpha^*)}{\tilde{\beta}(\alpha^*)} = \frac{1}{\gamma + \mu + \alpha^*}, \tag{1.7}$$

where the prime denotes the first derivative. The left-hand side of (1.7) describes the relative change in transmission for a change in disease-induced mortality, while the right-hand side represents the average duration of infection. Equation (1.7), then, captures the trade-off faced by the pathogen: increased disease-induced mortality will increase transmission but decrease the duration of infection, and these two effects must balance out at evolutionary equilibrium. This balance is a common theme, both in theoretical studies [8] and empirical studies [12]. Úbeda and Jansen showed that a similar balance exists in a model of hosts split into female and male groups, while Alizon [16] showed that an analogous balance must be maintained in the presence of transmission-recovery trade-offs, as well. If we assume a saturating functional form for transmission and model it as $\beta(\alpha) = \alpha^{1/2}$ (so that $\tilde{\beta} = \beta(\tilde{\alpha}) = \tilde{\alpha}^{1/2}$), as used by Day and Burns [19], then we can use (1.7) to derive an explicit expression for the evolutionary equilibrium: $\alpha^* = \gamma + \mu$.

Similar to our treatment of the epidemiological equilibria in the previous section, we can ask questions about the stability of this evolutionary equilibrium. Under what conditions do we expect the pathogen population to converge to this evolutionary equilibrium? Since fitness depends on both the mutant and resident traits, we need to concern ourselves with the stability of the evolutionary equilibrium from two directions: the mutant direction and the resident direction. If the evolutionary equilibrium resists invasion from nearby mutant strains, then $\alpha*$ must satisfy

$$\left.\frac{\partial^2 W}{\partial \tilde{\alpha}^2}\right|_{\tilde{\alpha}=\alpha=\alpha^*} \leq 0 \tag{1.8}$$

and we say it is evolutionarily stable (sensu [20]). If the evolutionary equilibrium attracts nearby resident populations, then α^* must satisfy

$$\frac{d}{d\alpha}\left[\left.\frac{\partial W}{\partial \tilde{\alpha}}\right|_{\tilde{\alpha}=\alpha}\right]_{\alpha=\alpha^*} \leq 0 \tag{1.9}$$

and we say it is convergence stable [21]. Strict versions of the inequalities (1.8) and (1.9) provide sufficient conditions for stability. Both of these stability conditions are important for establishing an endpoint of natural selection. An equilibrium can be evolutionarily stable but not convergence stable, in which case nearby mutant strategies cannot invade the population but nearby resident populations employing a different strategy will not necessarily have a lower fitness than the focal population. Alternatively, an equilibrium can be convergence stable but not evolutionarily stable, in which case nearby resident populations have a lower fitness than the focal population but a nearby mutant strategy could invade and replace the equilibrium strategy. We call an evolutionary equilibrium which is both evolutionarily stable and convergence stable a continuously stable strategy (CSS) [22].

In our example, the partial derivative in (1.8) is given by

$$\left.\frac{\partial^2 W}{\partial \tilde{\alpha}^2}\right|_{\tilde{\alpha}=\alpha=\alpha^*} = -\frac{1}{4(\gamma+\mu)^2}, \tag{1.10}$$

and the partial derivative in (1.9) is given by

$$\frac{d}{d\alpha}\left[\left.\frac{\partial W}{\partial \tilde{\alpha}}\right|_{\tilde{\alpha}=\alpha}\right]_{\alpha=\alpha^*} = -\frac{1}{4(\gamma+\mu)^2}. \tag{1.11}$$

Since both (1.10) and (1.11) are negative, the evolutionary equilibrium $\alpha^* = \gamma + \mu$ is a CSS and we expect that natural selection will, over time, push the pathogen population towards this level of disease-induced mortality.

It is worth noting that in finding the evolutionary equilibrium α^* and confirming that it is a CSS, we have maximized the basic reproductive number [3] of the pathogen. Other authors have shown that natural selection acts to maximize $\mathcal{R}_0$ [10, 12, 19], but this literature often focuses on the evolution of pathogen virulence. Virulence is defined to be the reduction in host fitness due to infection with the disease [23]. Host fitness is comprised of two components: survival and reproduction. In our example model, the pathogen is only able to influence host survival, through its rate of disease-induced mortality, but has no effect on host reproduction. In this case, it would be appropriate to refer to disease-induced mortality as pathogen virulence. However, in more complicated models where the pathogen is potentially able to also influence host reproduction (e.g., via vertical transmission, as in [15]), virulence will be more than just the pathogen's rate of disease-induced mortality.

1.3 Evolution of Hosts

We could also ask about modelling the evolution of changing host traits in (1.1). Doing so involves a similar adaptive-dynamics approach [5, 6, 7] as with pathogen evolution. In our example model, we will consider the clearance rate γ to be the host trait that is evolving.

First, we must determine the effects that will influence the evolution of host recovery. As in the case of pathogen evolution, hosts will also face a trade-off. One of the most common approaches is to model a trade-off between host clearance and reproduction. Biologically, a host has only a finite amount of resources and choosing to invest in immune function necessarily takes resources away from other life history traits, such as reproduction [24]. This idea has been extended to models of hosts categorized into female and male groups to show that different sexes are expected to evolve different levels of immune investment [25, 26, 27]. There is also a distinction made in the literature between modelling host immune maintenance versus activation. Immune maintenance considers the costs of diverting resources from reproduction to immune function in order to maintain an immune system at all times [28]; in this framework, all individuals incur the cost of investing in their immune system, regardless of disease status. Alternatively, immune activation refers to the act of diverting resources from reproduction to immune function in order to combat an active infection [19, 29]; here, the cost of investing in the immune system is paid only by infected individuals. We will focus here on immune system maintenance. As in [28], we suppose that there is a maximal birth rate $b_{\max}$ which is reduced at a cost c for investing resources in immune function, with the level of investment measured by γ. This allows us to write $b = b(\gamma)$ and model the birth rate as $b(\gamma) = b_{\max} - c\gamma$ [28].

Next, suppose that there is a resident host population governed by (1.1) and that this resident system has reached the EE previously derived. We then imagine introducing a mutant host whose clearance rate is given by $\hat{\gamma}$. These mutant hosts will create new mutant host offspring at a per-capita rate $\hat{b} = b(\hat{\gamma})$. If we denote the number of susceptible mutant hosts by $\hat{S} = \hat{S}(t)$ and the number of infected mutant hosts by $\hat{I} = \hat{I}(t)$, then we can approximate the dynamics of the mutant host population by the following linear system:

$$\begin{bmatrix} \frac{d\hat{S}}{dt} \\ \frac{d\hat{I}}{dt} \end{bmatrix} = \left(\underbrace{\begin{bmatrix} \hat{b} & \hat{b} \\ 0 & 0 \end{bmatrix}}_{F} - \underbrace{\begin{bmatrix} \beta\bar{I} + \mu & -\hat{\gamma} \\ -\beta\bar{I} & \hat{\gamma} + \mu + \alpha \end{bmatrix}}_{V} \right) \begin{bmatrix} \hat{S} \\ \hat{I} \end{bmatrix}, \tag{1.12}$$

where overbars denote the EE levels of resident hosts. The matrix F describes the per-capita rate of production of new mutant hosts, while the matrix $-V$ describes transitions of individuals between disease compartments and the loss of individuals from the population.

As in the case of pathogen evolution, we can define the fitness $W = W(\hat{\gamma}, \gamma)$ of the mutant host in different ways. One way is to use the instantaneous growth rate of the mutant host population, which is now defined as the largest eigenvalue, in the sense that it is the eigenvalue which serves as an upper bound on the real parts of all of the other eigenvalues, of the matrix $F - V$ [17]. When this eigenvalue is positive (resp. negative), the mutant host population will grow (resp. shrink). Alternatively, we can derive fitness from the next-generation matrix FV^{-1} [30, 31, 32]. The entries of this matrix describe the expected number of susceptible and infected mutant hosts that will be created by a single susceptible or infected mutant host, and we can use its dominant eigenvalue as a measure of fitness [30]. As discussed previously, regardless of how we measure fitness, we will arrive at the same evolutionary equilibrium [18].

In our example model, if we choose to measure fitness as the dominant eigenvalue of the next-generation matrix [30], we get the following expression:

$$W(\hat{\gamma}, \gamma) = \frac{\hat{b}(\beta \bar{I} + \hat{\gamma} + \mu + \alpha)}{\mu(\beta \bar{I} + \hat{\gamma} + \mu + \alpha) + \alpha\beta\bar{I}}. \tag{1.13}$$

The evolutionary equilibrium γ^* is then found by solving

$$\left.\frac{\partial W}{\partial \hat{\gamma}}\right|_{\hat{\gamma}=\gamma=\gamma^*} = 0. \tag{1.14}$$

Stability conditions can also be derived for this equilibrium, as we did with the evolutionary equilibrium of the pathogen. We say that the host evolutionary equilibrium γ^* is evolutionarily stable (sensu [20]) if

$$\left.\frac{\partial^2 W}{\partial \hat{\gamma}^2}\right|_{\hat{\gamma}=\gamma=\gamma^*} \leq 0, \tag{1.15}$$

and that it is convergence stable [21] if

$$\frac{d}{d\gamma}\left[\left.\frac{\partial W}{\partial \hat{\gamma}}\right|_{\hat{\gamma}=\gamma}\right]_{\gamma=\gamma^*} \leq 0. \tag{1.16}$$

As before, strict versions of these inequalities provide sufficient conditions for stability. An evolutionary equilibrium which satisfies both (1.15) and (1.16) is called a continuously stable strategy (CSS) [22].

Using the relationship between birth rate and clearance rate defined above, we can solve (1.14) to find the evolutionary equilibrium clearance rate

$$\gamma^* = \frac{b_{\max} - (\mu + \alpha) + \sqrt{\alpha[(1-c)(\mu+\alpha) - b_{\max}]}}{c}, \tag{1.17}$$

where $b_{\max}$ and c are chosen so that γ^* is both real and positive. We can also find the equilibrium birth rate b^* associated with γ^*: $b^* = \mu + \alpha - \sqrt{\alpha[(1-c)(\mu+\alpha) - b_{\max}]}$. To check the stability of γ^*, we evaluate conditions (1.15) and (1.16). Condition (1.15) is satisfied if and only if $b^* > \mu$, which must be true since we are working under the assumption that the EE of (1.1) is stable. Condition (1.16) is satisfied if and only if $(\mu + \alpha - b^*)b^* + \alpha b^* > 0$, which must be true because $b^* < \mu + \alpha$ is a necessary condition for the EE of (1.1) to be stable. Thus, the evolutionary equilibrium clearance rate (1.17) is a CSS. Over time, we expect natural selection to push the host population towards this clearance rate.

1.4 Host-Pathogen Coevolution

What if both host and pathogen traits are evolving? In our example model, the CSS levels of disease-induced mortality and clearance depend on each other, so that changes in one will cause changes in the other. To study the coevolution of hosts and pathogens, we look for a CSS pair (α^*, γ^*) which simultaneously satisfies conditions (1.6), (1.8), and (1.9) for the pathogen and conditions (1.14), (1.15), and (1.16) for the host. To find this pair, we would equate the expressions found above for α^* and γ^*.

While the adaptive-dynamics approach [5, 6, 7] discussed previously still applies, the trade-offs faced by hosts and pathogens can become more complicated when the two groups are co-evolving with one another. For example, if pathogens face at trade-off between transmission and clearance [15, 16], then hosts balancing their resource investments between reproduction and immune function can influence pathogen evolution through changing clearance rates. The outcome of such an interaction was explored by van Baalen [28] in the case of host immune maintenance. Coevolution, in this case, could lead to two possible stable evolutionary outcomes: a state in which hosts invest little in their immune systems and pathogens are relatively avirulent, and a state in which hosts invest heavily in their immune systems and pathogens express a higher level of virulence [28]. Conversely, the same outcome was not found by Day and Burns [19] when considering host immune activation instead of maintenance. Day and Burns [19] also highlight the importance of how virulence is measured. If virulence is measured not as disease-induced mortality but as case mortality, the probability of a host dying due to the disease, then virulence is not affected by coevolutionary dynamics [19].

Coevolution can also be studied in cases where hosts and pathogens evolve on different time scales. For example, Pharaon and Bauch [33] studied a model in which pathogen evolution responds to changes in host behaviour. Hosts choose whether or not to engage in prophylactic behaviour, such as wearing a mask or social distancing. To model the proportion of individuals engaging in prophylaxis, Pharaon and Bauch [33] use the replicator dynamic [34, 35], a differential equation which describes how the frequency of individuals adopting a given strategy (in this case, engaging in prophylaxis) changes due to natural selection. In particular, if $x = x(t)$ represents the frequency of susceptible individuals engaging in prophylaxis, then the replicator dynamic says that

$$\frac{dx}{dt} \propto x(1 - x)(W_x - \bar{W}), \tag{1.18}$$

where W_x represents the fitness of a susceptible individual engaging in prophylaxis and $\bar{W}$ represents the average fitness of a susceptible individual in the population [34, 35]. This provides an alternative way of studying evolution than adaptive dynamics [5, 6, 7]. Host behaviour then evolves on a much faster time scale than pathogen disease-induced mortality, and the model effectively assumes that hosts reach a quasi-equilibrium before analyzing the evolution of pathogens [33]. This methodology is in contrast to that described above of using an adaptive-dynamics approach [5, 6, 7] to study the evolution of both host and pathogen populations.

1.5 Multiple Pathogen Strains

One way in which the previous models on evolution can be extended is by considering the effects of multiple strains of the pathogen. Coinfection by multiple strains is a feature of many infectious diseases, such as influenza [36], malaria [37], and dengue [38].

One approach to studying coinfection is to pair an epidemiological model, such as (1.1), with a model of the within-host dynamics of the pathogen strains [39]. Authors following this approach have taken into account such things as pathogen exploitation of host resources [40], the production of molecules used as a public good by the group of coinfecting pathogens [41], and the interaction between pathogens and host lymphocytes [42]. Much of this literature assumes that different pathogen strains compete for resources within the host, and show that the exact nature of the interactions between strains will determine the evolutionary outcome.

An alternative approach is to use tools from kin selection theory. Instead of explicitly modelling interactions between pathogen strains within hosts, this approach summarizes those within-host dynamics by using the coefficient of relatedness between a focal pathogen strain and its coinfecting group [43, 44]. In doing so, some biological details are sacrificed but the resulting model yields evolutionary predictions less beholden to specific assumptions about population dynamics. The guiding principle of this approach is to consider the fitness of a focal pathogen strain as a function of the genotype of that focal strain [43, 44]. Doing so shows that, at evolutionary equilibrium, a focal pathogen strain must balance the benefit to itself of increased transmission against both the direct cost to itself of increased clearance and the indirect cost to its coinfecting group of decreased duration of infection [43]. One of the main predictions from this literature is that increased relatedness among coinfecting pathogen strains will select for reduced virulence [43, 44]. Effectively, the coinfecting pathogen strains will behave more cooperatively the more related they are to one another, in keeping with the ideas put forth by Hamilton [45].

One open question in this field of work is: How do these predictions change when multiple pathogen strains coevolve with hosts, and how do evolution and coevolution proceed when susceptible and infected hosts can be further subdivided into additional categories? As discussed previously, host-pathogen coevolution can produce new results and predictions than when considering pathogen evolution alone. It seems reasonable, then, to hypothesize that allowing hosts to coevolve with multiple coinfecting pathogen strains could generate predictions not seen in the above literature on multiple pathogen strains.

1.6 Multiple Types of Hosts

Another way in which we can build on the models discussed previously is to consider the effects of multiple types of hosts. Mathematically, in models with multiple types of hosts, the pathogen will exhibit a different level of virulence and have a different fitness in each type of host [17]. To make evolutionary predictions, we then look to track the direction in which natural selection pushes pathogen virulence within each type of host [17].

As an example, many pathogens affect female and male hosts differently, such as those that cause bacterial meningitis [46] or tuberculosis [47]. In modelling these scenarios, the host population is split into susceptible and infected females, and susceptible and infected males. The pathogen expresses a certain disease-induced mortality rate in female hosts and a potentially different disease-induced mortality rate in males, and we look for CSS values of both of these traits using the adaptive-dynamics techniques discussed previously [17]. The sexes are typically differentiated based on their level of immune system investment, and models predict that the pathogen will evolve a higher level of disease-induced mortality in the sex that invests more heavily in its immune system [48]. Other work has shown that, in the presence of vertical transmission from female hosts to newborn offspring, pathogens are expected to evolve a lower level of disease-induced mortality in females due to this additional transmission pathway [15]. Alternatively, we can look at host evolution, where previous authors have shown that sexual selection can shape sex differences in host immune defense [24, 25, 27] and susceptibility to infection [26], or differing transmission and disease-induced mortality rates between the sexes [29]. Notably, all of this work focuses either on pathogen evolution or on host evolution, but not on the coevolution of both groups. Given that coevolution has been shown to produce qualitatively different results than considering only the evolution of one group, it is reasonable to ask how these results on sex-specific differences change when hosts and pathogens evolve together.

Another example involves classifying hosts according to whether or not they engage in some prophylactic measure, such as hand washing or social distancing, to protect against an infectious disease. Much research has been conducted on hosts choosing to vaccinate against a disease [49]. In the case of human papillomavirus, for example, theory has predicted that vaccination can select for higher levels of pathogen virulence [50]. Other work has shown that the direction in which natural selection pushes a pathogen population depends on the mechanism by which the vaccine works [51, 52]. In contrast, we can also model impermanent types of behaviour, such as social distancing or wearing a mask, which hosts may choose to start or stop at any time. Work in this area has derived conditions under which a more virulent pathogen strain can or cannot successfully invade a resident population containing a less virulent strain [33]. However, this latter work considers only short-term pathogen competition, and does not make predictions about evolutionary stability or where natural selection will push a pathogen population over longer periods of time.

1.7 Contributions of this Thesis

Throughout this chapter, I have explored some of the key literature on evolutionary epidemiology and highlighted some questions that remain unanswered. I propose that coevolution and multiple types of hosts are important factors governing real host-pathogen systems, and that accounting for these factors in mathematical models can generate qualitatively different predictions than previous literature which neglects either of these effects. In the remaining chapters of this thesis, I provide three examples of original research supporting this claim. Each example will begin with a review of relevant literature in addition to the literature already discussed in this chapter. Matlab code used in Chapters 2 and 3 is available on the GitHub repository located at `https://github.com/evanjmitchell/doctoral-thesis`.

In Chapter 2, I study a population of hosts split into females and males, and investigate how coevolution of hosts and pathogens responds to the presence of multiple types of hosts. Female hosts show a stronger immune response than male hosts across many infectious diseases, while male hosts tend to experience a higher disease-induced mortality rate than female hosts. Previous evolutionary explanations of this phenomenon have focused exclusively on either host or pathogen evolution. Here, I build a coevolutionary model where both host and pathogen populations evolve in response to changes in either population. I also include the effects of vertical transmission, a crucial selective pressure felt only by female hosts and which has been neglected in previous theories. For high rates of vertical transmission, I predict that female hosts will evolve a higher level of immune system investment than male hosts while pathogens will evolve a higher rate of disease-induced mortality in males relative to females. By including the effects of vertical transmission and establishing this result in a coevolutionary setting, I provide a more complete explanation of the trend observed across a wide variety of infectious diseases.

In Chapter 3, I study a scenario in which hosts are able to change from one type to another. I build a model of sublethal disease effects where hosts are able to choose to engage in prophylactic measures that reduce the likelihood of disease transmission. This choice is mediated by utility costs and benefits associated with prophylaxis, and the fraction of hosts engaged in prophylaxis is also affected by population dynamics. As in [33], I model host behaviour using the replicator dynamic [34] and assume that it evolves to a quasi-equilibrium before studying the long-term evolution of pathogens. When prophylactic host behaviour occurs, I find that the level of pathogen host exploitation is reduced, by the action of selection, relative to the level that would otherwise be predicted in the absence of prophylaxis. This work emphasizes the significance of the transmission-recovery trade-off faced by the pathogen and the ability of the pathogen to influence host prophylactic behaviour.

In Chapter 4, I consider the possibility of multiple pathogen strains in addition to multiple types of hosts. I develop a general theoretical framework to link ideas from evolutionary epidemiology to those from kin selection theory to study the evolution of coinfecting pathogen strains. The main result is that pathogens will evolve to balance both the direct and indirect benefits of increased transmission with the associated direct and indirect costs of decreased duration of infection within each type of host. Importantly, the trait value which achieves this balance can differ between host types and is affected by coevolutionary dynamics. Furthermore, the more genetically related is a pathogen strain to its coinfecting group, the more it will reduce its own disease-induced mortality rate for the benefit of the whole group.

Finally, in Chapter 5, I provide some summarizing remarks and discuss possible directions for future research work.

Chapter 2

Female Reproduction and the Evolution of Sex-specific Differences in Immunity

2.1 Introduction

Many clinical studies on infectious diseases show a trend of female hosts maintaining a stronger immune system and experiencing a lower level of disease-induced mortality than male hosts [53]. This trend is seen across a wide variety of infectious diseases, such as bacterial meningitis [46], tuberculosis [47], and infections caused by *Staphylococcus aureus* [54]. These observations have been attributed to inherent genetic differences between the sexes [55, 56, 57, 58], but a full evolutionary explanation is not readily available. What selective pressures could have pushed females to invest more heavily in their immune system? How did evolution lead to pathogens that inflict a lower level of disease-induced mortality in females than in males?

Two theories currently exist to address the first of these questions. One theory argues that differences in immunity between the sexes are the result of females choosing males with attractive features as reproductive partners [24, 25, 26]. While male sex hormones may enhance their attractiveness, they also act as immune suppressants [24, 25, 26]. Thus, sexual selection for attractive males should result in a weaker immune response in males relative to females

[24, 25, 26, 27]. In this case, reduced immune response is simply the cost of being attractive and this cost is unique to males.

A second theory in shaping patterns of host immunity emphasizes the role of pathogen life-history traits. Different infection rates or disease-induced mortality rates in female versus male hosts can select for sex-specific levels of immune investment. In particular, if males experience a higher infection rate than females, or if females experience a higher disease-induced mortality rate, then natural selection leads to a greater immune response in females relative to males [29]. In this case, it is the pathogen, not the mating system, that leads selection to shape the host's response to infection in a sex-specific manner.

Both of these explanations neglect host-pathogen coevolution. They take, as given, that a pathogen exhibits a higher level of disease-induced mortality in one sex relative to the other and predict where this will lead host evolution. The subsequent evolutionary response from the pathogen is ignored.

In order to develop a more complete explanation of the pattern observed in clinical studies of increased immunity and decreased disease-induced mortality in females, we investigate the coevolution of both hosts and pathogens as a result of natural and sexual selection. Furthermore, we also include the possibility of a female infecting her newborn offspring via vertical transmission. Vertical transmission is observed in many infectious diseases, such as dengue [59], human papillomavirus [60], and hepatitis B [61], and is experienced exclusively by females. The possibility of vertical transmission means that a female investing more heavily in her immune system will reduce the likelihood of infecting her newborn offspring, conferring to her a fitness benefit. This benefit trades off against a cost to reproductive success. Vertical transmission adds an extra dimension to the evolutionary pressures felt by females, as there is now a reproductive benefit for females to invest in their immune system where before there was only a cost. This extra dimension is crucial to fully understand how selection shapes female immune investment and has been neglected in previous theories of the evolution of host immune response.

Here, we develop a model where female and male hosts can evolve different levels of immune-system investment (measured by their sex-specific rates of recovery) and pathogens can evolve sex-specific levels of disease-induced mortality. Asymmetry between the sexes is introduced via differences in the reproductive cost to immune investment and via the inclusion of vertical transmission. Our model predicts that sex differences in the reproductive cost to immune investment select for a stronger immune system and a higher disease-induced mortality rate in the sex that pays the lower cost, akin to previous non-sex-specific coevolutionary modelling [28]. Under the influence of vertical transmission, we predict that evolution can be driven to a state in which female hosts invest little in their immune system and pathogens exhibit lower levels of disease-induced mortality in female hosts, relative to male hosts. This result is similar to findings from sex-specific non-coevolutionary models [15]. The novel result is that the combination of vertical transmission and host-pathogen coevolution can select for a state in which pathogens exhibit a lower level of disease-induced mortality in heavily-defended female hosts. In this way, we identify specific evolutionary pressures that could have led to the previously unexplained trends observed in clinical studies across a wide variety of infectious diseases.

2.2 Model

2.2.1 Epidemiological Dynamics

We start with a population of N hosts classified according to their sex and disease status. At time t, there are $I_f = I_f(t)$ females infected with the pathogen and $S_f = S_f(t)$ females not infected. There are also $I_m = I_m(t)$ males infected with the pathogen and $S_m = S_m(t)$ males not infected. All uninfected individuals are susceptible to infection, and all infected individuals are also infectious.

Following the discussion of various mating functions in [62, 63], we model the host mating rate using the harmonic mean of the population sizes of females and males, given by

$$\frac{2(S_f + I_f)(S_m + I_m)}{N}. \tag{2.1}$$

The mating function is then multiplied by a per-capita birth rate, b. Assuming a one-to-one birth sex ratio, the total rate at which new hosts enter either the susceptible female or susceptible male classes is

$$\frac{b(S_f + I_f)(S_m + I_m)}{N}. \tag{2.2}$$

Hosts in every class experience a per-capita background mortality rate μ, and hosts infected by the pathogen experience an additional per-capita disease-induced mortality rate of α_f in females and α_m in males. Infective females and infective males also recover at rates γ_f and γ_m, respectively, and return immediately to their associated susceptible class.

Horizontal transmission to susceptible sex-i hosts in class S_i from infective sex-j hosts in class I_j occurs at a rate $S_i\beta_{ij}I_j$. We also include the possibility of vertical transmission from infective females to their offspring (as in [15]). If we assume that a proportion v of new hosts created by infective females are born with the disease, then we now have a flow of newborns into the infective female and male classes at a rate of

$$\frac{bvI_f(S_m + I_m)}{N}. \tag{2.3}$$

This leaves us with newborns entering the susceptible female and male classes at a rate of

$$\frac{b(S_f + (1 - v)I_f)(S_m + I_m)}{N}. \tag{2.4}$$

The model description is summarized schematically in figure 2.1 and mathematically with the following system of differential equations:

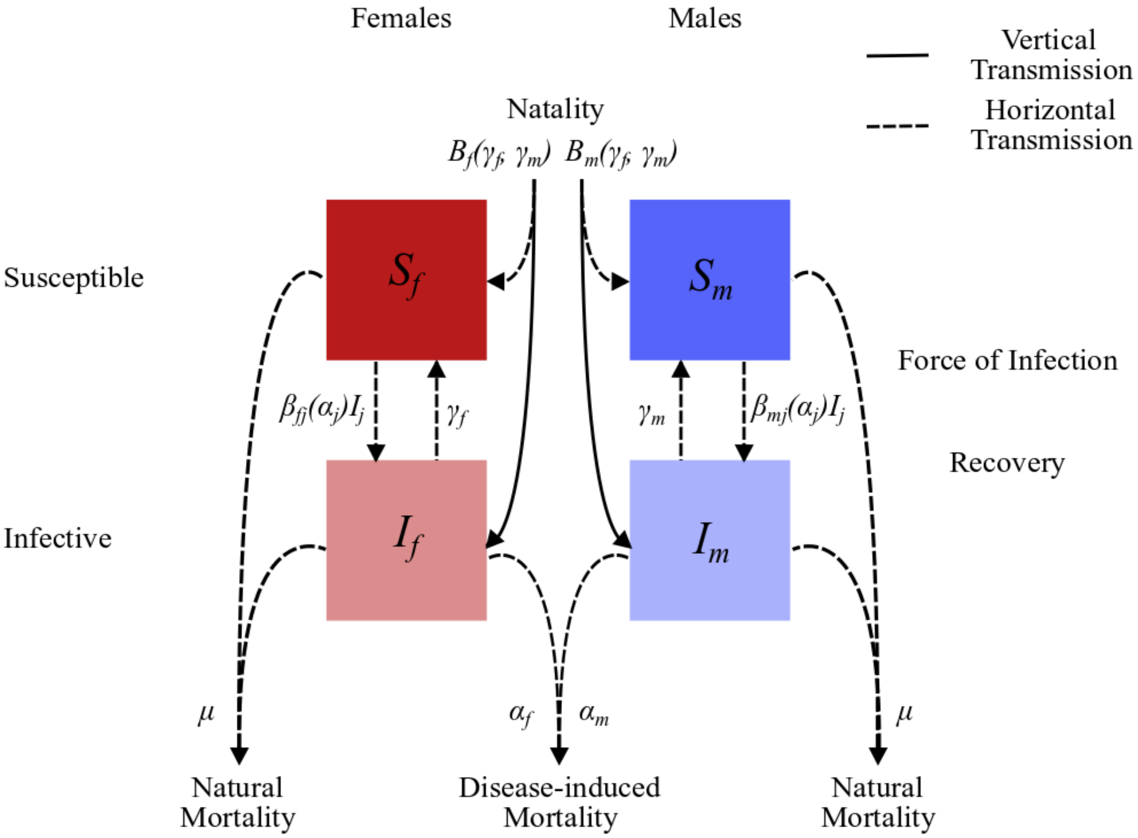
Females
Males
Vertical Transmission
Horizontal Transmission
Natality
$B_f(\gamma_f, \gamma_m)$
$B_m(\gamma_f, \gamma_m)$
Susceptible
S_f
S_m
Force of Infection
$\beta_{fj}(\alpha_j)I_j$
γ_f
γ_m
$\beta_{mj}(\alpha_j)I_j$
Recovery
Infective
I_f
I_m
μ
α_f
α_m
μ
Natural Mortality
Disease-induced Mortality
Natural Mortality

Figure 2.1: A schematic diagram of the model. B_f and B_m represent total birth rates given by the sum of equations (2.3) and (2.4). Dashed lines indicate routes of horizontal transmission while solid lines indicate routes of vertical transmission.

$$\frac{dS_f}{dt} = \frac{b(S_f + (1-v)I_f)(S_m + I_m)}{N} + \gamma_f I_f - S_f\beta_{ff}I_f - S_f\beta_{fm}I_m - \mu S_f \tag{2.5a}$$

$$\frac{dS_m}{dt} = \frac{b(S_f + (1-v)I_f)(S_m + I_m)}{N} + \gamma_m I_m - S_m\beta_{mf}I_f - S_m\beta_{mm}I_m - \mu S_m \tag{2.5b}$$

$$\frac{dI_f}{dt} = \frac{bvI_f(S_m + I_m)}{N} + S_f\beta_{ff}I_f + S_f\beta_{fm}I_m - (\gamma_f + \alpha_f + \mu)I_f \tag{2.5c}$$

$$\frac{dI_m}{dt} = \frac{bvI_f(S_m + I_m)}{N} + S_m\beta_{mf}I_f + S_m\beta_{mm}I_m - (\gamma_m + \alpha_m + \mu)I_m. \tag{2.5d}$$

As discussed in chapter 1 of this thesis, parameters are chosen so that there is a unique disease-free equilibrium, which coincides with the trivial equilibrium, and a unique endemic equilibrium. To achieve this, it is assumed that $b/2 \neq \mu$. Linear stability analysis of this system shows that the disease-free equilibrium, where no infected individuals are present, is unstable whenever $b/2 > \mu$. It is not possible to analytically find an endemic equilibrium of system (2.5), i.e., an equilibrium where hosts of all classes are present. Instead, we use numerical simulation to show that system (2.5) reaches an endemic equilibrium for a range of birth rates satisfying $b/2 > \mu$. However, if the birth rate becomes too large, the endemic equilibrium becomes unstable and the host population grows without bound. This indicates that there is a finite range of birth rate values to explore in analyzing our model.

2.2.2 Evolutionary Dynamics

To study how pathogen disease-induced mortality and host immune investment respond to selection, we assume that each faces a trade-off. The pathogen faces a trade-off between how efficiently it is able to transmit itself and how quickly it kills its host. Following many previous authors (e.g., [12, 8, 11]), we model the transmission constants β_{ij} as functions of the pathogen disease-induced mortality rates, α_f and α_m. In particular, we adapt the saturating functional form used in [28] to this sex-specific setting and write

$$\beta_{ij} = \beta_{ij}(\alpha_j) = \frac{\beta_{\max}\alpha_j}{\alpha_j + d}, \tag{2.6}$$

where larger values of $d > 0$ indicate a slower rate of saturation. By making β_{ij} independent of i, we are assuming that females and males are equally susceptible to infection.

Hosts face a trade-off between investing resources in their immune system and their reproductive success, as has been modelled by previous authors (e.g., [28, 19]). Hosts' level of immune investment is captured here by their sex-specific recovery rate, as in [28]. To relate the total birth rate b to the recovery rates γ_f and γ_m, we first suppose that the rate at which a female gives birth decays exponentially with increasing immune investment and write it as $b_{\max}e^{-k_f\gamma_f}$, where $b_{\max}$ is the maximal birth rate. The parameter $k_f > 0$ measures the rate of decay of a female's reproductive success due to increased investment in her immune system. For example, female sex hormones enhance the immune system, which in turn reduces the likelihood of conception and increases the chances of spontaneous abortion [64, 65, 66]. We also suppose that a male's probability of successfully mating with a female decays exponentially with increasing immune investment and express it as $e^{-k_m\gamma_m}$. It could be that a male is rejected by a potential female mate because he is not sufficiently attractive, and this decrease in reproductive success is captured by the parameter $k_m > 0$. The total per-capita birth rate in the population is then given by the product of the rate at which a female gives birth and the probability that a given male is successfully able to mate with a female, $b_{\max}e^{-k_f\gamma_f - k_m\gamma_m}$. If we take a first-order approximation to this exponential function, we can write $b_{\max}e^{-k_f\gamma_f - k_m\gamma_m} \approx b_{\max} - b_{\max}k_f\gamma_f - b_{\max}k_m\gamma_m$. We then interpret $b_{\max}k_f$ and $b_{\max}k_m$ as sex-specific reproductive costs to immune investment, and relabel them c_f and c_m, respectively. We consider host immune system maintenance (as in [28]) instead of immune system activation (as in [19]) so that hosts pay the reproductive cost to immune investment regardless of whether they are in a susceptible or infective class. We can now relate b to the recovery rates γ_f and γ_m via

$$b = b(\gamma_f, \gamma_m) = b_{\max} - c_f \gamma_f - c_m \gamma_m. \tag{2.7}$$

Equation (2.7) also generalizes the birth rate function used in [28] to this sex-specific setting.

Using an adaptive-dynamics approach [5, 6, 7], we can investigate how the pathogen and host traits change over evolutionary time. As in [28] and [19], we apply this approach to both the pathogen and host populations to study their coevolution. For the pathogen population, we introduce a rare mutant-type pathogen with disease-induced mortality rates $\tilde{\alpha}_f$ in female hosts and $\tilde{\alpha}_m$ in male hosts. The numbers $\tilde{I}_f$ and $\tilde{I}_m$ of female and male hosts, respectively, infected with this mutant strain change according to

$$\frac{d\tilde{I}_f}{dt} = \frac{bv\tilde{I}_f(\bar{S}_m + \bar{I}_m)}{\bar{N}} + \bar{S}_f \tilde{\beta}_{ff} \tilde{I}_f + \bar{S}_f \tilde{\beta}_{fm} \tilde{I}_m - (\gamma_f + \tilde{\alpha}_f + \mu)\tilde{I}_f \tag{2.8a}$$

$$\frac{d\tilde{I}_m}{dt} = \frac{bv\tilde{I}_f(\bar{S}_m + \bar{I}_m)}{\bar{N}} + \bar{S}_m \tilde{\beta}_{mf} \tilde{I}_f + \bar{S}_m \tilde{\beta}_{mm} \tilde{I}_m - (\gamma_m + \tilde{\alpha}_m + \mu)\tilde{I}_m, \tag{2.8b}$$

Overbars denote equilibrium levels of the resident host variables. We then apply a next-generation matrix approach [30] to (2.8) to find a fitness function for the pathogen. In particular, we write the matrix J of first-order partial derivatives of (2.8) as $J = F - V$ for matrices F and V. The pathogen's fitness $W_\alpha(\tilde{\alpha}_f, \tilde{\alpha}_m, \alpha_f, \alpha_m)$ is then defined as the dominant eigenvalue of the next-generation matrix FV^{-1} [30].

We follow a similar procedure for the host population by introducing a rare mutant-type host with recovery rate $\hat{\gamma}_f$ in females and $\hat{\gamma}_m$ in males. We denote the numbers of susceptible and infective female mutant-type hosts as $\hat{S}_f$ and $\hat{I}_f$, respectively, and the numbers of susceptible and infective male mutant-type hosts as $\hat{S}_m$ and $\hat{I}_m$, respectively. To account for the birth rate of new mutant hosts, we take a first-order approximation by considering only mutant hosts who are heterozygous for the mutation mating with resident (homozygous) wild-type hosts. They will produce new offspring at a rate $\hat{b}_f$ for matings between mutant females and resident males, and at a rate $\hat{b}_m$ for matings between mutant males and resident females. On average, half of these matings will result in new hosts heterozygous for the mutation, so new susceptible female or male mutant-type hosts are created at a total rate

$$\frac{\frac{\hat{b}_f}{2}(\hat{S}_f + (1-v)\hat{I}_f)(\bar{S}_m + \bar{I}_m) + \frac{\hat{b}_m}{2}(\bar{S}_f + (1-v)\bar{I}_f)(\hat{S}_m + \hat{I}_m)}{\bar{N}} \tag{2.9}$$

and new infective female or male mutant-type hosts are created at a total rate

$$\frac{\frac{\hat{b}_f}{2}v\hat{I}_f(\bar{S}_m + \bar{I}_m) + \frac{\hat{b}_m}{2}v\bar{I}_f(\hat{S}_m + \hat{I}_m)}{\bar{N}}. \tag{2.10}$$

The numbers of susceptible and infective mutant-type hosts then change according to

$$\begin{aligned}\frac{d\hat{S}_f}{dt} &= \frac{\frac{\hat{b}_f}{2}(\hat{S}_f + (1-v)\hat{I}_f)(\bar{S}_m + \bar{I}_m) + \frac{\hat{b}_m}{2}(\bar{S}_f + (1-v)\bar{I}_f)(\hat{S}_m + \hat{I}_m)}{\bar{N}} \\ &\quad + \hat{\gamma}_f\hat{I}_f - \hat{S}_f\beta_{ff}\bar{I}_f - \hat{S}_f\beta_{fm}\bar{I}_m - \mu\hat{S}_f\end{aligned} \tag{2.11a}$$

$$\frac{d\hat{I}_f}{dt} = \frac{\frac{\hat{b}_f}{2}v\hat{I}_f(\bar{S}_m + \bar{I}_m) + \frac{\hat{b}_m}{2}v\bar{I}_f(\hat{S}_m + \hat{I}_m)}{\bar{N}} + \hat{S}_f\beta_{ff}\bar{I}_f + \hat{S}_f\beta_{fm}\bar{I}_m - (\hat{\gamma}_f + \alpha_f + \mu)\hat{I}_f \tag{2.11b}$$

$$\begin{aligned}\frac{d\hat{S}_m}{dt} &= \frac{\frac{\hat{b}_f}{2}(\hat{S}_f + (1-v)\hat{I}_f)(\bar{S}_m + \bar{I}_m) + \frac{\hat{b}_m}{2}(\bar{S}_f + (1-v)\bar{I}_f)(\hat{S}_m + \hat{I}_m)}{\bar{N}} \\ &\quad + \hat{\gamma}_m\hat{I}_m - \hat{S}_m\beta_{mf}\bar{I}_f - \hat{S}_m\beta_{mm}\bar{I}_m - \mu\hat{S}_m\end{aligned} \tag{2.11c}$$

$$\frac{d\hat{I}_m}{dt} = \frac{\frac{\hat{b}_f}{2}v\hat{I}_f(\bar{S}_m + \bar{I}_m) + \frac{\hat{b}_m}{2}v\bar{I}_f(\hat{S}_m + \hat{I}_m)}{\bar{N}} + \hat{S}_m\beta_{mf}\bar{I}_f + \hat{S}_m\beta_{mm}\bar{I}_m - (\hat{\gamma}_m + \alpha_m + \mu)\hat{I}_m. \tag{2.11d}$$

We then apply a next-generation matrix approach [30], as described above, to (2.11) to find a fitness function $W_\gamma(\hat{\gamma}_f, \hat{\gamma}_m, \gamma_f, \gamma_m)$ for the host.

2.2.3 Methods of Analysis

Selection will move the pathogen's disease-induced mortality in a direction given by the sign of $\partial W_\alpha/\partial\tilde{\alpha}_f|_{\tilde{\alpha}_f=\alpha_f}$ in female hosts and $\partial W_\alpha/\partial\tilde{\alpha}_m|_{\tilde{\alpha}_m=\alpha_m}$ in male hosts. An endpoint of evolution will take the form of a pair (α_f^*, α_m^*) satisfying

$$\left.\frac{\partial W_\alpha}{\partial\tilde{\alpha}_i}\right|_{(\tilde{\alpha}_f,\tilde{\alpha}_m)=(\alpha_f,\alpha_m)=(\alpha_f^*,\alpha_m^*)} = 0, \tag{2.12}$$

for $i = f, m$. We then look for a continuously stable strategy (CSS) [22] of this process: an endpoint of evolution that both attracts nearby resident pathogen populations and resists invasion by nearby mutant pathogen populations. If such a point attracts nearby resident populations, then the matrix of first-order partial derivatives of the selection gradients of W_α must be negative definite. If this condition holds, we say the point is convergence stable [67, 68]. If the point resists invasion by nearby mutant populations, then the matrix of second-order partial derivatives of W_α must be negative definite. If this condition holds, we say the point is evolutionarily stable [67, 68]. We can also define analogous conditions on the host fitness function, W_γ. Ultimately, we look for a quadruple $(\gamma_f^*, \gamma_m^*, \alpha_f^*, \alpha_m^*)$ that simultaneously satisfies the above conditions on W_α and W_γ. Such a quadruple we call a coevolutionary continuously stable strategy (coCSS) [28, 19].

In general, finding this quadruple cannot be done analytically. Instead, we use a Matlab (version R2019a) algorithm, the code for which is available on the GitHub repository at `https://github.com/evanjmitchell/doctoral-thesis`, to find the coCSS levels of host recovery and pathogen disease-induced mortality numerically. This algorithm is based on the observation that locally asymptotically stable equilibrium solutions to the system

$$\frac{d\gamma_f}{dt} = \left.\frac{\partial W_\gamma}{\partial \hat{\gamma}_f}\right|_{(\hat{\gamma}_f,\hat{\gamma}_m)=(\gamma_f,\gamma_m)} \tag{2.13a}$$

$$\frac{d\gamma_m}{dt} = \left.\frac{\partial W_\gamma}{\partial \hat{\gamma}_m}\right|_{(\hat{\gamma}_f,\hat{\gamma}_m)=(\gamma_f,\gamma_m)} \tag{2.13b}$$

$$\frac{d\alpha_f}{dt} = \left.\frac{\partial W_\alpha}{\partial \tilde{\alpha}_f}\right|_{(\tilde{\alpha}_f,\tilde{\alpha}_m)=(\alpha_f,\alpha_m)} \tag{2.13c}$$

$$\frac{d\alpha_m}{dt} = \left.\frac{\partial W_\alpha}{\partial \tilde{\alpha}_m}\right|_{(\tilde{\alpha}_f,\tilde{\alpha}_m)=(\alpha_f,\alpha_m)} \tag{2.13d}$$

will be convergence-stable evolutionary equilibria in the sense described above. We numerically iterate this system until equilibrium has been reached to generate a candidate coCSS. Finally, we use a centred finite-difference approximation to compute the matrices of second-order partial derivatives of W_α and W_γ, evaluated at the candidate coCSS, and check that they are negative definite. This is done by computing the eigenvalues of these matrices and confirming that they are all negative.

2.3 Results

2.3.1 No Sex-Specific Differences

Before exploring the full model (2.5), we consider two special cases. The first case is when we strip away the sex differences from our model. In particular, we assume (i) that there is no vertical transmission, (ii) that females and males pay the same reproductive cost of immune investment (i.e., $c_f = c_m = c$), and (iii) that there are no sex-specific levels of recovery or disease-induced mortality so that $\gamma_f = \gamma_m = \gamma$ and $\alpha_f = \alpha_m = \alpha$ and $\beta_{ff} = \beta_{fm} = \beta_{mf} = \beta_{mm} = \beta$. We introduce new state variables $S = S_f + S_m$ for the total number of susceptible hosts and $I = I_f + I_m$ for the total number of infective hosts. When this system is at the endemic equilibrium, under these assumptions, we would expect to have $S_f = S_m = S/2$ and $I_f = I_m = I/2$. Since the evolutionary analysis is performed when the resident system is at equilibrium, we can reduce (2.5) to

$$\frac{dS}{dt} = \frac{b}{2}(S + I) + \gamma I - S\beta I - \mu S \tag{2.14a}$$

$$\frac{dI}{dt} = S\beta I - (\gamma + \alpha + \mu)I, \tag{2.14b}$$

where $b = b_{\max} - 2c\gamma$. We can then solve (2.14) to find a disease-free equilibrium $(S, I) = (0, 0)$ and an endemic equilibrium given by

$$S = \frac{\gamma + \alpha + \mu}{\beta} \quad \text{and} \quad I = \frac{(\gamma + \alpha + \mu)(b - 2\mu)}{\beta[2(\alpha + \mu) - b]}. \tag{2.15}$$

Linear stability analysis of the associated Jacobian matrix shows that the disease-free equilibrium is unstable when $b/2 > \mu$, in which case the system moves towards the endemic equilibrium (2.15), and that the endemic equilibrium remains stable as long as $b/2 < \alpha + \mu$.

The evolutionary analysis proceeds as outlined above. Detailed calculations, presented in Appendix A, show that we can analytically find the coCSS level of pathogen disease-induced mortality to be $\alpha = \sqrt{d(\gamma + \mu)}$, which matches the result found in the model used in [28] (and in the Discussion of [19]) to analyze host-pathogen coevolution in the absence of host sex differences. Solving for the coCSS level of host recovery is not possible analytically, but numerical simulation suggests that there are two possible outcomes: an unstable equilibrium characterized by an intermediate level of recovery, and a stable equilibrium characterized by a higher level of recovery. Selection, then, will push the host-pathogen system towards this stable equilibrium, corresponding qualitatively with predictions made in previous work [28].

We now relax the restriction that $\gamma_f = \gamma_m$ and $\alpha_f = \alpha_m$, and allow for sex-specific levels of recovery and disease-induced mortality. We continue to assume that there is no asymmetry between the sexes, i.e., both sexes pay the same reproductive cost of immune investment ($c_f = c_m = c$) and there is no vertical transmission ($v = 0$). Under these assumptions, model (2.5) reduces to

$$\frac{dS_f}{dt} = \frac{b(S_f + I_f)(S_m + I_m)}{N} + \gamma_f I_f - S_f\beta_{ff}I_f - S_f\beta_{fm}I_m - \mu S_f \tag{2.16a}$$

$$\frac{dS_m}{dt} = \frac{b(S_f + I_f)(S_m + I_m)}{N} + \gamma_m I_m - S_m\beta_{mf}I_f - S_m\beta_{mm}I_m - \mu S_m \tag{2.16b}$$

$$\frac{dI_f}{dt} = S_f\beta_{ff}I_f + S_f\beta_{fm}I_m - (\gamma_f + \alpha_f + \mu)I_f \tag{2.16c}$$

$$\frac{dI_m}{dt} = S_m\beta_{mf}I_f + S_m\beta_{mm}I_m - (\gamma_m + \alpha_m + \mu)I_m, \tag{2.16d}$$

where $b = b_{\max} - c(\gamma_f + \gamma_m)$.

Analysis again proceeds as described above, with detailed calculations presented in Appendix A. We are able to show that the coCSS level of pathogen disease-induced mortality is $\alpha_f = \sqrt{d(\gamma_f + \mu)}$ in female hosts and $\alpha_m = \sqrt{d(\gamma_m + \mu)}$ in male hosts. This corresponds qualitatively with results from previous authors that show that, in the presence of multiple types of hosts, we expect the pathogen to evolve levels of disease-induced mortality specific to each host type [15, 17]. The coCSS levels of host recovery cannot be found analytically, and we instead use the numerical procedure described previously. Numerical results confirm that the pathogen's level of disease-induced mortality evolves towards that found analytically. Moreover, the pathogen evolves the same level of disease-induced mortality in both female and male hosts (i.e., $\alpha_f = \alpha_m$) and this matches the disease-induced mortality level predicted in the previous result in the absence of any sex differences. This trend is also seen in the host population, as our numerical results suggest that female and male hosts will evolve the same level of recovery and that this communal level matches that found in the previous case with no sex differences.

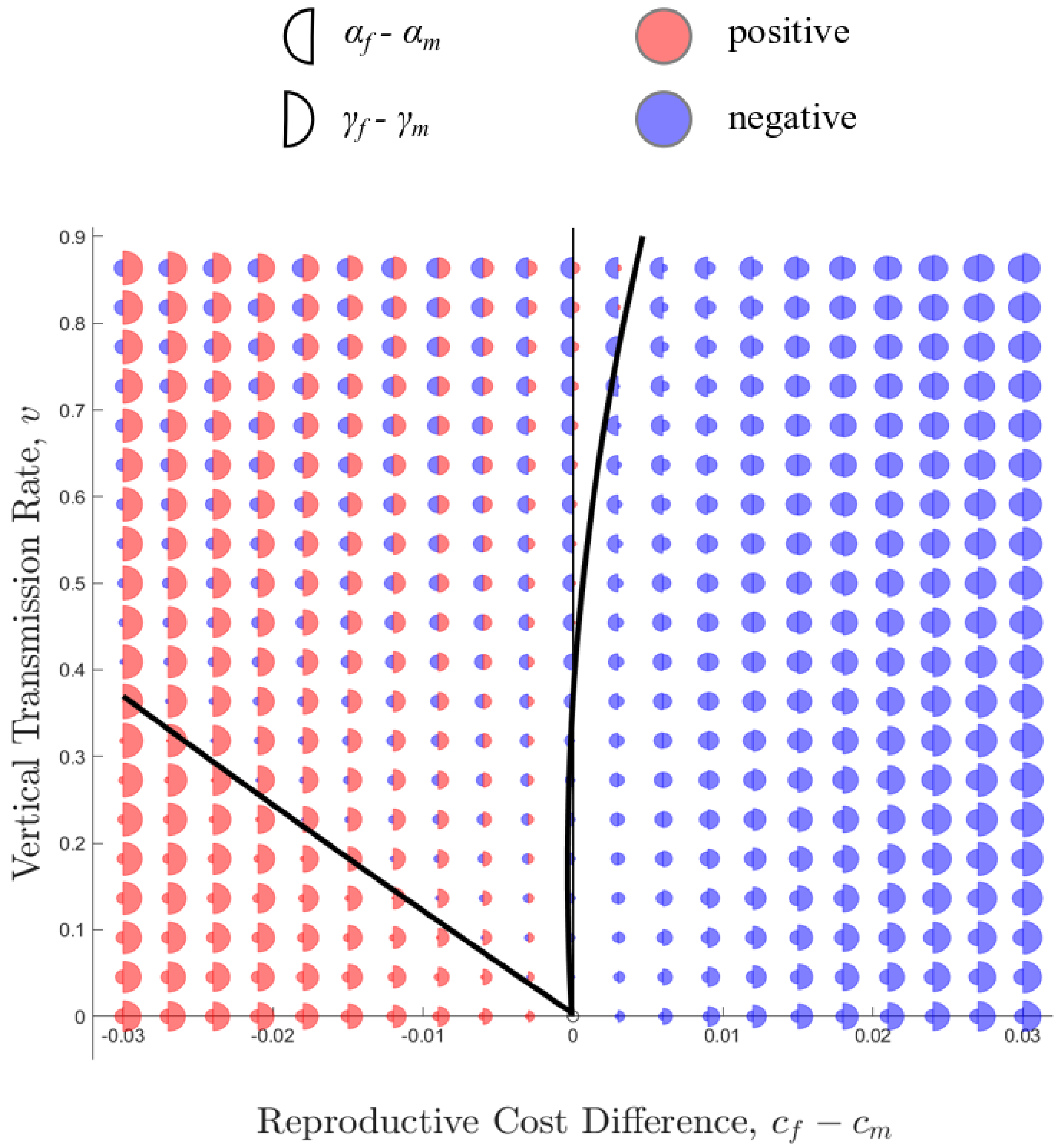

Figure 2.2: Results from numerical simulation of the full model (2.5) across a range of reproductive cost differences and vertical transmission rates. Solid black curves indicate boundaries between regions containing qualitatively different evolutionary patterns, interpolated using numerical results. Each point is split into two half-circles, with the area of the left half proportional to the sex difference in disease-induced mortality rates and the right half proportional to the sex difference in recovery rates. Red indicates a positive parameter difference, so that higher values of the given parameter are found in females relative to males. Blue indicates a negative parameter difference, so that higher values of the given parameter are found in males relative to females.

2.3.2 General Case

To analyze the full model with sex-specific differences, we use the numerical method described above. The results of this method are summarized in figure 2.2 and various aspects of this figure will be discussed in the following paragraphs. We used a range of parameter values chosen to satisfy the stability conditions presented previously, i.e., $b/2 > \mu$ but b cannot be so large that the endemic equilibrium becomes unstable and the population grows without bound (see table 2.1).

Table 2.1: Ranges tested for the various model parameters, along with the qualitative effect of an increase in a given parameter value on the results in figure 2.2.

Paramater	Range	Effect on Fig. 2.2 of Increasing Parameter Value
$b_{\max}$	$\{5, 10, 20\}$	boundary curves pulled towards vertical axis
μ	$\{1, 2, 4\}$	boundary curves pulled towards horizontal axis
$\beta_{\max}$	$\{10, 20, 50\}$	no noticeable effect
d	$\{1, 2, 5, 10\}$	right boundary curve pulled towards horizontal axis

The vertical axis of figure 2.2 has been partially explored in previous work on pathogen evolution in response to vertical transmission in hosts [15], and our results on disease-induced mortality evolution along this axis match those predictions. In particular, along the entire vertical axis our model predicts that pathogens will evolve a lower level of disease-induced mortality in female hosts relative to male hosts (figure 2.2). Our results also build on these predictions by including the coevolution of host recovery. For low rates of vertical transmission, we see female hosts evolve a lower level of recovery than male hosts. However, for sufficiently large rates of vertical transmission, the trend changes and we observe female hosts evolving a higher recovery rate than male hosts.

Restricting attention to the horizontal axis of figure 2.2, there is no vertical transmission and hosts pay a sex-specific reproductive cost to immune investment. Here, we find that the host sex that pays the lower cost to immune investment will evolve the higher recovery rate. Since the pathogen is now being cleared more quickly in this sex, there is selective pressure to evolve a higher level of disease-induced mortality in this sex relative to the other.

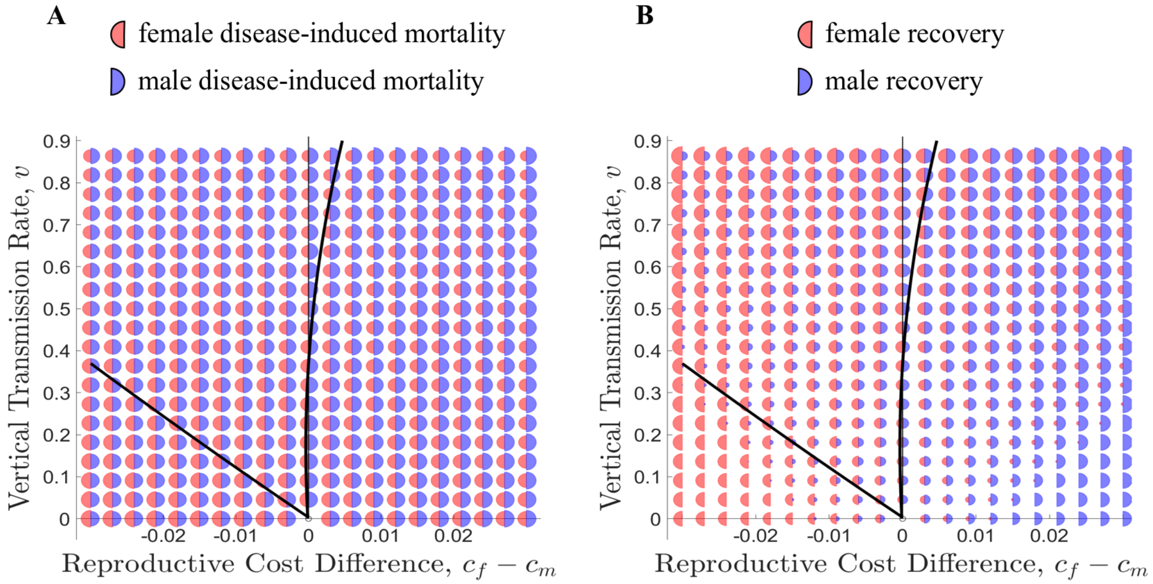

Figure 2.3: Evolutionary trends within each sex. Solid black curves are the same numerically interpolated boundaries identified in figure 2.2. **Panel A:** The area of the left half-circle is proportional to the coCSS level of female host disease-induced mortality, while the area of the right half-circle is proportional to the coCSS level of male host disease-induced mortality. **Panel B:** The area of the left half-circle is proportional to the coCSS level of female host recovery, while the area of the right half-circle is proportional to the coCSS level of male host recovery.

Finally, we investigate what happens when we move off of the axes and include both vertical transmission and sex-specific reproductive costs to immune investment. Here, we see the emergence of a region in which female hosts evolve a higher level of recovery while the pathogen evolves a lower level of disease-induced mortality than it does in male hosts (upper-left region in figure 2.2). This is a novel pattern not found in previous literature, and matches the observations from clinical research showing a stronger immune system and lower level of disease-induced mortality in female relative to male hosts across a wide range of infectious diseases. Of particular note is that both vertical transmission and host-pathogen coevolution are necessary conditions for the emergence of this pattern in our model.

In addition to looking at the evolutionary trends in one sex relative to the other, we can also look at how disease-induced mortality and recovery rates are changing in each sex independently. These results are shown in figure 2.3. Panel A of this figure shows that as we increase the degree of sexual asymmetry via an increase in the vertical transmission rate, we expect the pathogen's disease-induced mortality rate to decrease in females while remaining relatively unchanged in males. Increasing the degree of sexual asymmetry via an increase in the reproductive cost difference, conversely, has a less noticeable effect on disease-induced mortality rates in either sex. Panel B of figure 2.3 shows that we expect recovery rates in both sexes to increase when we increase the vertical transmission rate. Furthermore, increasing the reproductive cost difference has a more noticeable effect on recovery rates than it does on disease-induced mortality rates. In particular, as we magnify the cost difference in favour of one sex over the other, recovery rates will increase in the sex that pays the lower cost and decrease in the sex that pays the higher cost.

Lastly, we can also recast these results in terms of more easily measurable quantities of potential interest to public-health officials. In particular, we look at the effects on both the case mortality rates, χ_f in females and χ_m in males, and the expected lifetime of a host, defined as the sum of the average amount of time for which they are in either the susceptible or infected classes (see figure 2.4). Panel A of figure 2.4 shows that we expect the case mortality rate to be lower in females than males for almost all parameter values explored, with a greater difference for larger vertical transmission rates. As vertical transmission rates increase, we expect females will invest more in their immune system which should lower their case mortality relative to males. Panel B of figure 2.4 shows that females will have a longer expected lifetime than males for almost all parameter values explored, with this difference being amplified by larger rates of vertical transmission. Again, this is expected given our previous result of females investing more in their immune system for higher rates of vertical transmission, as they will be less likely than males to die prematurely due to the disease.

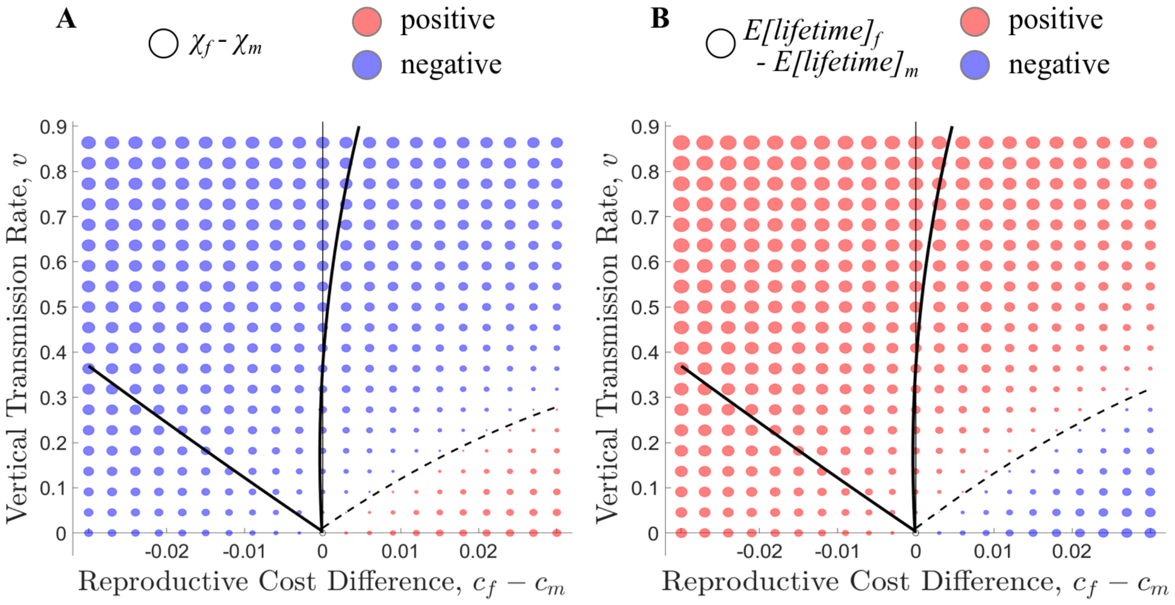

Figure 2.4: Results from numerical simulation of the full model (2.5) recast in terms of more easily measurable quantities of potential interest to public-health officials. Solid black curves are the same numerically interpolated boundaries identified in figure 2.2. **Panel A:** The area of each circle is proportional to the difference between female and male case mortality rates. Red indicates a positive difference, so that case mortality is higher in females than in males. Blue represents a negative difference, so that case mortality is higher in males than in females. The black dashed line indicates where the case mortality rate is the same in both sexes, interpolated using numerical results. **Panel B:** The area of each circle is proportional to the difference between the expected lifetime of females and males. Red indicates a positive difference, so that females have a longer expected lifetime than males. Blue indicates a negative difference, so that males have a longer expected lifetime than females. The black dashed line indicates where the expected lifetimes of both sexes are the same, interpolated using numerical results.

2.4 Discussion

We have considered a model in which asymmetry was introduced between host sexes via a difference in the reproductive cost to immune investment and the possibility of vertical transmission in female hosts. The former is a direct cost to hosts, while the latter can be viewed as an indirect cost to female hosts. In this way, we are treading on well-travelled ground, but we place these effects in a coevolutionary setting in order to develop a more complete explanation for the evolution of a greater immune response in females and increased disease-induced mortality in males.

If we consider only the effects of sex-specific reproductive costs to immune investment, our results predict that hosts and pathogens will coevolve to a state in which the sex that incurs the lower cost will invest more heavily in their immune system and experience a higher rate of disease-induced mortality. If a female host increases her immune investment due to a lower reproductive cost, this reduces the pathogen's fitness in female hosts relative to male hosts. This puts selective pressure on the pathogen to increase its disease-induced mortality rate in female hosts, which in turn puts pressure on female hosts to further increase their immune investment. Eventually, this process will settle into a state where female hosts invest more heavily in their immune system and the pathogen exhibits a higher disease-induced mortality rate in female hosts. The same argument holds if male hosts instead pay the lower reproductive cost to immune investment, *mutatis mutandis*. This result echoes previous work that studied host or pathogen evolution in isolation. For example, [48] found that higher host immune investment can select for higher pathogen disease-induced mortality, while [29] found that higher pathogen disease-induced mortality can select for an increased host immune investment. Our work establishes these outcomes as possible endpoints for host and pathogen populations evolving in tandem.

When we include vertical transmission, we change the nature of the trade-off felt by female but not male hosts. For female hosts, immune investment now benefits both survival and fecundity, where before it could only benefit survival. For low rates of vertical transmission, we predict decreased female immune investment since this added benefit is not yet enough to outweigh the reproductive cost of immune investment. However, as the rate of vertical transmission increases, the reproductive benefit to female immune investment increases. There is then a threshold rate of vertical transmission past which female hosts will invest more in their immune system than male hosts. Such a pattern is noted in [29], but is described as a result of male immunity being more sensitive to changes in disease-induced mortality than female immunity. Here, we show that this outcome is not only a viable endpoint of selection via coevolution of both hosts and pathogens, but also that this can be obtained as a result of considering the effects of female reproduction. Furthermore, this prediction matches the trend seen in clinical studies across a wide range of infectious diseases, and provides a more complete evolutionary explanation for this trend if the disease is able to be vertically transmitted.

Ewald [69] discusses the idea that vertical transmission should shift a host-pathogen population away from parasitism and towards a state of mutualism, similar to how beneficial microbes can evolve to increase their own fitness through increasing their host's fitness [70]. Our results support this hypothesis in female hosts for sufficiently large rates of vertical transmission. In our model, vertical transmission offers an additional transmission route to pathogens in a female host, so that it would be a fitness benefit to the pathogen to reduce its level of disease-induced mortality in order to survive longer inside a female host. This is a trend that has been shown in previous work on non-sex-specific models [71] and non-coevolutionary sex-specific models [15]. A reduction in disease-induced mortality will also confer a fitness benefit to female hosts. However, our results also suggest that this shift towards mutualism can be disrupted by the effects of differential reproductive costs to immune investment between host sexes. In particular, if female hosts incur a significantly smaller reproductive cost to immune investment than male hosts, then evolution can maintain a parasitic relationship between pathogens and female hosts for low levels of vertical transmission.

Our results also have potential implications for public health and personalized medicine. First, selection favours higher levels of immune investment in both sexes as the vertical transmission rate grows. Second, regardless of which sex is investing more in their immune system or has a higher disease-induced mortality rate, we generally expect females to experience a lower level of case mortality than males. The sex-related difference in case mortality is most apparent in the presence of large rates of vertical transmission, but we only ever predict increased case mortality in females if they simultaneously incur a higher reproductive cost to immune investment and the rate of vertical transmission is low. Finally, the pattern of increased immune investment and decreased disease-induced mortality in female hosts could, in turn, explain the observed pattern of greater prevalence of autoimmune diseases in females [72, 73, 74]. If females mount a strong immune response even when a pathogen exhibits a relatively weak rate of disease-induced mortality, due to the presence of strong vertical transmission, then they may have a higher likelihood of mistakenly attacking their own cells instead of those of the pathogen. If this is the case, we can speculate based on our model that implementing policies aimed at reducing the rate of vertical transmission could lower the risk of autoimmune disease in females, while still maintaining a lower level of case mortality than in males. More broadly, our work contributes to a growing body of research (e.g., [24, 25, 26, 27, 15]) that shows that host sex is an important component of conversations on infectious diseases.

Chapter 3

Prophylactic Host Behaviour Discourages Pathogen Exploitation

3.1 Introduction

Mathematical study of infectious diseases has a long history that predates even the well-known contributions of [1] and [2]. Mathematical study of the evolution of pathogens, however, is relatively recent. One avenue of inquiry has explored the ways in which natural selection shapes the virulent effects pathogens inflict on their hosts. Models have provided insight into the ways in which various factors—such as parasite reproductive rates [75], host density [76], relatedness among co-infecting pathogen strains [43], and multiple types of hosts [17]—modulate the expressed level of virulence. A key prediction emerging from this body of work is that, in many cases, selection acts to maximize the basic reproduction number [10, 19], i.e., the expected number of new infections caused by a single infective host [3]. In particular, adaptive levels of pathogen virulence balance a trade-off between the average duration of infection and the rate of disease transmission [12, 8]. As disease transmission rates slow, then, standard theory predicts selection will respond by shaping virulence in a way that decreases the duration of infection.

Mathematics has also contributed to our understanding of the ways in which host traits impact the evolution of pathogen virulence. Here, models have explored the effects of co-evolution with innate host defences [19, 28], use of antibiotics [77], vaccines and vaccination behaviour [49, 50], and other social factors related to hosts themselves [78]. It is this last item—namely, the effect of host social behaviour on pathogen evolution—on which we focus our attention in this paper. [79] discusses the idea of a “behavioural immune system” that complements the standard physiological immune system in humans. This behavioural immune system is comprised of various prophylactic measures, such as social distancing (e.g., avoiding handshakes when greeting) or improved personal hygiene (e.g., hand washing), that individuals may adopt to reduce the likelihood of infection [79]. Importantly, individuals can start and stop these behaviours as often as desired (e.g., as in [33]), as opposed to measures like vaccination that are, in a sense, irreversible.

Unfortunately, little is known about how hosts’ behavioural immune system impacts the evolution of pathogens. What work has been done in this area predicts that prophylactic behaviour exhibited by hosts can select for higher pathogen virulence, assuming that the perceived severity is higher for the more virulent strain and that the prophylactic measures are more effective against the less virulent strain [33]. This work, however, considers short-term evolutionary outcomes only, and does not consider the effects on host behavioural changes of factors outside of social learning. In particular, the model of host behavioural dynamics in [33] does not account for all the ways in which host demographics and disease dynamics could affect the proportion of susceptible individuals engaging in prophylaxis. In order to assess additional risks posed by pathogen evolution, then, different models are required.

We devise a model that tightly couples changes in the host’s behavioural immune system, host demographics, and disease dynamics, in a way that allows us to make predictions about the long-term evolution of pathogen host exploitation. We focus on pathogen exploitation instead of virulence as we are considering sublethal disease effects and low-risk host behaviours (e.g., hand washing). An important aspect of the host behaviours studied here is the relation between the utility cost associated with engaging in that behaviour, which may take many different forms, and the benefit in terms of a reduced likelihood of pathogen transmission. A simple example would be more frequent hand washing, where an individual engaging in this behaviour will benefit from a lower risk of contracting the disease at the cost of some extra time out of their day and having to spend more money on soap than they would otherwise. Another, more compelling, example is social distancing, which again reduces disease transmission but can have much more severe social and economic costs as can be seen in the current COVID-19 pandemic [80]. We find that prophylactic behaviour uniformly reduces the pathogen's exploitation below the level expected in the absence of such behaviour. Furthermore, we argue that the driving force behind our result is the modified nature of the transmission-recovery trade-off faced by the pathogen as a result of the inclusion of host prophylactic behaviour.

3.2 Model

3.2.1 Disease Dynamics

We begin with a version of an endemic SIR model of infectious-disease dynamics [4] modified in a way that separates a host population of total size N into two groups. Individuals in group $i = 0$ are those who do not take prophylactic measures that limit (but do not completely prevent) disease transmission, whereas those in group $i = 1$ do take such measures. Individuals in each group are further subdivided according to their disease status. Let S_i, I_i, and R_i denote the number of individuals in group i who are susceptible to infection, infective, and recovered from infection, respectively.

We assume that transmission is frequency-dependent. This is a common assumption when modelling sexually transmitted diseases (STDs) since contacts between individuals in those cases are generally not the result of random mixing [81, 82]. While we are not considering STDs here, some prophylactic behaviours may create similar contact patterns within the population. For example, in the case of social distancing, individuals intentionally limit their contact with others, and adding more people to the population may not greatly affect the average contact rate. This would make frequency-dependent transmission a more appropriate model.

Each individual encounters another at a fixed rate and, given that an encounter is between a susceptible and an infective, the likelihood of disease transmission depends on the groups to which individuals belong. If β_{ij} denotes the product of the probability of disease transmission from a j-infective to an i-susceptible and the per-capita encounter rate, then $S_i\beta_{ij}I_j/N$ gives us the total rate at which new infections are created in group i. Infective individuals recover at a fixed per-capita rate, γ, independent of their group. As a result of recovery, individuals are imbued with life-long immunity to future infection. Since we are considering sublethal disease effects, we do not include disease-related mortality (virulence) in our model.

Individuals can also switch groups. For now, we use the constants τ_{ij}, ϕ_{ij} and η_{ij} to represent the per-capita rates at which susceptible, infective, and recovered individuals, respectively, switch from group j to i. We expand on the details surrounding group switching later. We can summarize the description above using a system of differential equations. Scaling time so that the background death rate is unity (i.e., one time unit is equivalent to the average lifetime of an individual in the population), and matching birth and death rates, we get

$$\frac{dS_0}{dt} = N - S_0\frac{\beta_{00}}{N}I_0 - S_0\frac{\beta_{01}}{N}I_1 - S_0 + \tau_{01}S_1 - \tau_{10}S_0 \tag{3.1a}$$

$$\frac{dS_1}{dt} = -S_1\frac{\beta_{10}}{N}I_0 - S_1\frac{\beta_{11}}{N}I_1 - S_1 - \tau_{01}S_1 + \tau_{10}S_0 \tag{3.1b}$$

$$\frac{dI_0}{dt} = S_0\frac{\beta_{00}}{N}I_0 + S_0\frac{\beta_{01}}{N}I_1 - (1+\gamma)I_0 + \phi_{01}I_1 - \phi_{10}I_0 \tag{3.1c}$$

$$\frac{dI_1}{dt} = S_1\frac{\beta_{10}}{N}I_0 + S_1\frac{\beta_{11}}{N}I_1 - (1+\gamma)I_1 - \phi_{01}I_1 + \phi_{10}I_0 \tag{3.1d}$$

$$\frac{dR_0}{dt} = \gamma I_0 - R_0 + \eta_{01}R_1 - \eta_{10}R_0 \tag{3.1e}$$

$$\frac{dR_1}{dt} = \gamma I_1 - R_1 - \eta_{01}R_1 + \eta_{10}R_0. \tag{3.1f}$$

Here, we make the assumption that all newborns enter the S_0 compartment. While realistically we might expect a fraction to enter the S_1 compartment (e.g., through cultural vertical transmission of prophylactic behaviours), the presence of the switching terms allows individuals in the S_0 compartment to immediately move into the S_1 compartment if they choose to do so, justifying our choice of modelling births as entering only the S_0 compartment.

Note that the differential equations in (3.1) sum to zero, and so total population size N is constant. This, along with the fact that group membership among recovered individuals is of no consequence, allows us to omit (3.1e) and (3.1f). We now use $u_i = S_i/N$ and $v_i = I_i/N$ to denote the fraction of susceptible and infective individuals, respectively, in group i. Similarly, we use $u = u_0 + u_1$ and $v = v_0 + v_1$ to denote the total fraction of susceptible and infective individuals, respectively. The dynamics of u and v can then be modelled by the following set of differential equations:

$$\frac{du}{dt} = 1 - \left[y(\beta_{01}(1-x) + \beta_{11}x) + (1-y)(\beta_{00}(1-x) + \beta_{10}x)\right] uv - u \tag{3.2a}$$

$$\frac{dv}{dt} = \left[y(\beta_{01}(1-x) + \beta_{11}x) + (1-y)(\beta_{00}(1-x) + \beta_{10}x)\right] uv - (1+\gamma)v. \tag{3.2b}$$

We also track the fraction of susceptible and infected individuals taking prophylactic measures using $x = u_1/u$ and $y = v_1/v$, respectively. Given this definition of x, we can derive the following differential equation to describe how the proportion of susceptible individuals engaging in prophylaxis changes due to various factors:

$$\frac{dx}{dt} = -\overbrace{\frac{x}{u}}^{\text{births}} \overbrace{-\tau_{01}x + \tau_{10}(1-x)}^{\text{group switching}} + \overbrace{(\beta_{00}(1-y)v + \beta_{01}yv)(1-x)x}^{\text{infection of hosts not engaged in prophylaxis}} - \underbrace{(\beta_{10}(1-y)v + \beta_{11}yv)x(1-x)}_{\text{infection of hosts engaged in prophylaxis}}. \tag{3.2c}$$

The first term represents the fact that births increase the pool of individuals not engaging in prophylactic measures, which in turn reduces the relative proportion of susceptible individuals engaging in prophylactic measures. The τ_{ij} terms capture the effects of susceptible individuals switching between engaging and not engaging in prophylaxis. The final two terms correspond to infection. In one case, infection reduces the pool of individuals not engaging in prophylaxis and subsequently increases the relative proportion of individuals engaging in prophylaxis. Conversely, the proportion of susceptible individuals engaging in prophylaxis is directly reduced by infection of these individuals. Similarly, we can define the differential equation for y as:

$$\frac{dy}{dt} = -\overbrace{\phi_{01}y + \phi_{10}(1-y)}^{\text{group switching}} - \overbrace{(\beta_{00}(1-y) + \beta_{01}y)(1-x)uy}^{\text{infection of hosts not engaged in prophylaxis}} + \underbrace{(\beta_{10}(1-y) + \beta_{11}y)xu(1-y)}_{\text{infection of hosts engaged in prophylaxis}}. \tag{3.2d}$$

The first term represents the effects of infective individuals switching between engaging and not engaging in prophylaxis. The latter two terms correspond to infection in the same vein as in equation (3.2c).

Equations (3.2c) and (3.2d) capture dynamic features of the proportion of hosts engaged in prophylaxis not found in previous work. The switching terms in the modelling undertaken by [33] account for utility costs and benefits of prophylaxis, but neglect changes due to demographics (births) and infection. Our equations, therefore, combine multiple processes to establish a more realistic model of changing host behaviour.

We now return to the issue of group switching and the details surrounding the switching terms τ_{ij} and ϕ_{ij}, ultimately replacing these constants with functions of x, y, and v. Individuals do not always adhere to beneficial measures such as taking medications [83], exercise regimes [84], or dietary restrictions [85], so we include group switching in our model to account for these types of effects. Following [33], we use the replicator dynamic [34] to model the total rate at which individuals move from one group to another. We assume that the decision to switch groups is driven by utility, as discussed in [86]. Specifically, an individual's utility will be determined by their risk of infection less the utility cost of taking prophylactic measures. For an i-susceptible, the risk of infection it faces will be quantified by the force of infection,

$$\sum_j -\frac{\beta_{ij}I_j}{N} = -\left(\beta_{i0}(1-y) + \beta_{i1}y\right)v.$$

Consequently, the utility of a susceptible individual adopting prophylactic measures is

$$-\left(\beta_{10}(1-y)+\beta_{11}y\right)v-\chi$$

where χ is the utility cost to engaging in prophylaxis. Infective individuals have no risk of infection, so they only pay the utility cost of the prophylactic measure should they choose to engage in it. Thus, $-\chi$ represents the utility of an infective individual engaging in prophylaxis. A susceptible (resp. infective) individual will then choose to switch into a given group when the utility of an individual in that group exceeds the utility of the average susceptible (resp. infective) in the population. This replicator-dynamics model of switching gives us

$$-\tau_{01}x+\tau_{10}(1-x)=kx(1-x)[y(\beta_{01}-\beta_{11})+(1-y)(\beta_{00}-\beta_{10})]v-k\chi x \tag{3.3}$$

and

$$-\phi_{01}y+\phi_{10}(1-y)=-k\chi y \tag{3.4}$$

where k is a constant that reflects the rate at which individuals change their behaviour based on the behaviour of others in the population (see Appendix B for a more detailed derivation of equations 3.3 and 3.4). We note that our model of switching makes the simplification (made in [33]) of assuming individuals have up-to-date information about the global state of the population. Our final model of disease dynamics can now be stated as,

$$\frac{du}{dt}=1-\left[y(\beta_{01}(1-x)+\beta_{11}x)+(1-y)(\beta_{00}(1-x)+\beta_{10}x)\right]uv-u \tag{3.5a}$$

$$\frac{dv}{dt}=\left[y(\beta_{01}(1-x)+\beta_{11}x)+(1-y)(\beta_{00}(1-x)+\beta_{10}x)\right]uv-(1+\gamma)v \tag{3.5b}$$

$$\frac{dx}{dt}=\frac{-x}{u}+(k+1)x(1-x)\left[y(\beta_{01}-\beta_{11})+(1-y)(\beta_{00}-\beta_{10})\right]v-k\chi x \tag{3.5c}$$

$$\frac{dy}{dt}=-\left[y(\beta_{01}(1-x)y-\beta_{11}x(1-y))+(1-y)(\beta_{00}(1-x)y-\beta_{10}x(1-y))\right]u-k\chi y. \tag{3.5d}$$

A sample trajectory of this system is shown in figure 3.1, panel A.

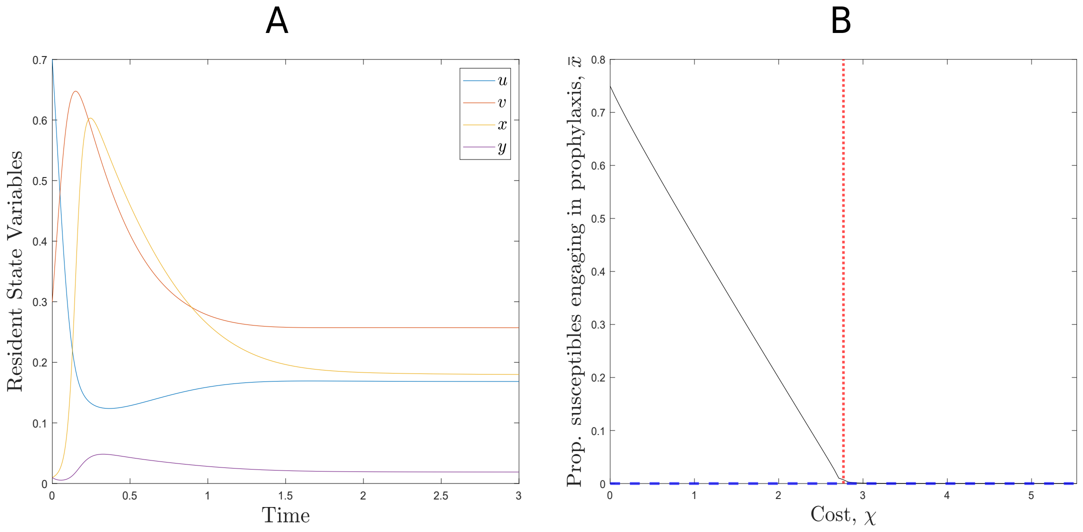

Figure 3.1: Panel A shows a sample trajectory for the resident system (3.5). As described in the main text, time has been rescaled so that one time unit is equivalent to the average lifetime of an individual in the population. Panel B shows a bifurcation plot indicating the cost threshold (dotted red line) at which the endemic equilibrium without prophylaxis (dashed blue line) and the endemic equilibrium with prophylaxis (solid black line) undergo an exchange of stability. Parameter values are: $\kappa = 5, \beta_{\max} = 70.4721, k = 5.1745$, and $\varepsilon = 0.5951$. The initial condition used in panel A was: $u = 0.7$, $v = 0.3$, $x = 0.01$, and $y = 0.01$.

Note that, if no individual in the population takes prophylactic measures, then $x = y = 0$ and we recover the standard endemic SIR model (Appendix C). When some fraction of the population takes prophylactic measures, however, standard predictions of the SIR model may or may not hold. The linear stability analysis presented in Appendix C shows that the endemic equilibrium without individuals engaging in prophylaxis remains stable as long as

$$\chi > \mathcal{R}_0 - \left(\frac{k+1}{k}\right)\left(\frac{\beta_{10}}{\beta_{00}}(\mathcal{R}_0 - 1) + 1\right) \triangleq \chi_c, \tag{3.6}$$

where $\mathcal{R}_0 = \beta_{00}/(1+\gamma)$ is the basic reproductive number [3] of the system in the absence of prophylactic measures. Below this threshold, the cost to taking prophylactic measures is low enough that the system moves towards a new endemic equilibrium $(\hat{u}, \hat{v}, \hat{x}, \hat{y})$ at which some non-zero fractions of susceptible and infective individuals adopt prophylactic measures (figure 3.1, panel B). It is this new endemic equilibrium that will frame the evolutionary model we pursue in the next section.

3.2.2 Evolutionary Dynamics

We consider the evolution of the level of pathogen exploitation of its host, denoted $\xi > 0$. Exploitation affects disease transmission, with a greater ξ value corresponding to a greater β_{ij}. To reflect this, we now write $\beta_{ij}(\xi)$ where

$$\beta_{ij}(\xi) = \frac{\beta_{\max}(1-\varepsilon)^{i+j}\xi}{\kappa+\xi}. \tag{3.7}$$

In words, we are treating β_{ij} as an increasing function of ξ that saturates at a value of $\beta_{\max}(1-\varepsilon)^{i+j}$, where ε is the probability that the prophylactic measures prevent disease transmission. We assume that prophylactic measures taken by individuals fail independently, so $(1-\varepsilon)^2$ gives the probability that the disease is transmitted between two individuals engaging in prophylaxis. The rate at which transmission saturates is controlled by $\kappa > 0$, with larger values of this constant corresponding to a reduced rate of saturation.

Exploitation also affects recovery. To reflect this assumption, we write $\gamma(\xi)$, where $\gamma(\xi) = c\xi$ for a constant c with units of inverse time (the exploitation level ξ is dimensionless). Without loss of generality, we take $c = 1$. Here, increased exploitation acts to reduce the expected duration $1/(1+\gamma(\xi))$ of an infection. This penalty of larger ξ, then, trades off against the transmissibility benefits described above. Previous authors have either assumed (or shown) that such trade-offs exist, though they are often mediated by disease-related mortality [10, 13, 11] or viral load [14]. Here, we follow [15] and [16] by assuming the trade-off faced by the pathogen involves recovery. For example, through increased viral load making it more likely that the pathogen is detected by the host's immune system, or increased exploitation leading to more antigens presented on the surfaces of target cells.

We use an adaptive dynamics approach to model the evolution of pathogen exploitation under the primary influence of natural selection ([5, 6, 7]; and see [19, 15, 30] for examples specifically related to virulence evolution). We introduce a rare mutant pathogen with exploitation trait ξ_m into a resident pathogen population with exploitation trait ξ. It is assumed that the resident system has reached equilibrium prior to introducing the mutant, that there is no co-infection, and that the prophylactic measures are equally effective at preventing transmission of both strains.

Let v_m denote the fraction of individuals in the population infected with the mutant strain. While the mutant is rare, its dynamics are well approximated by

$$\begin{aligned}\frac{dv_m}{dt} = [y_m(\beta_{01}(\xi_m)(1-\bar{x}) + \beta_{11}(\xi_m)\bar{x}) + (1-y_m)(\beta_{00}(\xi_m)(1-\bar{x}) + \beta_{10}(\xi_m)\bar{x})]\bar{u}v_m \\ - (1+\gamma(\xi_m))v_m, \quad (3.8a)\end{aligned}$$

where overbars denote equilibrium values of the respective variables. As we do with the resident population, we can also track the proportion of individuals infected with the mutant strain engaging in prophylaxis. Denoting this proportion by y_m, we can describe its dynamics by

$$\begin{aligned}\frac{dy_m}{dt} = -[y_m(\beta_{01}(\xi_m)(1-\bar{x})y_m - \beta_{11}(\xi_m)\bar{x}(1-y_m)) \\ + (1-y_m)(\beta_{00}(\xi_m)(1-\bar{x})y_m - \beta_{10}(\xi_m)\bar{x}(1-y_m))]\bar{u} - k\chi y_m. \quad (3.8b)\end{aligned}$$

If the mutant strain becomes common and the mutant-free equilibrium becomes unstable, we say that the mutant has successfully invaded the resident population. Provided the system is sufficiently close to an evolutionarily steady state, a mutant who successfully invades will become the new resident [5].

Since v_m does not appear in (3.8b), we can first solve for the equilibrium value $\bar{y}_m$ of y_m, substitute that value into (3.8a), and study (3.8a) alone. If the right-hand side of (3.8a) is positive (resp. negative), the mutant invades (resp. is eliminated) because it is favoured (resp. disfavoured) by natural selection. The sign of the right-hand side of (3.8a) is the same as the sign of the difference between

$$W(\xi_m, \xi) = \frac{\beta_{\text{avg}}(\xi_m, \xi)\, \bar{u}(\xi)}{1 + \gamma(\xi_m)} \tag{3.9}$$

and unity, where

$$\beta_{\text{avg}}(\xi_m, \xi) = \begin{bmatrix} 1 - \bar{x}(\xi) & \bar{x}(\xi) \end{bmatrix} \begin{bmatrix} \beta_{00}(\xi_m) & \beta_{01}(\xi_m) \\ \beta_{10}(\xi_m) & \beta_{11}(\xi_m) \end{bmatrix} \begin{bmatrix} 1 - \bar{y}_m(\xi_m) \\ \bar{y}_m(\xi_m) \end{bmatrix}$$

represents an average transmission rate taking into account the different groups of susceptible and infective individuals. W then has a clear biological interpretation, made in previous work [19], in terms of the basic reproductive number of the mutant strain. In particular, an infection with the mutant strain lasts an average of $1/(1 + \gamma)$ time units and an average of $\beta_{\text{avg}}\bar{u}$ new infections are created during this time. If this quantity is larger than one (resp. smaller than one), then the mutant population will grow (resp. shrink). Writing W as we have done in equation (3.9) also highlights the transmission-recovery trade-off described above, captured through the β_{avg} and γ terms. Through the $\bar{y}_m$ terms, the pathogen is also able to influence whether a new infection occurs in an individual engaging or not engaging in prophylaxis. We can, therefore, use W as an invasion fitness function in the adaptive dynamics analysis, even though the derivation of the function proceeded in a non-standard way.

Following the discussion above, the direction of evolution of ξ that is favoured by natural selection is given by the sign of $\partial W/\partial \xi_m|_{\xi_m=\xi}$. Consequently, the selective process is at equilibrium whenever $\xi = \bar{\xi}$ where $\bar{\xi}$ satisfies

$$\left.\frac{\partial W}{\partial \xi_m}\right|_{\xi_m=\xi=\bar{\xi}} = 0. \tag{3.10}$$

An equilibrium value $\bar{\xi}$, i.e., one that satisfies condition (3.10), may or may not be stable. If the equilibrium value $\bar{\xi}$ attracts nearby resident populations, then

$$\frac{d}{d\xi}\left[\left.\frac{\partial W}{\partial \xi_m}\right|_{\xi_m=\xi}\right]_{\xi=\bar{\xi}} \leq 0 \tag{3.11}$$

and we say that $\bar{\xi}$ is convergence stable [21]. If the equilibrium $\bar{\xi}$ resists invasion from nearby mutants, then

$$\left.\frac{\partial^2 W}{\partial \xi_m^2}\right|_{\xi_m=\xi=\bar{\xi}} \leq 0 \tag{3.12}$$

and we say that $\bar{\xi}$ is evolutionarily stable (sensu [20]). A sufficient condition for either type of stability is obtained by replacing the weak inequality with a strict one. It is the strict sufficient versions that we use here. When $\bar{\xi}$ is both convergence stable and evolutionarily stable, we say it is a continuously stable strategy (CSS) [22].

3.3 Results

3.3.1 Simple Cases

There are two special cases that can be analyzed with relative ease. The first special case assumes the cost of prophylaxis exceeds the threshold χ_c. In this case, no one in a population supporting the resident endemic disease is adopting prophylactic measures and so $\bar{x} = \bar{y} = 0$. The equilibrium value of y_m can be shown to be $\bar{y}_m = 0$ (see Appendix D) and so the fitness function simplifies to

$$W(\xi_m, \xi) = \frac{\beta_{00}(\xi_m)\bar{u}(\xi)}{1 + \gamma(\xi_m)} = \frac{\mathcal{R}_0(\xi_m)}{\mathcal{R}_0(\xi)}. \tag{3.13}$$

The mutant strain is then able to invade (resp. is eliminated) if $W(\xi_m, \xi)$ exceeds (resp. is less than) unity; equivalently, if $\mathcal{R}_0(\xi_m)$ exceeds or is less than $\mathcal{R}_0(\xi)$. More importantly, the CSS level of exploitation, $\bar{\xi}$, will maximize $\mathcal{R}_0(\xi)$ and so $\bar{\xi} = \sqrt{\kappa}$. This will serve as a benchmark against which more general results will be compared.

The second special case assumes that prophylactic measures are cost-free, i.e., $\chi = 0$. Since

$\chi < \chi_c$, the system moves towards an endemic equilibrium where some non-zero proportions of susceptible and infective individuals are engaging in prophylaxis. While the replicator dynamics predict that all individuals will begin adopting prophylactic measures in the absence of cost, the terms noted in equations (3.2c) and (3.2d) relating to demographics and disease dynamics counteract this effect. This will result in the evolution of intermediate levels of the proportions of susceptible and infective individuals engaging in prophylaxis. Under the assumption of zero cost, the distribution of the mutant strain, captured by $\bar{y}_m$, does not depend on the mutant exploitation level and so the pathogen is not able to influence whether new infections occur in individuals engaging or not engaging in prophylaxis. In this case, the selection gradient simplifies and results in a CSS of $\bar{\xi} = \sqrt{\kappa}$ (see Appendix D). This is the same result as the benchmark established in our first special case, despite the presence of individuals taking prophylactic measures. Absence of cost, it seems, decouples the pathogen's evolution from the evolution of host behaviour due to the pathogen no longer being able to influence the relative proportions of infections in individuals engaged or not engaged in prophylaxis.

3.3.2 Evolution Near the Critical Cost

In general, the model cannot be explored analytically. However, there are certain analytical results we can derive for cost values other than those discussed in the previous section. In particular, we can show that for any cost value, there is a unique stable equilibrium value of y_m on the interval $[0, 1]$. Moreover, we can show that the derivative of this equilibrium value with respect to the mutant exploitation ξ_m is always positive, and that this complicates the relationship between pathogen exploitation and transmissibility (see Appendix E for a derivation of these results). This leads to a change in the evolutionarily stable level of pathogen exploitation away from that which would be expected in the absence of prophylaxis.

If we are near the critical cost χ_c we can derive quasi-analytic results to predict the direction of this change in the CSS value of ξ. When the cost χ is slightly below its critical threshold χ_c, we can approximate the CSS exploitation level as $\bar{\xi} \approx \sqrt{\kappa} + \sigma(\chi - \chi_c)$ where $\chi - \chi_c < 0$ and σ

is a constant such that

$$\sigma \propto -\frac{\partial}{\partial \bar{x}}\left[\left.\frac{\partial W}{\partial \xi_m}\right|_{\xi_m=\xi}\right]_{\substack{\chi\,=\,\chi_c \\ \xi\,=\,\sqrt{\kappa}}}\ . \tag{3.14}$$

If σ is positive (resp. negative), then $\bar{\xi}$ is below (resp. above) the benchmark value of $\sqrt{\kappa}$. As equation (3.14) shows, whether we are above or below this benchmark depends on how small changes in cost lead to small changes in the proportion of susceptible individuals engaged in prophylaxis which, in turn, lead to changes in the selection gradient acting on exploitation (see Appendix F for a derivation of equation 3.14).

We can show with a quasi-analytic approach that equation (3.14) is always positive. Our evidence relies on first choosing feasible values of our parameters. In particular, we need $\mathcal{R}_0 > 1$. If $\mathcal{R}_0 > 1$, then we need also to choose the probability $\varepsilon > \frac{1}{k+1}\frac{\mathcal{R}_0}{\mathcal{R}_0-1}$, thus ensuring that $\chi_c > 0$. To ensure that $\varepsilon < 1$, we then need to choose $k > \frac{1}{\mathcal{R}_0-1}$.

Using feasible parameters and working to zeroth order in $\chi - \chi_c$, we use the computer algebra software (CAS) Maple (version 2019.1) to investigate the sign of σ as described in equation (3.14). We find that the requirement that $\mathcal{R}_0 > 1$ necessarily restricts our choices of maximal transmissibility, $\beta_{\max}$, to values that lie above the curve traced out by $(1+\sqrt{\kappa})^2$ (figure 3.2, panel A). The CAS shows that nullclines of the partial derivative in (3.14) never exceed the $(1+\sqrt{\kappa})^2$ curve for the wide range of feasible parameters we investigated (figure 3.2, panel B). Thus, the sign of σ does not change provided the $\mathcal{R}_0 > 1$ restriction is met. Moreover, test points show that the sign of σ itself is positive when feasible model parameters are chosen. Based on CAS investigations described in Appendix G, then, we conclude that, just below the critical cost, selection acts to reduce the CSS level of host exploitation exhibited by the pathogen.

3.3.3 Evolution for Arbitrary Cost

Our results can be extended numerically for costs that are possibly much smaller than the critical value, χ_c, using a Matlab (version R2019a) procedure available on the GitHub repos-

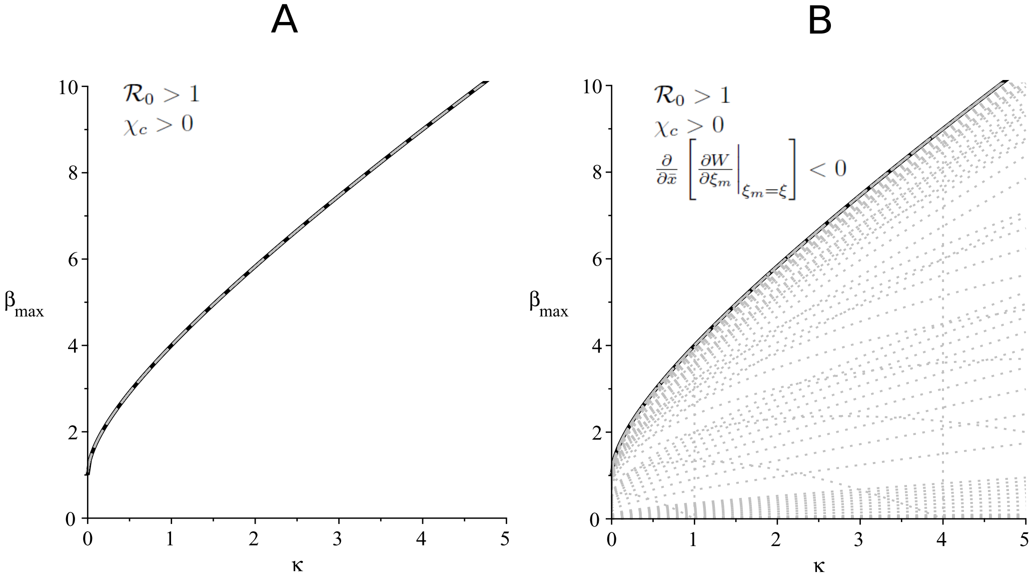

Figure 3.2: Panel A shows the curve $\chi_c = 0$ (dashed grey) overlaying the curve $\mathcal{R}_0 = 1$ (solid black), and the region of parameter space where $\chi_c > 0$ and $\mathcal{R}_0 > 1$. Dotted grey curves represent the roots of the partial derivative on the right-hand side of equation (3.14) and panel B shows that these all occur on or below the black and dashed grey curves (note that vertical dotted grey lines are an artifact of jump discontinuities). Choosing parameter values in the region above the curves in panel A results in the partial derivative on the right-hand side of equation (3.14) being negative, as noted in panel B. The implication is that the parameter σ is positive and so pathogen exploitation will decrease relative to the benchmark level of $\sqrt{\kappa}$ close to the cost threshold χ_c.

itory at `https://github.com/evanjmitchell/doctoral-thesis`. We build the procedure around the observation that locally asymptotically stable equilibrium solutions to $d\xi/dt = (\partial W/\partial \xi_m)|_{\xi_m=\xi}$ are also convergence-stable evolutionary equilibria as defined by conditions (3.10) and (3.11), respectively. As a result, numerical iteration of this differential equation can be used to find candidate CSS strategies. The evolutionary stability of candidate CSS strategies can be confirmed with a centred finite-difference approximation of (3.12). Since the error is on the order of the square of the distance between ξ values used in the approximation, we consider any value within this error to satisfy the ESS condition (3.12).

The results of our numerical procedure confirm that the benchmark CSS level of $\bar{\xi} = \sqrt{\kappa}$ is obtained when $\chi = 0$ and $\chi = \chi_c$. Second, numerical results confirm the reduction in the CSS level of pathogen exploitation for χ slightly smaller than χ_c. Third, and most important, numerical results indicate that the CSS exploitation level $\bar{\xi}$ changes in a simple way as cost is reduced from its critical value to its natural lower limit at zero (figure 3.3). In particular, as cost is reduced $\bar{\xi}$ decreases monotonically from the benchmark value until it reaches a minimum. Once at the minimum, the direction of selection changes and $\bar{\xi}$ increases monotonically, ultimately returning to the benchmark when cost disappears.

This pattern holds for a wide range of parameter values chosen to satisfy the conditions described in the previous section. Specifically, we investigate four different values of κ: $\kappa = 0.1$, $\kappa = 1$, $\kappa = 10$, and $\kappa = 100$. For each of these values, we choose five values of $\beta_{\max}$ above the $(1 + \sqrt{\kappa})^2$ threshold: $\beta_{\max} = (1 + \sqrt{\kappa})^2 + 5$, $\beta_{\max} = (1 + \sqrt{\kappa})^2 + 10$, $\beta_{\max} = (1 + \sqrt{\kappa})^2 + 50$, $\beta_{\max} = (1 + \sqrt{\kappa})^2 + 100$, and $\beta_{\max} = (1 + \sqrt{\kappa})^2 + 500$. We then choose five values of k ($k = 1/(\mathcal{R}_0 - 1) + 5$, $k = 1/(\mathcal{R}_0 - 1) + 10$, $k = 1/(\mathcal{R}_0 - 1) + 50$, $k = 1/(\mathcal{R}_0 - 1) + 100$, and $k = 1/(\mathcal{R}_0 - 1) + 500$) and five values of ε spread evenly between the threshold $\mathcal{R}_0/((k+1)(\mathcal{R}_0 - 1))$ and 1, for a total of 500 combinations of parameter values.

Although the decline in the CSS value of exploitation shown in figure 3.3 appears modest, recall that one time unit is equivalent to the average lifetime of an individual in the population. This means that the change in the duration of infection as $\bar{\xi}$ changes is on the order of years. For

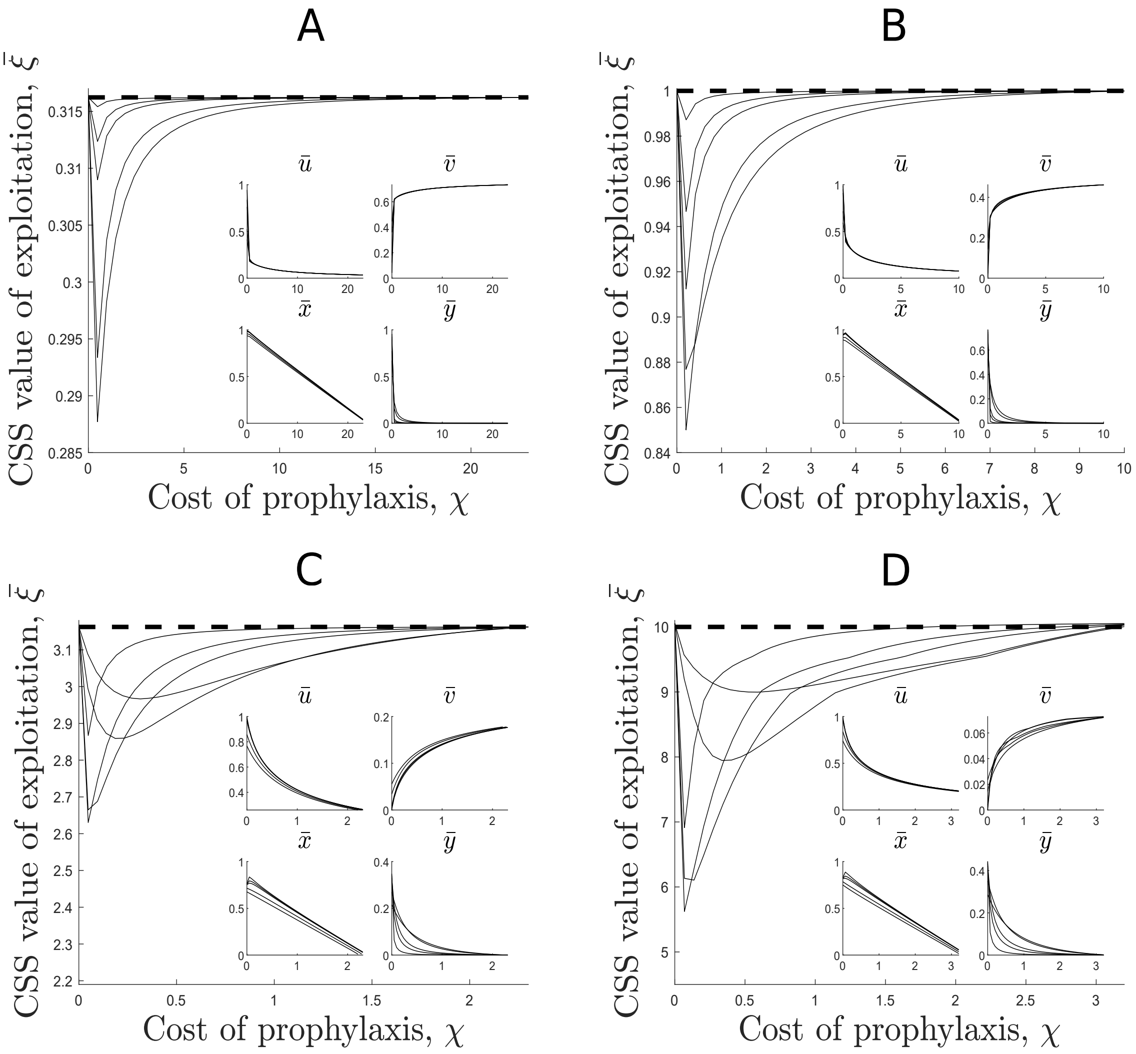

Figure 3.3: Plots of the CSS level of pathogen exploitation found using the numerical procedure described in the main text. Panel A contains sample results for $\kappa = 0.1$, panel B for $\kappa = 1$, panel C for $\kappa = 10$, and panel D for $\kappa = 100$. Inset figures show the equilibrium values of the epidemiological variables u, v, x, and y. The cost values presented are all below the critical cost threshold χ_c. In all cases, the CSS level of exploitation is lower than the benchmark value $\bar{\xi} = \sqrt{\kappa}$, plotted as a dashed black line, observed in the absence of prophylaxis.

example, if the average lifespan of an individual in the population is 79 years, then a decrease from $\bar{\xi} = 1$ to $\bar{\xi} = 0.86$ (as seen in figure 3.3, panel B) corresponds to an increase in the duration of infection of approximately three years.

3.4 Discussion

We study the impact of measures taken by hosts to limit disease transmission. Here, the willingness among hosts to engage in these prophylactic behaviours responds to changing utility costs and benefits. We focus on long-term evolution of a pathogen, defined by successive mutations until an equilibrium state is reached [86], alongside the rapid evolution of host behaviour. We find that when prophylactic behaviour among hosts occurs, pathogen host exploitation is always lower than it is in the absence of prophylaxis. Moreover, we find that stable exploitation is lowest for an intermediate frequency of prophylactic behaviour among hosts (indirectly, intermediate cost of prophylaxis).

This study contributes to the growing body of work that shows host behaviour, in general, influences pathogen evolution. Much of this work has considered vaccination behaviour, in particular, and has described both beneficial and detrimental evolutionary outcomes. In the case of human papillomavirus (HPV), for example, theoretical work predicted HPV vaccination will select for higher levels of virulence [50]. By contrast, empirical evidence suggests that vaccination can actually limit the ecological opportunity open to certain HPV types [87]. In keeping with the mixed nature of results, [51, 52] find that the direction of selection acting on pathogen virulence depends on the mechanism by which vaccination works.

More closely related to the current study are the conclusions of [33]. They show that host prophylactic behaviour in response to an endemic disease can allow for the invasion of a pathogen strain that is more virulent than the resident, and that the conditions for such a result are an increased perceived severity for the more virulent strain and more effective prophylactic measures against the less virulent strain. While our model considers sublethal disease effects and does not explicitly include virulence, the positive relationship between pathogen exploitation and virulence allows us to predict that such an outcome cannot occur in our model. This is a result of the fact that our benchmark result, established in the absence of prophylactic behaviour, is our worst case scenario. For example, consider a mutant pathogen with an exploitation level $\xi > \sqrt{\kappa}$. When the cost is above its critical value so that no one is engaging in prophylaxis, then this mutant cannot invade a resident population at the CSS $\bar{\xi} = \sqrt{\kappa}$. If we then decrease the cost below its critical value so that individuals begin to take prophylactic measures, the CSS exploitation level decreases away from $\bar{\xi} = \sqrt{\kappa}$ and so the mutant is still unable to invade the resident population.

The discrepancy between our prediction and those of [33] is due to the differences in how we model the dynamics of host behaviour. In addition to looking at actual risk instead of perceived risk (as in [33]), the evolution of host behaviour in our work is not governed solely by the replicator dynamics. Our model consists of additional terms to represent the effects of births and infection on the proportion of individuals engaging in prophylactic behaviour. Moreover, we track the proportion of infective individuals taking prophylactic measures, which adds an extra layer of complexity to the relationship between pathogen exploitation and transmissibility (Appendix E). These key differences are missing from previous work [33] and lead us to the conclusion that, for all feasible sets of parameter values, we expect a decrease in pathogen exploitation away from the benchmark value found in the absence of prophylactic behaviour. To obtain a more direct comparison to previous work, future iterations of our model should explicitly include virulence and explore the subsequent predictions on pathogen evolution.

To get some intuition into the decrease in exploitation that we find in this paper, we need to understand two things. In the absence of prophylaxis, standard theory (e.g., [19, 15, 16]) predicts that increased pathogen exploitation results in a decrease in the duration of infection and an increase in transmission, leading to a balance between these two competing effects at evolutionary equilibrium. In our model, increasing exploitation still reduces the duration of infection, but it affects transmission in a more complicated way. This more complicated effect on tranmissibility disrupts the balance that would be achieved in standard models. As we show in Appendix E, there is a benefit to increased exploitation through a direct increase in transmission, but also a marginal cost through increased exposure to the host behavioural immune system. In fact, the marginal cost is indirect as it results in fewer mutant infections in hosts not engaging in prophylaxis (i.e., smaller $1 - \bar{y}_m$). Ultimately, this added cost tips the scales in favour of lower pathogen exploitation.

We have already pointed to specific differences between our work and similar work of others [33]. While those differences will undoubtedly affect the model predictions, the intuition developed above suggests a more concrete explanation for the contrast is possible. In particular, [33] do not expose mutant infectives to host prophylactic behaviour in a way that differs from resident infectives. Granted, [33] do allow for the efficacy of prophylaxis to differ between resident and mutant strains, but the host landscape looks the same from both resident and mutant perspectives in that model. In our model, mutant infections in individuals engaging in prophylaxis happen in different proportions than resident infections (i.e., $\bar{y}_m \neq \bar{y}$ in general). Simply put, the host landscape in our model differs meaningfully between resident and mutant infectives.

Arguably, our main result is reminiscent of other pathogens that control host behaviour for their own gain. While our model pathogens are not directly controlling hosts like the pathogen *Ophiocordyceps unilateralis* does with the ant *Camponotus leonardi* [88] (or *Schistocephalus solidus* with the stickleback fish *Gasterosteus aculeatus* [89], or *Leucochloridium paradoxum* with the snail *Succinea putris* [90]), one might speculate that ours indirectly manipulate the hosts' economic agency. This suggests that there may be some cryptic parasite manipulation to further investigate.

As with any modelling endeavour, we have made some simplifying assumptions to reduce the mathematical complexity of our model. For example, we have assumed that individuals instantly update their behaviour when receiving new information about the progression of the disease. In reality, there is a time delay between receiving information and deciding to modify behaviour. Previous work has studied the effects of including a delay in the form of waning immunity either independently [91] or together with a delay in the form of a latent period following infection [92], and found that this can create periodicity in the model solutions. Other work has also investigated the effects of these delays on effective vaccination strategies [93]. Future work could extend our model to include the lag in information gain and behaviour modification, with the expectation that this would cause oscillations in the predicted exploitation level.

One could also relax the assumption that individuals sample from all other individuals in the population when deciding whether or not to take prophylactic measures. Epidemic models have previously been extended to include spatial structure through the use of networks, with different types of networks providing qualitatively different predictions [94]. Others have studied the interaction between network models and host heterogeneities in the case of sexually transmitted diseases [95], and the effects of adaptive networks where individuals may build and sever connections during the progression of a disease [96]. Networks could be incorporated here to explore the decoupling of social interactions related to disease transmission and those related to information transmission. Based on previous work [97], it is expected that this decoupling could lead to a lower level of pathogen exploitation.

It is tempting to use our evolutionary predictions to inform public-health policy. While pathogen exploitation does reach a minimum value for an intermediate level of cost of prophylaxis, our results (figure 3.3) also show that lowering the cost even farther below this level leads to fewer infections even if those infections are from a more exploitative pathogen strain. Moreover, the pathogen's exploitation is always below the level predicted in the absence of individuals engaging in prophylactic behaviour. There is a balance, then, between the level of cost that is optimal for minimizing prevalence and the level optimal for minimizing pathogen exploitation. It is important to recognize that efforts to minimize the cost of prophylaxis will result in a pathogen strain that is more exploitative of its host than it otherwise might be. More broadly, our work suggests that conversations about disease management and infection should be more inclusive towards the effects of human behaviour.

Chapter 4

Cooperation between Related Coinfecting Pathogen Strains in Multiple Types of Hosts

4.1 Introduction

A theoretical framework was presented in [43] for studying the evolution of disease-induced mortality among groups of coinfecting pathogen strains. This framework has its underpinnings in the Price equation [98, 99], and links tools from evolutionary game theory and kin selection theory in an epidemiological setting. Starting with a definition of fitness as the basic reproductive number $\mathcal{R}_0$ [3] of a focal pathogen strain, the disease-induced mortality rates of both the focal pathogen and its group are assumed to depend on the genotype of the individual pathogen strains [43, 44]. From this interpretation, the evolutionary equilibrium level of disease-induced mortality of a focal pathogen strain will depend on its genetic relatedness to its coinfecting group. The more related is a group of coinfecting pathogens, the greater is the incentive to reduce their individual disease-induced mortality rate to prolong the duration of infection of the whole group [43]. However, this framework is only developed in epidemiological models with a single type of host. How do these ideas extend to situations where multiple types of hosts are present, in which fitness is not defined in such a straightforward way?

Analyses of models with multiple types of hosts usually follow an adaptive-dynamics approach [5, 6, 7]. A resident host-pathogen system is assumed to have reached an equilibrium state, after which a mutant pathogen strain is introduced and tracked in the population. The fitness of this mutant strain can be defined as the instantaneous growth rate of the host population infected with the mutant strain [17] or, equivalently, as the basic reproductive number [3] of the mutant strain, which must take into account all types of hosts and is defined as the dominant eigenvalue of the next-generation matrix [17, 30, 31, 32]. Fitness is then maximized within each type of host, striking a balance between the pathogen's rate of transmission and its duration of infection [17].

Here, we investigate how these tools and ideas on pathogen evolution in multiple types of hosts connect to those from kin selection theory discussed in a single-host setting in [43, 44]. To do this, we present a theoretical framework for studying the evolution of disease-induced mortality among groups of related coinfecting pathogen strains in multiple types of hosts (e.g., females and males; large and small; juveniles, young adults, and adults). We discuss how fitness can be defined as either the instantaneous growth rate of a focal pathogen lineage or as the basic reproductive number $\mathcal{R}_0$ [3] of that focal lineage, and establish the equivalence between these two measures. We then study how the inclusion of genetic relatedness [43, 44] affects fitness and provide a biological interpretation of the resulting evolutionary equilibrium conditions. In general, we find that pathogens must balance the direct individual and indirect group benefits of increased transmission against the associated direct individual and indirect group costs of shorter duration of infection, within each type of host. This reflects the ideas of Hamilton [45] that greater relatedness should push for greater cooperation among a group of individuals.

Following the presentation of the theoretical framework, we work through two examples to illustrate using these ideas in practice. The first example considers a model of an infectious disease circulating in a population of juvenile and adult hosts. The second example extends the framework to a model in which hosts coevolve with pathogens, in the setting of a sexually transmitted infection circulating in a population of female and male hosts. We then conclude with some summarizing remarks.

4.2 Theoretical Framework

Suppose we have a population of hosts categorized into n different types. Hosts are further classified according to their disease status. Individual hosts are infected by a group of pathogens made up of various genetically related strains. The disease-induced mortality rate of an individual pathogen strain will be expressed as a vector $\boldsymbol{\alpha}$, where each element α_i represents the pathogen's disease-induced mortality rate in a host of type i. The average disease-induced mortality rate of a group of infecting pathogens will be expressed as a vector $\boldsymbol{\alpha}_g$, where each element α_{g_i} represents the average disease-induced mortality rate of a group of pathogens infecting a host of type i. In what follows, we assume that pathogens face a trade-off between transmission and disease-induced mortality, whereby increased disease-induced mortality will result in increased transmission but also a decreased duration of infection. This is a common trade-off modelled by other authors in the case of multiple pathogen strains [43], coevolution with hosts [28, 19], and vector-transmitted diseases [11]. The trade-off faced by pathogens need not involved disease-induced mortality, though, and could instead involve other traits such as the degree to which pathogens exploit their host's resources [15], viral load [14], or pathogen growth rate [16].

To study the evolution of pathogen disease-induced mortality, we begin by assuming that there is a host-pathogen system that has reached equilibrium. We then fix attention on a specific pathogen strain and track its lineage in the population. The disease-induced mortality rate of this focal strain can be expressed as the vector $\tilde{\boldsymbol{\alpha}}$. As before, the elements $\tilde{\alpha}_i$ of this vector represent the disease-induced mortality rate of the focal strain in a host of type i. An infecting pathogen group containing this focal strain will have an average group disease-induced mortality rate expressed as the vector $\tilde{\boldsymbol{\alpha}}_g$, where each element $\tilde{\alpha}_{g_i}$ represents the average disease-induced mortality rate of a pathogen group infecting a host of type i and containing the focal strain. We can express the densities of all types of hosts infective with a pathogen group containing the focal strain, at time t, as the $n \times 1$ column vector $\tilde{\mathbf{I}} = \tilde{\mathbf{I}}(t)$. The dynamics of the focal pathogen strain are then approximated by the linear system

$$\frac{d\tilde{\mathbf{I}}}{dt} = [F(\tilde{\boldsymbol{\alpha}}, \tilde{\boldsymbol{\alpha}}_g, \boldsymbol{\alpha}, \boldsymbol{\alpha}_g) - V(\tilde{\boldsymbol{\alpha}}, \tilde{\boldsymbol{\alpha}}_g, \boldsymbol{\alpha}, \boldsymbol{\alpha}_g)]\tilde{\mathbf{I}}, \tag{4.1}$$

where F and V are $n \times n$ matrices.

The matrix F contains all terms related to the production of new pathogens (e.g., transmission). In particular, the entry f_{ij} in the ith row and jth column of F represents the rate at which hosts of type j infective with the focal pathogen strain create new infections in hosts of type i susceptible to infection. By this definition, all entries of F must be non-negative, i.e., F must be a non-negative matrix.

The matrix $-V$ contains all terms related to transitions between infective classes of hosts infective with the focal pathogen strain (e.g., juvenile infective hosts maturing into adult infective hosts), as well as terms related to loss of hosts infective with the focal strain (e.g., recovery, natural mortality, disease-induced mortality). In particular, the entry v_{ij} in the ith row and jth column of $-V$ represents the sum of the rate at which hosts of type j infective with the focal strain transition to hosts of type i infective with the focal strain, and the rate at which hosts of type i leave their corresponding infective class. If $\tilde{I}_i$ represents the density of hosts of type i infective with the focal pathogen strain, then loss of individuals from class $\tilde{I}_i$ will occur, to first-order in the frequency of the focal strain, at a rate proportional to $\tilde{I}_i$. Terms representing the loss of hosts infective with the focal strain, then, will appear only on the main diagonal of the matrix $-V$. Entries off the main diagonal of $-V$ must represent only transitions into class $\tilde{I}_i$ from class $\tilde{I}_j$, $j \neq i$, and so must be non-negative. Such a matrix, where all entries off the main diagonal are non-negative, is called a Metzler matrix. Since F is non-negative, the entries off the main diagonal of the matrix $F - V$ must be non-negative and so $F - V$ is also a Metzler matrix.

We can then find a positive constant c such that $(F - V) + cI$ is a non-negative matrix, where I is the $n \times n$ identity matrix. Specifically, we can choose any $c > |\min_i v_{ii}|$, where v_{ii} represents the ith entry on the main diagonal of $-V$. For any such c, the entries on the main diagonal of $(F - V) + cI$ will be strictly positive, and so $(F - V) + cI$ is a non-negative matrix. We now consider the graph associated with the matrix $(F - V) + cI$. Nodes in this graph represent the densities of hosts of each type infective with a pathogen group containing the focal strain. The entries of $(F - V) + cI$ represent directed connections between these nodes, with the ijth entry describing the creation of new infections in type-i hosts by infected type-j hosts (e.g., transmission) and the transition of infected type-j hosts to infected type-i hosts (e.g., maturation). Assuming that a host of type i can either be infected by a host of type j or by a host of type k, who can themselves be infected by a host of type j (or possibly by a host of some other type, forming an "infection chain" that eventually links to a host of type j), there will always be a path leading from node j to node i in the graph of $(F - V) + cI$. Hence, the graph of $(F - V) + cI$ is irreducible [100]. Furthermore, since the entries on the main diagonal of $(F - V) + cI$ are strictly positive, loops (i.e., paths of length one) will exist from node i to itself. This means that the greatest common divisor of the lengths of the paths of $(F - V) + cI$ must be one. Together with the fact that the graph is irreducible, this allows us to say that $(F - V) + cI$ is a primitive matrix [100].

The Perron-Frobenius Theorem for primitive non-negative matrices tells us that $(F-V)+cI$ has a dominant real eigenvalue $\Lambda + c > 0$ with associated real positive left and right eigenvectors $\mathbf{w}^T$ and $\mathbf{u}$, respectively [100]. Moreover, all other eigenvectors of $(F - V) + cI$ must be negative [100]. In other words, the spectrum of the matrix $(F - V) + cI$, defined as the set of all eigenvalues of the matrix, is contained within the circle of radius $\Lambda + c$ centred at the origin in the complex plane. It has been shown [101] that shifting a matrix by a constant multiple c of the identity matrix preserves the eigenvectors of that matrix, but shifts the spectrum of the matrix by the constant c. This means that the spectrum of the matrix $F-V$ is contained within the circle of radius $\Lambda + c$ centred at the point $(-c, 0)$ in the complex plane. Importantly, the dominant eigenvalue of the matrix $F - V$ is Λ, with associated positive left and right eigenvectors $\mathbf{w}^T$ and $\mathbf{u}$, respectively.

We express the evolutionary equilibrium of (4.1) as a vector $\boldsymbol{\alpha}^*$, where each element α_i^* represents the equilibrium level of the trait in a type-i host. At evolutionary equilibrium, all pathogen strains must exhibit the same disease-induced mortality rate in each type of host, i.e., $\tilde{\boldsymbol{\alpha}} = \boldsymbol{\alpha} = \boldsymbol{\alpha}^*$. If all pathogens exhibit the same rate of disease-induced mortality, then the average disease-induced mortality rate of a group of infecting pathogens will match this equilibrium level, i.e., $\tilde{\boldsymbol{\alpha}}_g = \boldsymbol{\alpha}_g = \boldsymbol{\alpha}^*$. By definition, at this evolutionary equilibrium, the focal pathogen population must not be changing and so

$$\mathbf{0} = (F^* - V^*)\bar{\mathbf{I}}, \tag{4.2}$$

where $\mathbf{0}$ represents the $n \times 1$ zero column vector, $\bar{\mathbf{I}}$ represents the vector of equilibrium densities of infective hosts of each type evaluated at the evolutionary equilibrium, and F^* and V^* represent the matrices F and V evaluated at the evolutionary equilibrium, respectively.

Equation (4.2) shows that $\mathbf{I}$ is a positive right eigenvector for the matrix $F - V$. Since the only positive eigenvectors of $(F - V) + cI$ are those associated with the dominant eigenvalue, and since eigenvectors are preserved by shifting the matrix by cI, we can conclude that $\mathbf{u} = \mathbf{I}$ is a right eigenvector associated with the dominant eigenvalue Λ of $F - V$. The positive left eigenvector $\mathbf{w}^T$ associated with Λ must satisfy $\mathbf{w}^T(F - V) = \Lambda\mathbf{w}^T$. As long as the densities of infected hosts are still changing (i.e., $\Lambda \neq 0$), we can rewrite this as $\mathbf{w}^T = (\mathbf{w}^T/\Lambda)(F - V)$. Since the ijth entry of $F - V$ represents the net number of new type-i infected hosts created by a type-j infected host, this allows us to interpret the ith element of $\mathbf{w}^T$ as the reproductive value of a type-i infected host in the sense that w_i^T represents the average number of infected hosts of any type created by a type-i infected host, discounted by the growth rate Λ of the infected host population.

We can then define a fitness function for the focal pathogen lineage in one of two ways. The first is to define it as the growth rate of the infected host population, given by the dominant eigenvalue Λ of the matrix $F - V$. Equivalently, we can express this in terms of the associated left and right eigenvectors and define fitness as $W_1(\tilde{\boldsymbol{\alpha}}, \tilde{\boldsymbol{\alpha}}_g, \boldsymbol{\alpha}, \boldsymbol{\alpha}_g) = \mathbf{w}^T(F - V)\mathbf{u}$. The second way is to follow a standard adaptive-dynamics approach [5, 6, 7] and define fitness as the average number of new infections created by a host infected with the focal pathogen strain. This can be expressed as the dominant eigenvalue Λ_{NGM} of the next-generation matrix FV^{-1} or, equivalently, in terms of the associated left and right eigenvectors $\mathbf{w}_{\text{NGM}}^T$ and $\mathbf{u}_{\text{NGM}}$, respectively [30]. The left eigenvector associated with the dominant eigenvalue of the next-generation matrix is the same as the left eigenvector of the dominant eigenvalue of the matrix $F - V$, i.e., $\mathbf{w}_{\text{NGM}}^T = \mathbf{w}^T$, while the right eigenvector associated with the dominant eigenvalue of the next-generation matrix is given by $\mathbf{u}_{\text{NGM}} = F\mathbf{u}$. We can then express the fitness of the focal pathogen strain as $W_2(\tilde{\boldsymbol{\alpha}}, \tilde{\boldsymbol{\alpha}}_g, \boldsymbol{\alpha}, \boldsymbol{\alpha}_g) = \mathbf{w}^T FV^{-1}(F\mathbf{u})$.

While these two fitness functions have different interpretations, they are related to one another [18]. In particular, if we multiply W_1 by the dominant eigenvalue Λ_{NGM} of the next-generation matrix and use the fact that the left and right eigenvectors of the next-generation matrix associated with Λ_{NGM} are $\mathbf{w}^T$ and $F\mathbf{u}$, respectively, we get:

$$\Lambda_{\text{NGM}}\mathbf{w}^T(F - V)\mathbf{u} = \mathbf{w}^T FV^{-1}(F - V)\mathbf{u} = \mathbf{w}^T FV^{-1}(F\mathbf{u}) - \mathbf{w}^T(F\mathbf{u}) = W_2 - 1, \tag{4.3}$$

where we have assumed that the eigenvectors $\mathbf{w}^T$ and $F\mathbf{u}$ have been rescaled so that $\mathbf{w}^T(F\mathbf{u}) = 1$. Dividing both sides of (4.3) by $\Lambda_{\text{NGM}} \neq 0$ and using the fact that W_2 can be equivalently expressed as Λ_{NGM}, we have that

$$W_1 = 1 - \frac{1}{W_2}. \tag{4.4}$$

Equation (4.4) shows that W_1 is positive (resp. negative) if and only if W_2 is greater than one (resp. less than one).

To find the evolutionary equilibrium $\boldsymbol{\alpha}^*$, we adapt the procedure used in [43, 44] and consider the genotypic values x_i and $\tilde{x}_i$ of a typical pathogen strain and the focal strain, respectively, in a host of type i. We write the genotypic value of a typical pathogen strain as the vector $\mathbf{x}$ and that of the focal pathogen strain as the vector $\tilde{\mathbf{x}}$. The disease-induced mortality rate of a typical strain, $\boldsymbol{\alpha}$, will depend on the pathogen's genotype in each type of host, $\mathbf{x}$. Similarly, the disease-induced mortality rate of the focal strain, $\tilde{\boldsymbol{\alpha}}$, will depend on the focal pathogen's genotype in each type of host, $\tilde{\mathbf{x}}$. One can translate the genotypic value into a continuous phenotype by assuming that the latter is a product of the presence of a genetic allele and the rate at which that allele changes the phenotype, as is done in [43]. The equilibrium $\boldsymbol{\alpha}^*$ is then found by solving the system $dW_i/d\tilde{\mathbf{x}}|_{\tilde{\mathbf{x}}=\mathbf{x}=\mathbf{x}^*} = \mathbf{0}$, where $\mathbf{x}^*$ represents the genotype of a pathogen strain at the evolutionary equilibrium $\boldsymbol{\alpha}^*$ [43, 44]. From equation (4.4), we have $dW_1/d\tilde{\mathbf{x}} = (1/W_2^2)(dW_2/d\tilde{\mathbf{x}})$ and so $dW_1/d\tilde{\mathbf{x}} = \mathbf{0}$ if and only if $dW_2/d\tilde{\mathbf{x}} = \mathbf{0}$. This means that we can analyze either W_1 or W_2 and arrive at the same evolutionary equilibrium. Using W_1, and the fact that the dominant eigenvalue of $F - V$ is zero at equilibrium, the ith equation in the system $dW_1/d\tilde{\mathbf{x}} = \mathbf{0}$ is

$$0 = \frac{\partial W_1}{\partial \tilde{x}_i} = \mathbf{w}^T \left(\frac{\partial F}{\partial \tilde{\alpha}_i} \frac{\partial \tilde{\alpha}_i}{\partial \tilde{x}_i} + \frac{\partial F}{\partial \tilde{\alpha}_{g_i}} \frac{\partial \tilde{\alpha}_{g_i}}{\partial \tilde{x}_i} \right) \mathbf{u} - \mathbf{w}^T \left(\frac{\partial V}{\partial \tilde{\alpha}_i} \frac{\partial \tilde{\alpha}_i}{\partial \tilde{x}_i} + \frac{\partial V}{\partial \tilde{\alpha}_{g_i}} \frac{\partial \tilde{\alpha}_{g_i}}{\partial \tilde{x}_i} \right) \mathbf{u}, \tag{4.5}$$

where all terms are evaluated when $\tilde{\alpha}_i = \alpha_i = \tilde{\alpha}_{g_i} = \alpha_{g_i} = \alpha_i^*$. If we divide both sides of equation (4.5) by $\partial\tilde{\alpha}_i/\partial\tilde{x}_i$, we can rewrite this equation as

$$\underbrace{\mathbf{w}^T \left(\frac{\partial F}{\partial \tilde{\alpha}_i} + r_i \frac{\partial F}{\partial \tilde{\alpha}_{g_i}} \right) \mathbf{u}}_{\text{I}} = \underbrace{\mathbf{w}^T \left(\frac{\partial V}{\partial \tilde{\alpha}_i} + r_i \frac{\partial V}{\partial \tilde{\alpha}_{g_i}} \right) \mathbf{u}}_{\text{II}}, \tag{4.6}$$

where $r_i = \frac{\partial\tilde{\alpha}_{g_i}/\partial\tilde{x}_i}{\partial\tilde{\alpha}_i/\partial\tilde{x}_i}$ is the genetic relatedness of the focal pathogen strain to the infecting group of pathogens to which it belongs [43, 44].

To interpret equation (4.6) biologically, we identify two terms. Term I measures the change in two types of benefits conferred to the focal pathogen for increasing its disease-induced mortality rate: a direct benefit of increased personal transmission and an indirect benefit, weighted by the focal pathogen's relatedness to its group, of increased group transmission. Similarly, term II measures the change in two types of costs incurred by the focal pathogen for increasing its disease-induced mortality rate: a direct cost of decreased personal duration of infection and an indirect cost, weighted by the focal pathogen's relatedness to its group, of decreased group duration of infection. Equation (4.6) then says that, at evolutionary equilibrium, these benefits and costs must balance out within each type of host. Moreover, the more related is the focal pathogen to its infecting group, the more the indirect benefit and cost will affect the evolutionarily stable trait value α^*.

4.3 Illustrative Examples

4.3.1 Example 1: Infections in Age-structured Host Populations

Our first example considers an infectious disease circulating in a population of hosts classified according to their age. Such models have been studied in the cases of tuberculosis [102] and pertussis [103], and have been used to explore the effects on evolution of different contact patterns between susceptible and infected individuals [104]. At time t, there will be $I_j = I_j(t)$ juvenile hosts infected with the disease and $S_j = S_j(t)$ juvenile hosts susceptible to infection. There will also be $I_a = I_a(t)$ adult hosts infected with the disease and $S_a = S_a(t)$ adult hosts susceptible to infection. All infected hosts are also infective.

Adult hosts will produce juvenile offspring at a per-capita rate b. We assume that juvenile hosts cannot reproduce, but they will mature into adults at a per-capita rate m. Both juveniles and adults will experience a natural mortality rate μ.

Infected juvenile hosts will transmit the disease to susceptible juveniles at a per-capita rate $S_j\beta_j$ and to susceptible adults at a per-capita rate $S_a\beta_j$. Infected adult hosts will transmit the disease to susceptible juveniles at a per-capita rate $S_j\beta_a$ and to susceptible adults at a per-capita rate $S_a\beta_a$. Juvenile hosts will recover from infection at a per-capita rate γ_j and they will die due to the infection at a per-capita rate α_{g_j}, where α_{g_j} is an average disease-induced mortality rate across the group of infecting pathogen strains. Similarly, adult hosts will recover from infection at a per-capita rate γ_a and they will die due to the infection at a per-capita rate α_{g_a}, where α_{g_a} is an average disease-induced mortality rate across the group of infecting pathogen strains.

The model is summarized by the following system of differential equations:

$$\frac{dS_j}{dt} = b(S_a + I_a) + \gamma_j I_j - S_j\left(\beta_j I_j + \beta_a I_a\right) - (m + \mu)S_j \tag{4.7a}$$

$$\frac{dS_a}{dt} = mS_j + \gamma_a I_a - S_a\left(\beta_j I_j + \beta_a I_a\right) - \mu S_a \tag{4.7b}$$

$$\frac{dI_j}{dt} = S_j\left(\beta_j I_j + \beta_a I_a\right) - (\gamma_j + m + \mu + \alpha_{g_j})I_j \tag{4.7c}$$

$$\frac{dI_a}{dt} = mI_j + S_a\left(\beta_j I_j + \beta_a I_a\right) - (\gamma_a + \mu + \alpha_{g_a})I_a. \tag{4.7d}$$

To study the evolution of disease-induced mortality, we assume pathogens face a trade-off between transmission and recovery, as previous authors have done [43, 11, 10, 13]. To capture this, we follow [43] and treat transmission and recovery as functions of the focal pathogen's disease-induced mortality rate in juvenile hosts, α_j, and adult hosts, α_a. We then write $\beta_j = \beta_j(\alpha_j)$, $\beta_a = \beta_a(\alpha_a)$, $\gamma_j = \gamma_j(\alpha_j)$, and $\gamma_a = \gamma_a(\alpha_a)$. We suppose that (4.7) has reached an endemic equilibrium. While it is not possible to find and analyze the stability of this equilibrium analytically, numerical simulation suggests that an endemic equilibrium exists and is stable for some sets of parameter values. We then track a focal pathogen lineage with disease-induced mortality rates $\tilde{\alpha}_j$ and $\tilde{\alpha}_a$ in juvenile and adult hosts, respectively. An infecting group of pathogens containing this focal strain will have an average group disease-induced mortality rate of $\tilde{\alpha}_{g_j}$ in juvenile hosts and $\tilde{\alpha}_{g_a}$ in adult hosts. If we use the vector $\tilde{\mathbf{I}} = (\tilde{I}_j, \tilde{I}_a)^T$ to denote the densities of juvenile and adult hosts infected with a group of pathogens containing the focal strain, then we can approximate the dynamics of the focal strain with the following linear system:

$$\frac{d\tilde{\mathbf{I}}}{dt} = \left(\underbrace{\begin{bmatrix} \bar{S}_j \tilde{\beta}_j & \bar{S}_j \tilde{\beta}_a \\ \bar{S}_a \tilde{\beta}_j & \bar{S}_a \tilde{\beta}_a \end{bmatrix}}_{F} - \underbrace{\begin{bmatrix} \tilde{\gamma}_j + m + \mu + \tilde{\alpha}_{g_j} & 0 \\ -m & \tilde{\gamma}_a + \mu + \tilde{\alpha}_{g_a} \end{bmatrix}}_{V} \right) \tilde{\mathbf{I}}, \tag{4.8}$$

where $\tilde{\beta}_j = \beta_j(\tilde{\alpha}_j)$, $\tilde{\beta}_a = \beta_a(\tilde{\alpha}_a)$, $\tilde{\gamma}_j = \gamma_j(\tilde{\alpha}_j)$, $\tilde{\gamma}_a = \gamma_a(\tilde{\alpha}_a)$, and overbars denote equilibrium densities hosts. Given that all model parameters are positive, the entries off the main diagonal of $F - V$ will be non-negative and so $F - V$ is a Metzler matrix.

In order to investigate the evolutionary equilibrium condition given in (4.6), we first need to find the left and right eigenvectors $\mathbf{w}^T$ and $\mathbf{u}$, respectively, associated with the dominant eigenvalue of the matrix $F - V$. As discussed previously, at evolutionary equilibrium, the left eigenvector $\mathbf{w}^T$ can be interpreted as the reproductive value of infected juvenile and adult hosts, while the right eigenvector $\mathbf{u}$ can be interpreted as the equilibrium numbers of infected juvenile and adult hosts. The left eigenvector $\mathbf{w}^T$ is found by solving

$$\mathbf{0} = \mathbf{w}^T(F - V), \tag{4.9}$$

where F and V are evaluated at the evolutionary equilibrium $\boldsymbol{\alpha}^* = (\alpha_j^*, \alpha_a^*)$. From this, we get that the left eigenvector is given by

$$\mathbf{w}^T = \begin{bmatrix} \frac{\beta_j^* \bar{S}_a + m}{\gamma_j^* + \mu + \alpha_j^* + m - \beta_j^* \bar{S}_j} w_a & w_a \end{bmatrix}, \tag{4.10}$$

where w_a is the reproductive value of a focal pathogen in an infected adult host, asterisks denote traits evaluated at the evolutionary equilibrium $\boldsymbol{\alpha}^*$, and overbars denote equilibrium numbers of hosts. The right eigenvector $\mathbf{u}$ is found by solving

$$\mathbf{0} = (F - V)\mathbf{u} \tag{4.11}$$

where F and V are evaluated at α^*, and is given by

$$\mathbf{u} = \begin{bmatrix} \frac{\beta_a^* \bar{S}_j}{\gamma_j^* + \mu + \alpha_j^* + m - \beta_j^* \bar{S}_j} \bar{I}_a \\ \bar{I}_a \end{bmatrix}, \tag{4.12}$$

where $\bar{I}_a$ is the equilibrium number of adult hosts infected with the focal pathogen strain.

We can now use these eigenvectors to analyze the evolutionary equilibrium condition (4.6). In juvenile hosts, this equilibrium condition becomes

$$\frac{\beta_j'}{\beta_j^*} = \frac{\gamma_j' + r_j}{\gamma_j^* + \mu + \alpha_j^* + m} \left(\frac{1 + \overbrace{\frac{m}{\beta_j^* \bar{S}_a}}^{\text{I}}}{1 + \underbrace{\frac{\frac{m}{\gamma_j^* + \mu + \alpha_j^* + m} \bar{S}_j}{\bar{S}_a}}_{\text{II}}} \right), \tag{4.13}$$

where primes denote first derivatives and r_j represents the relatedness of the focal pathogen strain to its coinfecting group in a juvenile host. On the left-hand side of (4.13), we have the benefit to the focal pathogen for increasing its disease-induced mortality, measured as the rate of change of transmission relative to the transmission rate itself. On the right-hand side of (4.13), we have the cost, both direct and indirect, to the focal pathogen for increasing its disease-induced mortality rate, measured as the rate of change of the duration of infection relative to the duration of infection itself. This cost has a compounding effect attached to it to capture the fact that if the focal pathogen increases its disease-induced mortality in a juvenile host to the point where it kills the juvenile host before it is able to mature into an adult, it will miss out on all of the possible infections it could have created in that matured juvenile host. Term I in (4.13) measures the rate at which an infected juvenile host matures into an infected adult host relative to the rate at which an infected juvenile host is able to create infections in susceptible adults. If a juvenile host infected with the focal pathogen is able to create new infections in susceptible adults much faster than it matures into an infected adult itself, then this decreases the compounding effect on the cost to the focal pathogen. Term II in (4.13) measures the potential number of adult infections that could be created by infecting juveniles and waiting for them to mature relative to the potential number of adult infections that could be created in susceptible adults. If there are fewer juvenile hosts who will survive to mature into adults after being infected by the focal pathogen strain, then this will increase the compounding effect on the cost to the focal strain for increasing its disease-induced mortality rate.

The effect of increased relatedness can be seen analytically in (4.13). In particular, if the focal pathogen strain is more related to its coinfecting group in a juvenile host, this will increase the cost associated with increased disease-induced mortality. To maintain the equilibrium balance, (4.13) then says that evolution will push for reduced disease-induced mortality in order to reduce the transmission rate β_j^*. This effect is depicted graphically in figure 4.1. The slope of the solid curve is the ratio of the rate of change of transmission to the rate of change of duration of infection, while the slope of the dashed and dotted lines is given by the ratio of transmission to duration of infection, multiplied by the compounding effect in brackets in (4.13). These slopes are equal at the intersection point marked by the black square. The dotted line shows that, for increased relatedness, the evolutionary equilibrium occurs at a lower rate of transmission and a higher duration of infection, both of which are achieved by reducing disease-induced mortality.

In adult hosts, the equilibrium condition is given by

$$\frac{\beta_a'}{\beta_a^*} = \frac{\gamma_a' + r_a}{\gamma_a^* + \mu + \alpha_a^*} \left(\frac{1 - \frac{\beta_j^* \bar{S}_j}{\gamma_j^* + \mu + \alpha_j^* + m}}{\frac{1}{\gamma_a^* + \mu + \alpha_a^*} \left(\beta_a^* \bar{S}_a + \frac{m}{\gamma_j^* + \mu + \alpha_j^* + m} \beta_a^* \bar{S}_j \right)} \right), \tag{4.14}$$

where r_a is the relatedness of the focal pathogen to its coinfecting group in an adult host. The numerator of the fraction in the brackets in (4.14) can be simplified slightly by making the observation that, at equilibrium, neither the infected juvenile nor infected adult populations can be growing or shrinking. In particular, when one juvenile host leaves the infected compartment at the end of the duration of infection of a juvenile host, it must be replaced simultaneously by

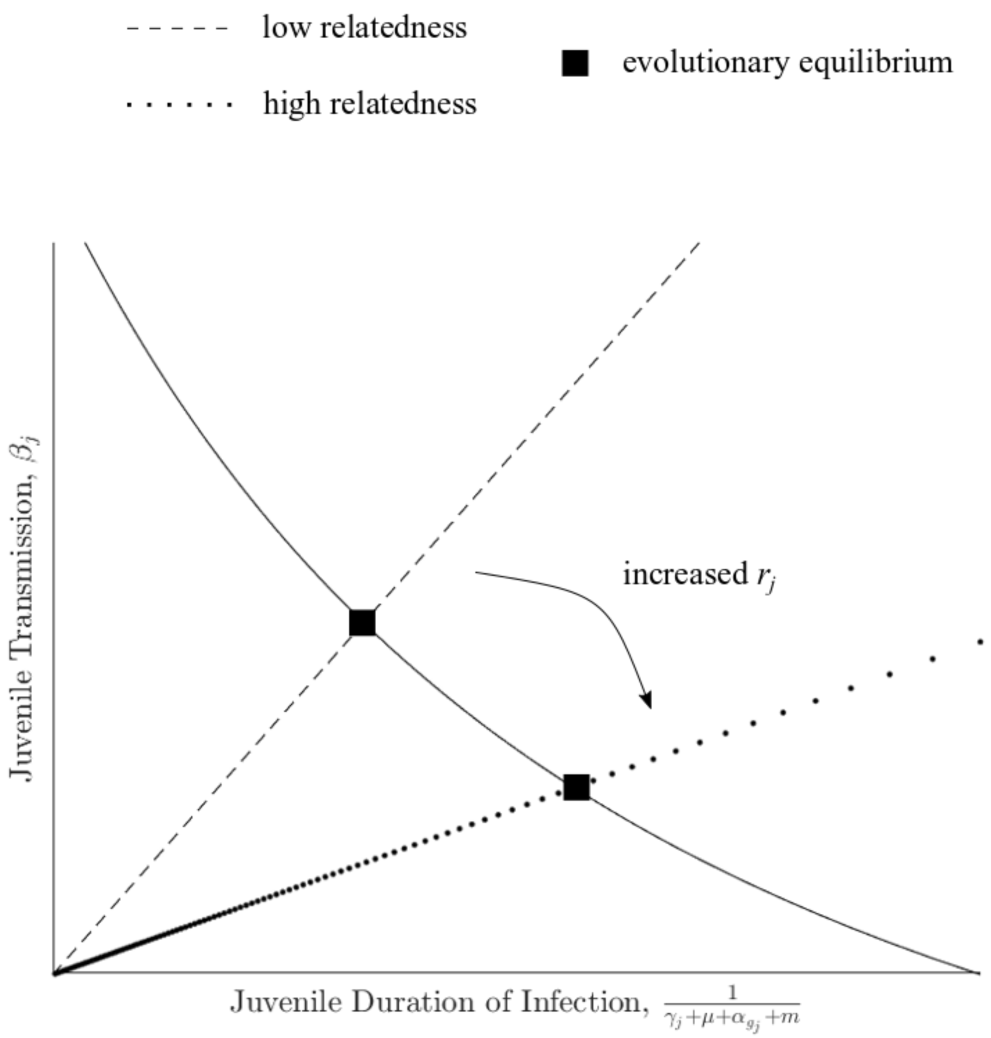

Figure 4.1: Graphical depiction of the effect of increasing relatedness between the focal pathogen strain and its coinfecting group. The slope of the solid curve is given by β'_j/D'_j, where D_j is the duration of infection of a juvenile host. The slope of the dashed and dotted lines is given by β_j/D_j multiplied by the compounding effect given in brackets in (4.13). Equation (4.13) is satisfied when these two slopes are equal in magnitude, which occurs at the point of intersection marked by the black square. Increasing relatedness r_j will increase D'_j, which will drag the intersection point farther right along the horizontal axis. This new intersection point is characterized by reduced transmission and increased duration of infection, achieved via a reduction in disease-induced mortality.

a new infected juvenile host. This replacement infected juvenile can be created either by an infected juvenile host or by an infected adult host. The total number of new juvenile infections created by an infected juvenile host over the duration of infection of a juvenile host is given by $\frac{\beta_j^*\bar{S}_j}{\gamma_j^*+\mu+\alpha_j^*+m}$. Similarly, the total number of new juvenile infections created by an infected adult host over the duration of infection of a *juvenile* host is given by $\frac{\beta_a^*\bar{S}_j}{\gamma_j^*+\mu+\alpha_j^*+m}$. The total number of new juvenile infections created over the duration of infection of a juvenile host is then given by the sum of these two terms and must be equal to one at evolutionary equilibrium. This allows us to replace the numerator of the fraction inside the brackets in (4.14) and write the adult host equilibrium condition as

$$\frac{\beta_a'}{\beta_a^*} = \frac{\gamma_a'+r_a}{\gamma_a^*+\mu+\alpha_a^*}\left(\frac{\overbrace{\frac{\beta_a^*\bar{S}_j}{\gamma_j^*+\mu+\alpha_j^*+m}}^{\text{I}}}{\underbrace{\frac{1}{\gamma_a^*+\mu+\alpha_a^*}\left(\beta_a^*\bar{S}_a+\frac{m}{\gamma_j^*+\mu+\alpha_j^*+m}\beta_a^*\bar{S}_j\right)}_{\text{II}}}\right). \tag{4.15}$$

As in the juvenile equilibrium condition, the left-hand side of (4.15) measures the benefit to the focal pathogen for increasing its disease-induced mortality rate and the right-hand side measures the associated cost. Term I in (4.15) measures the total number of new infected juvenile hosts created by an infected adult host over the duration of infection of a juvenile host. Term II in (4.15) measures the total number of new infected adult hosts created by an infected adult over the duration of infection of an adult host, both from direct infection of susceptible adults and maturation of infected juveniles into infected adults. As with juvenile hosts, increased relatedness of the focal pathogen strain to its coinfecting group in adult hosts will push for reduced disease-induced mortality.

4.3.2 Example 2: Sexually Transmitted Infections

For our second example, we study a system where hosts and pathogens are allowed to coevolve. We consider a sexually transmitted infection (STI) circulating in a population of female and male hosts. Hosts are further classified according to their disease status. At time t, there are $I_f = I_f(t)$ female hosts infected with the disease and $S_f = S_f(t)$ female hosts susceptible to infection. Similarly, there are $I_m = I_m(t)$ male hosts infected with the disease and $S_m = S_m(t)$ male hosts susceptible to infection. All infected hosts are also infective.

Females will have an average of $M = M(N_f, N_m)$ mating events with males, where N_f is the total number of female hosts and N_m is the total number of male hosts. As discussed in [62, 63], a common functional form for M uses the harmonic mean of the numbers of female and male hosts, i.e.,

$$M(N_f, N_m) = \frac{2N_f N_m}{N_f + N_m}. \tag{4.16}$$

Mating events will lead to the production of new offspring at a per-capita rate b. Assuming a one-to-one birth sex ratio, the total birth rate of both female and male hosts is given by

$$\frac{bN_f N_m}{N_f + N_m}. \tag{4.17}$$

Female and male hosts will also experience a per-capita natural mortality rate μ.

As in previous models of STIs (e.g., [62, 105, 106]), transmission of the disease between females and males will occur at a rate proportional to the average number of mating events M. Infected males will transmit the disease to susceptible females at a frequency-dependent, per-capita rate

$$\frac{S_f}{N_f}\frac{\beta_m}{N_m} M(N_f, N_m) = S_f \frac{2\beta_m}{N_f + N_m}. \tag{4.18}$$

Similarly, transmission from infected females to susceptible males will occur at a frequency-dependent, per-capita rate

$$\frac{S_m}{N_m}\frac{\beta_f}{N_f}M(N_f, N_m) = S_m\frac{2\beta_f}{N_f + N_m}. \tag{4.19}$$

Female hosts can then recover from infection at a rate γ_f, in which case they are again susceptible to infection, or die due to the disease at a rate α_{g_f}. Similarly, male hosts can recover at a rate γ_m, in which case they are again susceptible to infection, or die due to the disease at a rate α_{g_m}. As discussed previously, we assume that hosts are infected by a group of pathogens and so the disease-induced mortality rates α_{g_f} and α_{g_m} represent averages across infecting pathogen groups.

The mathematical model is summarized by the following system of differential equations:

$$\frac{dS_f}{dt} = \frac{bN_fN_m}{N_f + N_m} + \gamma_f I_f - S_f\frac{2\beta_m}{N_f + N_m}I_m - \mu S_f \tag{4.20a}$$

$$\frac{dS_m}{dt} = \frac{bN_fN_m}{N_f + N_m} + \gamma_m I_m - S_m\frac{2\beta_f}{N_f + N_m}I_f - \mu S_m \tag{4.20b}$$

$$\frac{dI_f}{dt} = S_f\frac{2\beta_m}{N_f + N_m}I_m - (\gamma_f + \mu + \alpha_{g_f})I_f \tag{4.20c}$$

$$\frac{dI_m}{dt} = S_m\frac{2\beta_f}{N_f + N_m}I_f - (\gamma_m + \mu + \alpha_{g_m})I_m. \tag{4.20d}$$

To study host evolution, we first suppose that female and male hosts have some level η_f and η_m, respectively, of investment in their immune system. A host's level of immune investment will affect both the rate at which it clears an infection, γ_f or γ_m, and their birth rate, b. To reflect this, we now write $\gamma_f = \gamma_f(\eta_f)$, $\gamma_m = \gamma_m(\eta_m)$, and $b = b(\eta_f, \eta_m)$. In general, increased immune investment will result in a faster rate of clearance at the cost of a lower birth rate, as has been modelled by previous authors [19, 28]. Our goal is then to find the evolutionary equilibrium level of female and male host immune investment η_f^* and η_m^*, respectively.

We start by assuming that system (4.20) has reached an endemic equilibrium where hosts of all classes are present in some numbers. As with the previous example, finding this equilibrium is not possible analytically, but numerical simulation suggests that it exists and is stable for some sets of parameter values. We then consider a host lineage where females and males have a level of immune investment $\hat{\eta}_f$ and $\hat{\eta}_m$, respectively, different from that of the equilibrium host population. Female hosts of the focal lineage will clear an infection at a rate $\hat{\gamma}_f = \gamma_f(\hat{\eta}_f)$, while male hosts of the focal lineage will clear an ifnection at a rate $\hat{\gamma}_m = \gamma_m(\hat{\eta}_m)$. All hosts of the focal lineage will have a per-capita birth rate given by $\hat{b} = b(\hat{\eta}_f, \hat{\eta}_m)$. The numbers of susceptible and infected female hosts of this focal lineage will be denoted by $\hat{S}_f$ and $\hat{I}_f$, respectively. Similarly, the numbers of susceptible and infected male hosts of this focal lineage will be denoted by $\hat{S}_m$ and $\hat{I}_m$, respectively. If we use the vector $\hat{\mathbf{H}} = (\hat{S}_f, \hat{S}_m, \hat{I}_f, \hat{I}_m)$ to denote the number of hosts of the focal lineage in each disease category, then the dynamics of the focal lineage can be approximated by the linear system

$$\frac{d\hat{\mathbf{H}}}{dt} = \left(\overbrace{\begin{bmatrix} \frac{\hat{b}\bar{N}_m}{\bar{N}_f+\bar{N}_m} & \frac{\hat{b}\bar{N}_f}{\bar{N}_f+\bar{N}_m} & \frac{\hat{b}\bar{N}_m}{\bar{N}_f+\bar{N}_m} & \frac{\hat{b}\bar{N}_f}{\bar{N}_f+\bar{N}_m} \\ \frac{\hat{b}\bar{N}_m}{\bar{N}_f+\bar{N}_m} & \frac{\hat{b}\bar{N}_f}{\bar{N}_f+\bar{N}_m} & \frac{\hat{b}\bar{N}_m}{\bar{N}_f+\bar{N}_m} & \frac{\hat{b}\bar{N}_f}{\bar{N}_f+\bar{N}_m} \\ 0 & 0 & 0 & 0 \\ 0 & 0 & 0 & 0 \end{bmatrix}}^{F_h} \right. \tag{4.21}$$

$$\left. - \underbrace{\begin{bmatrix} \frac{2\beta_m \bar{I}_m}{\bar{N}_f+\bar{N}_m} + \mu & 0 & -\hat{\gamma}_f & 0 \\ 0 & \frac{2\beta_f \bar{I}_f}{\bar{N}_f+\bar{N}_m} + \mu & 0 & -\hat{\gamma}_m \\ \frac{2\beta_m \bar{I}_m}{\bar{N}_f+\bar{N}_m} & 0 & \hat{\gamma}_f + \mu + \alpha_{g_f} & 0 \\ 0 & \frac{2\beta_f \bar{I}_f}{\bar{N}_f+\bar{N}_m} & 0 & \hat{\gamma}_m + \mu + \alpha_{g_m} \end{bmatrix}}_{V_h} \right) \hat{\mathbf{H}},$$

where overbars denote equilibrium levels of the respective variables. Finding the dominant eigenvalue of the matrix $F_h - V_h$ is computationally intensive, so we instead work with the dominant eigenvalue Λ_{NGM_h} of the next-generation matrix $F_h V_h^{-1}$ [30] and define host fitness was $W_h(\hat{\eta}_f, \hat{\eta}_m, \eta_f, \eta_m) = \Lambda_{\mathrm{NGM}_h}$. Differentiating W_h with respect to the level of female host immune investment $\hat{\eta}_f$, and evaluating at $\hat{\eta}_f = \eta_f = \eta_f^*$ and $\hat{\eta}_m = \eta_m = \eta_m^*$, gives the evolutionary equilibrium condition that must be satisfied by female hosts:

$$\frac{\partial \hat{b}/\partial \hat{\eta}_f}{\hat{b}} = \frac{\partial \hat{\gamma}_f/\partial \hat{\eta}_f}{G_f(\hat{\gamma}_f, \hat{\gamma}_m, \beta_f, \beta_m, \alpha_{g_f}, \alpha_{g_m})}, \tag{4.22}$$

for a function G_f. Similarly, we can differentiate W_h with respect to male host immune investment $\hat{\eta}_m$, evaluate at $\hat{\eta}_f = \eta_f = \eta_f^*$ and $\hat{\eta}_m = \eta_m = \eta_m^*$, and find the evolutionary equilibrium condition that must be satisfied by male hosts:

$$\frac{\partial \hat{b}/\partial \hat{\eta}_m}{\hat{b}} = \frac{\partial \hat{\gamma}_m/\partial \hat{\eta}_m}{G_m(\hat{\gamma}_f, \hat{\gamma}_m, \beta_f, \beta_m, \alpha_{g_f}, \alpha_{g_m})}, \tag{4.23}$$

for a function G_m. Equations (4.22) and (4.23) show that, at evolutionary equilibrium, hosts must balance the benefit of increased clearance rate against the cost of decreased reproduction. Importantly, pathogen evolution will affect host evolution through the functions G_f and G_m.

To study the evolution of pathogen disease-induced mortality, we first assume that system (4.20) has reached an endemic equilibrium where hosts of all classes are present in some numbers. Furthermore, as in the previous example, we assume that pathogens face a trade-off of increased transmission and decreased duration of infection for increased disease-induced mortality. To capture this, as in [43], we treat transmission and recovery as functions of individual pathogen disease-induced mortality, i.e., $\beta_f = \beta_f(\alpha_f)$, $\beta_m = \beta_m(\alpha_m)$, $\gamma_f = \gamma_f(\alpha_f)$, and $\gamma_m = \gamma_m(\alpha_m)$, where α_f and α_m are the disease-induced mortality rates of a pathogen strain in female and male hosts, respectively. We then track a focal pathogen lineage with disease-induced mortality rate expressed as the vector $\tilde{\boldsymbol{\alpha}} = (\tilde{\alpha}_f, \tilde{\alpha}_m)$, where $\tilde{\alpha}_f$ and $\tilde{\alpha}_m$ are the focal pathogen's disease-induced mortality rates in female and male hosts, respectively. A group of infecting pathogens containing this focal strain will have an average group disease-induced mortality rate expressed as the vector $\tilde{\boldsymbol{\alpha}}_g = (\tilde{\alpha}_{g_f}, \tilde{\alpha}_{g_m})$, where $\tilde{\alpha}_{g_f}$ and $\tilde{\alpha}_{g_m}$ are the average group disease-induced mortality rates in female and male hosts, respectively. If we use the vector

$\tilde{\mathbf{I}} = (\tilde{I}_f, \tilde{I}_m)^T$ to denote the densities of hosts infected with a group of pathogens containing the focal strain, then the dynamics of the mutant strain are approximated by the linear system

$$\frac{d\tilde{\mathbf{I}}}{dt} = \left(\underbrace{\begin{bmatrix} 0 & \bar{S}_f \frac{2\tilde{\beta}_m}{\bar{N}_f + \bar{N}_m} \\ \bar{S}_m \frac{2\tilde{\beta}_f}{\bar{N}_f + \bar{N}_m} & 0 \end{bmatrix}}_{F_p} - \underbrace{\begin{bmatrix} \tilde{\gamma}_f + \mu + \tilde{\alpha}_{g_f} & 0 \\ 0 & \tilde{\gamma}_m + \mu + \tilde{\alpha}_{g_m} \end{bmatrix}}_{V_p} \right) \tilde{\mathbf{I}}, \tag{4.24}$$

where $\tilde{\beta}_f = \beta_f(\tilde{\alpha}_f)$, $\tilde{\beta}_m = \beta_m(\tilde{\alpha}_m)$, $\tilde{\gamma}_f = \gamma_f(\tilde{\alpha}_f)$, $\tilde{\gamma}_m = \gamma_m(\tilde{\alpha}_m)$, and overbars denote equilibrium densities of hosts.

To analyze the evolutionary equilibrium condition (4.6), we first need to find the left and right eigenvectors $\mathbf{w}^T$ and $\mathbf{u}$, respectively, associated with the dominant eigenvalue of the matrix $F_p - V_p$. As discussed previously, at equilibrium, this dominant eigenvalue is zero and the associated left and right eigenvectors can be interpreted as reproductive value and equilibrium numbers of individuals infected with the focal pathogen strain, respectively. The left eigenvector $\mathbf{w}^T$ is found by solving

$$\mathbf{0} = \mathbf{w}^T (F_p - V_p) \tag{4.25}$$

and is given by

$$\mathbf{w}^T = \begin{bmatrix} \frac{\frac{2\beta_f^*}{\bar{N}_f + \bar{N}_m} \bar{S}_m}{\gamma_f^* + \mu + \alpha_f^*} w_m & w_m \end{bmatrix}, \tag{4.26}$$

where asterisks denote traits evaluated at the evolutionary equilibrium $\boldsymbol{\alpha}^* = (\alpha_f^*, \alpha_m^*)$ and w_m is the reproductive value of the focal pathogen strain in a male host. The right eigenvector $\mathbf{u}$ is found by solving

$$\mathbf{0} = (F_p - V_p)\mathbf{u} \tag{4.27}$$

and is given by

$$\mathbf{u} = \begin{bmatrix} \frac{\frac{2\beta_m^*}{\bar{N}_f + \bar{N}_m} \bar{S}_f}{\gamma_f^* + \mu + \alpha_f^*} \bar{I}_m \\ \bar{I}_m \end{bmatrix}, \tag{4.28}$$

where $\bar{I}_m$ is the equilibrium number of male hosts infected with the focal pathogen strain.

We can then construct the evolutionary equilibrium conditions from (4.6). The equilibrium condition for female hosts is given by

$$\frac{\beta_f'}{\beta_f^*} = \frac{\gamma_f' + r_f}{\gamma_f^* + \mu + \alpha_f^*}, \tag{4.29}$$

where primes denote first derivatives and r_f is the relatedness of the focal pathogen strain to its coinfecting group in a female host. As in the previous example, the left-hand side of (4.29) represents the benefit to the focal pathogen strain for increasing its disease-induced mortality, while the right-hand side represents the associated direct and indirect costs. The more related is the focal pathogen strain to its coinfecting group, the higher will be the cost and so evolution will push for reduced disease-induced mortality to maintain the benefit-cost balance.

The equilibrium condition for male hosts is given by

$$\frac{\beta_m'}{\beta_m^*} = \frac{\gamma_m' + r_m}{\gamma_m^* + \mu + \alpha_m^*} \underbrace{\left(\frac{\gamma_f^* + \mu + \alpha_f^*}{\frac{2\beta_m^*}{\bar{N}_f + \bar{N}_m}\bar{S}_f}\right)}_{\mathrm{I}} \underbrace{\left(\frac{\gamma_m^* + \mu + \alpha_m^*}{\frac{2\beta_f^*}{\bar{N}_f + \bar{N}_m}\bar{S}_m}\right)}_{\mathrm{II}}, \tag{4.30}$$

where r_m is the relatedness of the focal pathogen strain to its coinfecting group in male hosts. Term I represents the inverse of the number of new infections created in female hosts over the duration of infection of a female host, while term II represents the inverse of the number of new infections created in male hosts over the duration of infection of a male host. At equilibrium, both of these quantities must be one so that the infected host population is neither growing nor shrinking. This allows us to simplify (4.30) to

$$\frac{\beta_m'}{\beta_m^*} = \frac{\gamma_m' + r_m}{\gamma_m^* + \mu + \alpha_m^*}. \tag{4.31}$$

As with female hosts, male hosts must balance the benefits of increased disease-induced mortality against the associated direct and indirect costs. The more related is the focal pathogen to its coinfecting group, the lower will be the equilibrium disease-induced mortality rate. Unlike in the previous age-structured model example, here, the evolutionary equilibrium conditions are symmetric between the two host types.

4.4 Discussion

Here, we have presented a general framework for studying the evolution of disease-induced mortality among groups of related coinfecting pathogen strains in a host population classified into different types. Two examples were discussed to show how this general framework can be used in practice.

The first example considers an infectious disease circulating in a population of hosts split into juveniles and adults. Our theoretical framework shows that the evolutionary equilibrium conditions are asymmetric between host types. Pathogens in adult hosts must balance their direct benefit with their direct and indirect costs. However, in juvenile hosts, pathogens have an extra risk of killing their host before it matures into an adult, missing out on any infections it could have caused in the matured juvenile host. This creates an asymmetry between the equilibrium conditions of juvenile and adult hosts.

The second of these examples explores host-pathogen coevolution in the case of a STI circulating in a population of female and male hosts. A pathogen strain that increases its disease-induced mortality rate will gain a direct benefit of increased personal transmission, but it will also incur both a direct cost of a higher likelihood of being cleared by the host's immune system and an indirect cost of a reduced duration of infection for the entire coinfecting pathogen group. As in [43], these benefits and costs must balance out at evolutionary equilibrium. In this scenario, the equilibrium conditions are symmetric between host types. Furthermore, the degree of relatedness between coinfecting pathogen strains will also influence the coevolution of host immune investment.

In both examples, we find that increased relatedness among a group of coinfecting pathogen strains will select for cooperation as individual strains reduce their disease-induced mortality rate in order to prolong the duration of infection of the group, in keeping with the ideas put forth by Hamilton [45] on inclusive fitness. Such an effect of relatedness has been shown by Frank [43] in single-host models. Experimental studies on the *Microbotryum violaceum* [107] and *Microbotryum lychnidis-dioicae* [108] plant fungi have shown that competition to infect a host is fiercer between less related strains. Theoretical work on spatially structured populations [97] has shown that increased pathogen dispersal will result in lower relatedness among strains on a given patch of hosts, which will, in turn, select for greater virulence. While our framework does not include spatial structure, it does confirm that reduced relatedness among strains should select for higher disease-induced mortality.

Our theory has its underpinnings in the Price equation [109, 110], which provides a general mathematical framework for understanding the effects associated with natural selection. The Price equation has been extended previously to describe problems in evolutionary epidemiology concerning the evolution of multiple pathogen strains [98], the evolutionary effects of demographic stochasticity [99], and relatedness among coinfecting pathogen strains [43, 44]. In each of these cases, a methodology based on the Price equation provides an interpretation of the biological forces governing pathogen evolution under natural selection. Our work adds to this literature by extending these ideas to situations involving multiple types of hosts and, potentially, coevolution between hosts and pathogens.

One important limitation of this framework is that we are not able to make any conclusions about evolutionary stability [20, 22] or convergence stability [21]. Doing so would require specifying the functional relationship between transmission and clearance and disease-induced mortality, as well as establishing the dependence of pathogen relatedness to disease-induced mortality. However, by sacrificing the ability to determine stability criteria, we are able to make conclusions about the biological forces shaping evolutionary equilibria in more general settings.

Our work also provides a more straightforward approach to studying pathogen coinfection. Most analyses of coinfecting strains involve explicitly modelling complex within-host pathogen dynamics [39]. They take into account such things as pathogen exploitation of host resources [40], the production of molecules used as a public good by the group of coinfecting pathogens [41], and the interaction between pathogens and host lymphocytes [42], to make predictions about the evolution of disease-induced mortality. Our framework gives up some of these details by capturing the within-host dynamics by the genetic relatedness of coinfecting pathogen strains, but this allows us to make more general predictions about how pathogen strains should interact with one another without the need for additional modelling assumptions.

Much of this previous work on coinfecting pathogen strains has also focused on the evolution of pathogen virulence. Throughout this paper, we have been careful to refer to the evolution of pathogen disease-induced mortality instead of virulence. Virulence is generally defined to be the reduction in host fitness due to infection by the pathogen [10, 11, 111, 23]. Host fitness is comprised of two components: reproduction and survival. In our first example on an age-structured model, pathogens only affect host survival and not host reproduction, so it would be appropriate to refer to disease-induced mortality as virulence. However, in the second example, pathogens affect both host survival and reproduction. Host survival is affected directly by pathogen disease-induced mortality. Host reproduction is affected indirectly through the effect of disease-induced mortality on host clearance. Higher disease-induced mortality will push for hosts to invest more in their immune systems, taking away resources from reproduction and lowering their reproductive success. This adds an additional dimension to the effect of the pathogen on host fitness, and means that pathogen virulence is not necessarily equivalent to pathogen disease-induced mortality. Depending on the model under study, then, the evolutionary consequences of pathogen relatedness on virulence may be more complex than just the consequences of relatedness on disease-induced mortality alone.

Chapter 5

Conclusion

5.1 Summary

In this thesis, I have provided three pieces of evidence to support the claim that host-pathogen coevolution and multiple types of hosts are important forces governing real-world populations and that they lead to theoretical predictions not found in research that excludes either of these effects. From a practical point of view, these new predictions can provide additional perspective for conversations on the spread and management of infectious diseases.

I began, in Chapter 2, with a model of host-pathogen coevolution in a scenario where hosts are categorized into female and male groups. The goal was to develop a theoretical explanation of the differences in immune investment and disease-induced mortality observed between the sexes across a wide variety of infectious disease data. Previous authors have studied how differences in host immune investment [24, 25, 27] or pathogen disease-induced mortality [15] could have evolved, but without considering the effects of coevolution this does not provide a complete explanation for how both hosts and pathogens could have evolved to the point that is observed in clinical data. I have contributed to this discussion by showing that coevolutionary forces, responding to inherent differences between types of hosts due to vertical transmission and sex-specific costs to immune investment, can lead to a state in which female hosts invest heavily in their immune systems while pathogens exhibit increased disease-induced mortality in male hosts.

One feature of the model used in Chapter 2 is that host type is fixed. In Chapter 3, I relax this assumption by instead considering a model where hosts are able to change their type. In particular, hosts are categorized according to whether or not they choose to engage in prophylactic behaviour (e.g., hand washing, social distancing) to reduce their likelihood of transmitting an infectious disease. While both hosts and pathogens are evolving in this scenario, they are doing so on different time scales. I modelled host evolution using the replicator dynamic [34] and assumed that host behaviour reached a quasi-equilibrium before considering the evolution of the pathogen. The main finding was that accounting for these multiple types of hosts and their coevolution with pathogens gives rise to the prediction that the level of the pathogen's exploitation of its host will be lower than it would be in the absence of these effects.

Both of the models in Chapters 2 and 3 considered only a single pathogen strain. In Chapter 4, I relax this assumption and instead consider coinfection of hosts by multiple, genetically related pathogen strains. Much of the literature on coinfecting pathogen strains uses complex models of within-host pathogen dynamics [39] to take into account such things as pathogen exploitation of host resources [40], the production of molecules as a public good used by pathogens [41], and interactions between pathogens and host immune cells [16]. Instead, I provide a framework based on kin selection theory [43] for analyzing these kinds of models in the presence of multiple types of hosts. As an illustrative example, I consider a scenario in which hosts are coevolving with pathogens, and show how the relatedness between coinfecting pathogen strains can affect the evolution of host immune investment and how this, in turn, feeds back into affecting pathogen evolution.

The nature of the topics under investigation in this thesis makes it challenging to compare results to empirical observations. Data sets on costs and levels of immune investment, on the proportion of a population engaging in prophylactic behaviours at any given time, or on the relatedness among a group of coinfecting pathogen strains are not readily available or easily measured. Instead, I have chosen to focus on theoretical predictions. Experimental studies could be designed, though, to test these predictions. For example, one could survey groups of individuals over the course of a flu season and ask them to report on how often they engaged in some prophylactic behaviour, such as hand washing or wearing a mask. This could give a sense of the prevalence of these behaviours in the larger population, but care would need to be taken to account for the fact that individuals knowing they will be surveyed could cause them to engage in those behaviours more often and artificially inflate the observed rate of engagement in prophylaxis.

5.2 Future Directions

Part of the goal in Chapter 2 was to develop an evolutionary explanation for the trend observed across a wide variety of infectious diseases of increased immune investment in females and increased pathogen disease-induced mortality in males. Previous literature, which neglected host-pathogen coevolution, only addressed half of this trend. Authors have explained sex differences in host immune investment as resulting from sexual selection acting on males [24, 25, 26], sex differences in pathogen life history traits [29], and female reproduction (Chapter 2 of this thesis). Other authors have provided explanations of the evolution of sex-specific levels of pathogen disease-induced mortality as a result of inherent differences in host immune investment [48] or vertical transmission [15]. While the coevolutionary model I have investigated is able to provide a more complete explanation of the trend observed in clinical data, it hinges on the possibility of vertical transmission. One open question that remains in this area, then, is: How could hosts and pathogens have coevolved to a state of high female immune investment and high male disease-induced mortality, for diseases in which vertical transmission does not occur? In their work on pathogen evolution in response to sex-specific differences in hosts, Cousineau and Alizon [48] show how changing the structure of the transmission rate can influence the level of virulence to which natural selection pushes the pathogen. In particular, they show how allowing a particular sex to infect only the same sex, only the opposite sex, or a mixture of both sexes can select for different levels of virulence [48]. However, this is only done in the case of pathogen evolution, so the coevolutionary consequences of this are not clear. Investigating the role of contact patterns between the sexes on host-pathogen coevolution could provide an alternate explanation for patterns of immune investment and disease-induced mortality that does not rely on vertical transmission.

One of the assumptions made in Chapter 3 is that hosts have information on the entire population when deciding whether or not to engage in prophylactic behaviour. In human populations, though, we know that hosts will make decisions based on their interactions with only a subset of the population. Modelling such structure within the host population typically involves using networks. In the case of epidemic models, previous authors have studied the effects of different types of networks [94], sexually transmitted diseases spreading on networks of female and male hosts [95], and adaptive networks where individual hosts can change who they are connected to over time [96]. Networks have been discussed as a way to model not only infectious diseases but also the spread of information between individuals [78], or as a way to explain pathogen adaptation from an inclusive-fitness perspective [97]. While this literature links the ideas of spatial structure and infectious diseases, it is still unknown how this affects predictions in scenarios where hosts are able to switch between different types. The model presented in Chapter 3 of this thesis could be extended to study the consequences of a network structure on predictions of the coevolution of host behaviour and pathogen exploitation. For example, Wild, Gardner, and West [97] show that limited pathogen dispersal in a spatially structured population can select for lower levels of virulence. However, in a spatially structured host population split into those engaging and not engaging in prophylactic behaviours, pathogens with limited dispersal that find themselves in a group of hosts engaging in prophylaxis may no longer be at a selective advantage for lowering their virulence. Conversely, if the pathogen reduces its virulence within a group of hosts, that creates less incentive for those hosts to engage in prophylactic behaviours. If the fraction of hosts engaging in prophylaxis drops too low, the results presented in Chapter 3 suggest that natural selection will push for increased pathogen virulence. Predicting the exact endpoint of host-pathogen coevolution in such a setting requires further study of spatially structured coevolution models.

This idea of spatial structure can also be extended to scenarios like those discussed in Chapter 4. Here, I have considered the effects of relatedness among pathogen strains on the coevolution of hosts and pathogens, but I have not considered the effects of relatedness among hosts. Hamilton's [45] ideas on inclusive fitness pertain to hosts, as well, and so we would expect to see closely related hosts cooperating with each other. In particular, if hosts are clustered into groups and are closely related to those within their group, we would expect them to invest more heavily in their immune systems in order to protect not only themselves but also those around them. As seen in the sex-specific modelling of Cousineau and Alizon [48], this increased immune investment could then select for higher pathogen virulence within that host group. Understanding the interplay between host relatedness, pathogen relatedness, and host-pathogen coevolution would involve extending the framework developed in Chapter 4 to include spatially clustered and genetically related host groups.

Bibliography

[1] R. Ross. An application of the theory of probabilities to the study of a priori pathometry.—Part I. *Proc. R. Soc. A*, 92(638):204–230, 1916. https://doi.org/10.1098/rspa.1916.0007.

[2] W. O. Kermack and A. G. McKendrick. A contribution to the mathematical theory of epidemics. *Proc. R. Soc. A*, 115(772):700–721, 1927. https://doi.org/10.1098/rspa.1927.0118.

[3] J. M. Heffernan, R. J. Smith, and L. M. Wahl. Perspectives on the basic reproductive ratio. *J. R. Soc. Interface*, 2:281–293, 2005. https://doi.org/10.1098/rsif.2005.0042.

[4] N. F. Britton. *Essential Mathematical Biology*. Springer, 2003. ISBN: 9781852335366.

[5] F. Dercole and S. Rinaldi. *Analysis of Evolutionary Processes: The Adaptive Dynamics Approach and Its Applications*. Princeton University Press, 2008. ISBN: 9780691120065.

[6] U. Dieckmann and R. Law. The dynamical theory of coevolution: a derivation from stochastic ecological processes. *J. Math. Biol.*, 34:579–612, 1996. https://doi.org/10.1007/BF02409751.

[7] J. A. J. Metz, R. M. Nisbet, and S. A. H. Geritz. How should we define 'fitness' for general ecological scenarios? *Trends Ecol. Evol.*, 7(6):198–202, 1992. https://doi.org/10.1016/0169-5347(92)90073-K.

[8] C. E. Cressler, D. V. McLeod, C. Rozins, J. van den Hoogen, and T. Day. The adaptive evolution of virulence: a review of theoretical predictions and empirical tests. *Parasitology*, 143(7):915–930, 2016. https://doi.org/10.1017/S003118201500092X.

[9] S. A. Frank. Models of parasite virulence. *Q. Rev. Biol.*, 71(1):37–78, 1996. https://doi.org/10.1086/419267.

[10] R. M. Anderson and R. M. May. Coevolution of hosts and parasites. *Parasitology*, 85:411–426, 1982. https://doi.org/10.1017/S0031182000055360.

[11] P. W. Ewald. Host-parasite relations, vectors, and the evolution of disease severity. *Annu. Rev. Ecol. Evol. Syst.*, 14:465–485, 1983. https://doi.org/10.1146/annurev.es.14.110183.002341.

[12] S. Alizon and Y. Michalakis. Adaptive virulence evolution: the good old fitness-based approach. *Trends Ecol. Evol.*, 30(5):248–254, 2015. https://doi.org/10.1016/j.tree.2015.02.009.

[13] T. Day. On the evolution of virulence and the relationship between various measures of mortality. *Proc. R. Soc. B*, 269:1317–1323, 2002. https://doi.org/10.1098/rspb.2002.2021.

[14] C. Fraser, K. Lythgoe, G. E. Leventhal, G. Shirreff, T. D. Hollingsworth, S. Alizon, and S. Bonhoeffer. Virulence and pathogenesis of HIV-1 infection: an evolutionary perspective. *Science*, 343(6177):1243727, 2014. https://doi.org/10.1126/science.1243727.

[15] F. Úbeda and V. A. A. Jansen. The evolution of sex-specific virulence in infectious diseases. *Nat. Commun.*, 7, 2016. https://doi.org/10.1038/ncomms13849.

[16] S. Alizon. Transmission-recovery trade-offs to study parasite evolution. *Am. Nat.*, 172(3):E113–E121, 2008. https://doi.org/10.1086/589892.

[17] S. Gandon. Evolution of multihost parasites. *Evolution*, 58(3):455–469, 2004. https://doi.org/10.1111/j.0014-3820.2004.tb01669.x.

[18] L. Lehmann, C. Mullon, E. Akçay, and J. Van Cleve. Invasion fitness, inclusive fitness, and reproductive numbers in heterogeneous populations. *Evolution*, 70(8):1689–1702, 2016. https://doi.org/10.1111/evo.12980.

[19] T. Day and J. G. Burns. A consideration of patterns of virulence arising from host-parasite coevolution. *Evolution*, 57(3):671–676, 2003. https://doi.org/10.1111/j.0014-3820.2003.tb01558.x.

[20] J. Maynard Smith. *Evolution and the Theory of Games*. Cambridge University Press, 1982. ISBN: 0521288843.

[21] F. B. Christiansen. On conditions for evolutionary stability for a continuously varying character. *Am. Nat.*, 138(1):37–50, 1991. https://doi.org/10.1086/285203.

[22] I. Eshel. Evolutionary and continuous stability. *J. Theor. Biol.*, 103(1):99–111, 1983. https://doi.org/10.1016/0022-5193(83)90201-1.

[23] A. F. Read. The evolution of virulence. *Trends Microbiol.*, 2(3):73–76, 1994. https://doi.org/10.1016/0966-842X(94)90537-1.

[24] M. Zuk and A. M. Stoehr. Immune defense and host life history. *Am. Nat.*, 160(S4):S9–S22, 2002. https://doi.org/10.1086/342131.

[25] M. Zuk. The sicker sex. *PLoS Pathog.*, 5(1):e1000267, 2009. https://doi.org/10.1371/journal.ppat.1000267.

[26] M. Zuk and A. M. Stoehr. Sex differences in susceptibility to infection: an evolutionary perspective. In S. Klein and C. Roberts, editors, *Sex Hormones and Immunity to Infection*. Springer, Berlin, Heidelberg, 2010. ISBN: 978-3-642-02154-1.

[27] A. M. Stoehr and H. Kokko. Sexual dimorphism in immunocompetence: what does life-history theory predict? *Behav. Ecol.*, 17(5):751–756, 2006. https://doi.org/10.1093/beheco/ark018.

[28] M. van Baalen. Coevolution of recovery ability and virulence. *Proc. R. Soc. B*, 265:317–325, 1998. https://doi.org/10.1098/rspb.1998.0298.

[29] O. Restif and W. Amos. The evolution of sex-specific immune defences. *Proc. R. Soc. B*, 277(1691):2247–2255, 2010. https://doi.org/10.1098/rspb.2010.0188.

[30] A. Hurford, D. Cownden, and T. Day. Next-generation tools for evolutionary invasion analyses. *J. R. Soc. Interface*, 7:561–571, 2010. https://doi.org/10.1098/rsif.2009.0448.

[31] P. van den Driessche and J. Watmough. Reproduction numbers and sub-threshold endemic equilibria for compartmental models of disease transmission. *Math. Biosci.*, 180:29–48, 2002. https://doi.org/10.1016/S0025-5564(02)00108-6.

[32] O. Diekmann, J. A. P. Heesterbeek, and M. G. Roberts. The construction of next-generation matrices for compartmental epidemic models. *J. R. Soc. Interface*, 7:873–885, 2010. https://doi.org/10.1098/rsif.2009.0386.

[33] J. Pharaon and C. T. Bauch. The influence of social behaviour on competition between virulent pathogen strains. *J. Theor. Biol.*, 455:47–53, 2018. https://doi.org/10.1016/j.jtbi.2018.06.028.

[34] P. D Taylor and L. B. Jonker. Evolutionary stable strategies and game dynamics. *Math. Biosci.*, 40:145–156, 1978. https://doi.org/10.1016/0025-5564(78)90077-9.

[35] P. Schuster and K. Sigmund. Replicator dynamics. *J. Theor. Biol.*, 100(3):533–538, 1983. https://doi.org/10.1016/0022-5193(83)90445-9.

[36] G. B. Sharp, Y. Kawaoka, D. J. Jones, W. J. Bean, S. P. Pryor, V. Hinshaw, and R. G. Webster. Coinfection of wild ducks by influenza A viruses: distribution patterns and

biological significance. *J. Virol.*, 71(8):6128–6135, 1997. https://doi.org/10.1128/jvi.71.8.6128-6135.1997.

[37] J. C. de Roode, M. E. H. Helinski, M. A. Anwar, and A. F. Read. Dynamics of multiple infection and within-host competition in genetically diverse malaria infections. *Am. Nat.*, 166(5), 2005. https://doi.org/10.1086/491659.

[38] O. Balmer and M. Tanner. Prevalence and implications of multiple-strain infections. *Lancet*, 11(11):868–878, 2011. https://doi.org/10.1016/S1473-3099(11)70241-9.

[39] S. Alizon, J. C. de Roode, and Y. Michalakis. Multiple infections and the evolution of virulence. *Ecol. Lett.*, 16:556–567, 2013. https://doi.org/10.1111/ele.12076.

[40] T. Kamiya, N. Mideo, and S. Alizon. Coevolution of virulence and immunosuppression in multiple infections. *J. Evol. Biol.*, 31:995–1005, 2018. https://doi.org/10.1111/jeb.13280.

[41] M. T. Sofonea, S. Alizon, and Y. Michalakis. From within-host interactions to epidemiological competition: a general model for multiple infections. *Philos. Trans. R. Soc. B*, 370, 2015. https://doi.org/10.1098/rstb.2014.0303.

[42] S. Alizon and M. van Baalen. Multiple infections, immune dynamics, and the evolution of virulence. *Am. Nat.*, 172(4):E150–E168, 2008. https://doi.org/10.1086/590958.

[43] S. A. Frank. A kin selection model for the evolution of virulence. *Proc. R. Soc. B*, 250:195–197, 1992. https://doi.org/10.1098/rspb.1992.0149.

[44] P. D. Taylor and S. A. Frank. How to make a kin selection model. *J. Theor. Biol.*, 180(1):27–37, 1996. https://doi.org/10.1006/jtbi.1996.0075.

[45] W. D. Hamilton. The genetical evolution of social behaviour. *J. Theor. Biol.*, 7(1):1–16, 1964. https://doi.org/10.1016/0022-5193(64)90038-4.

[46] T. C. Washburn, D. N. Medearis, and B. Childs. Sex differences in susceptibility to infections. *Pediatrics*, 35(1):57–64, 1965.

[47] C. B. Holmes, H. Hausler, and P. Nunn. A review of sex differences in the epidemiology of tuberculosis. *Int. J. Tuberc. Lung D.*, 2(2):96–104, 1998.

[48] S. V. Cousineau and S. Alizon. Parasite evolution in response to sex-based host heterogeneity in resistance and tolerance. *J. Evol. Biol.*, 27(12):2753–2766, 2014. https://doi.org/10.1111/jeb.12541.

[49] C. T. Bauch and D. J. D. Earn. Vaccination and the theory of games. *Proc. Natl. Acad. Sci. U.S.A.*, 101(36):13391–13394, 2004. https://doi.org/10.1073/pnas.0403823101.

[50] C. L. Murall, C. T. Bauch, and T. Day. Could the human papillomavirus vaccines drive virulence evolution? *Proc. R. Soc. B*, 282, 2015. https://doi.org/10.1098/rspb.2014.1069.

[51] S. Gandon, M. J. Mackinnon, S. Nee, and A. F. Read. Imperfect vaccines and the evolution of pathogen virulence. *Nature*, 414:751–756, 2001. https://doi.org/10.1038/414751a.

[52] S. Gandon, M. Mackinnon, S. Nee, and A. Read. Imperfect vaccination: some epidemiological and evolutionary consequences. *Proc. R. Soc. B*, 270(1520):1129–1136, 2003. https://doi.org/10.1098/rspb.2003.2370.

[53] D. Gemmati, K. Varani, B. Bramanti, R. Piva, G. Bonaccorsi, A. Trentini, M. C. Manfrinato, V. Tisato, A. Carè, and T. Bellini. “Bridging the Gap” Everything that could have been avoided if we had applied gender medicine, pharmacogenetics and personalized medicine in the gender-omics and sex-omics era. *Int. J. Mol. Sci.*, 21(1):296, 2020. https://doi.org/10.3390/ijms21010296.

[54] J. Fischer, N. Jung, N. Robinson, and C. Lehmann. Sex differences in immune responses to infectious diseases. *Infection*, 43:399–403, 2015. https://doi.org/10.1007/s15010-015-0791-9.

[55] E. N. Fish. The X-files in immunity: sex-based differences predispose immune responses. *Nat. Rev. Immunol.*, 8:737–744, 2008. https://doi.org/10.1038/nri2394.

[56] M. A. Ingersoll. Sex differences shape the response to infectious diseases. *PLoS Pathog.*, 13(12), 2017. https://doi.org/10.1371/journal.ppat.1006688.

[57] S. L. Klein. The effects of hormones on sex differences in infection: from genes to behavior. *Neurosci. Biobehav. Rev.*, 24(6):627–638, 2000. https://doi.org/10.1016/S0149-7634(00)00027-0.

[58] C. W. Roberts, W. Walker, and J. Alexander. Sex-associated hormones and immunity to protozoan parasites. *Clin. Microbiol. Rev.*, 14(3):476–488, 2001. https://doi.org/10.1128/CMR.14.3.476–488.2001.

[59] J. K. Chye, C. T. Lim, K. B. Ng, J. M. H. Lim, R. George, and S. K. Lam. Vertical transmission of dengue. *Clin. Infect. Dis.*, 25(6):1374–1377, 1997. https://doi.org/10.1086/516126.

[60] A. C. Freitas, F. C. Mariz, M. A. R. Silva, and A. L. S. Jesus. Human papillomavirus vertical transmission: review of current data. *Clin. Infect. Dis.*, 56(10):1451–1456, 2013. https://doi.org/10.1093/cid/cit066.

[61] I. Gentile and G. Borgia. Vertical transmission of hepatitis B virus: challenges and solutions. *Int. J. Womens Health*, 6:605–611, 2014. https://dx.doi.org/10.2147

[62] L. Berec. Mate search and mate-finding Allee effect: on modeling mating in sex-structured population models. *Theor. Ecol.*, 11:225–244, 2018. https://doi.org/10.1007/s12080-017-0361-0.

[63] H. Caswell and D. E. Weeks. Two-sex models: chaos, extinction, and other dynamic consequences of sex. *Am. Nat.*, 128(5):707–735, 1986. https://doi.org/10.1086/284598.

[64] K. W. Beagley and C. M. Gockel. Regulation of innate and adaptive immunity by the female sex hormones oestradiol and progesterone. *FEMS Immunol. Med. Microbiol.*, 38(1):13–22, 2003. https://doi.org/10.1016/S0928-8244(03)00202-5.

[65] M. Cutolo, A. Sulli, S. Capellino, B. Villaggio, P. Montagna, B. Seriolo, and R. H. Straub. Sex hormones influence on the immune system: basic and clinical aspects in autoimmunity. *Lupus*, 13(9):635–638, 2004. https://doi.org/10.1191

[66] I. J. Tan, E. Peeva, and G. Zandman-Goddard. Hormonal modulation of the immune system - A spotlight on the role of progestogens. *Autoimmun. Rev.*, 14:536–542, 2015. http://dx.doi.org/10.1016/j.autrev.2015.02.004.

[67] T. Day and P. D. Taylor. Evolutionary dynamics and stability in discrete and continuous games. *Evol. Ecol. Res.*, 5:605–613, 2003.

[68] O. Leimar. Multidimensional convergence stability. *Evol. Ecol. Res.*, 11:191–208, 2009.

[69] P. W. Ewald. Transmission modes and evolution of the parasitism-mutualism continuum. *Ann. N. Y. Acad. Sci.*, 503(1):295–306, 1987. https://doi.org/10.1111/j.1749-6632.1987.tb40616.x.

[70] J. S. Ayres. Cooperative microbial tolerance behaviors in host-microbiota mutualism. *Cell*, 165(6):1323–1331, 2016. https://doi.org/10.1016/j.cell.2016.05.049.

[71] M. Lipsitch, M. A. Nowak, D. Ebert, and R. M. May. The population dynamics of vertically and horizontally transmitted parasites. *Proc. R. Soc. B*, 260(1359):321–327, 1995. https://doi.org/10.1098/rspb.1995.0099.

[72] D. Fairweather and N. R. Rose. Women and autoimmune diseases. *Emerg. Infect. Dis.*, 10(11):2005–2011, 2004. https://dx.doi.org/10.3201

[73] N. Gleicher and D. H. Barad. Gender as risk factor for autoimmune diseases. *J. Autoimmun.*, 28(1):1–6, 2007. https://doi.org/10.1016/j.jaut.2006.12.004.

[74] S. T. Ngo, F. J. Steyn, and P. A. McCombe. Gender differences in autoimmune disease. *Front. Neuroendocrinol.*, 35(3):347–369, 2014. https://doi.org/10.1016/j.yfrne.2014.04.004.

[75] H. J. Bremermann and J. Pickering. A game-theoretical model of parasite virulence. *J. Theor. Biol.*, 100(3):411–426, 1983. https://doi.org/10.1016/0022-5193(83)90438-1.

[76] H. Knolle. Host density and the evolution of parasite virulence. *J. Theor. Biol.*, 136(2):199–207, 1989. https://doi.org/10.1016/S0022-5193(89)80226-7.

[77] T. C. Reluga. Simple models of antibiotic cycling. *Math. Med. Biol.*, 22(2):187–208, 2005. https://doi.org/10.1093/imammb/dqi002.

[78] C. T. Bauch and A. P. Galvani. Social factors in epidemiology. *Science*, 342:47–49, 2013. https://doi.org/10.1126/science.1244492.

[79] M. Schaller. The behavioural immune system and the psychology of human sociality. *Philos. Trans. R. Soc. B*, 366:3418–3426, 2011. https://doi.org/10.1098/rstb.2011.0029.

[80] R. M. Anderson, H. Heesterbeek, D. Klinkenberg, and T. D. Hollingsworth. How will country-based mitigation measures influence the course of the covid-19 epidemic? *Lancet*, 395(10228):P931–P934, 2020. https://doi.org/10.1016/S0140-6736(20)30567-5.

[81] J. Antonovics, Y. Iwasa, and M. P. Hassell. A generalized model of parasitoid, venereal, and vector-based transmission processes. *Am. Nat.*, 145(5):661–675, 1995. https://doi.org/10.1086/285761.

[82] H. McCallum, N. Barlow, and J. Hone. How should pathogen transmission be modelled? *Trends Ecol. Evol.*, 16(6):295–300, 2001. https://doi.org/10.1016/S0169-5347(01)02144-9.

[83] L. Osterberg and T. Blaschke. Adherence to medication. *N. Engl. J. Med.*, 353(5):487–497, 2005. https://doi.org/10.1056/NEJMra050100.

[84] J. Robison and M. A. Rogers. Adherence to exercise programmes. *Sports Med.*, 17(1):39–52, 1994. https://doi.org/10.2165/00007256-199417010-00004.

[85] S. R. Patton. Adherence to diet in youth with type 1 diabetes. *J. Am. Diet. Assoc.*, 111(4):550–555, 2011. https://doi.org/10.1016/j.jada.2011.01.016.

[86] C. Matessi and C. Di Pasquale. Long-term evolution of multilocus traits. *J. Math. Biol.*, 34:613–653, 1996. https://doi.org/10.1007/BF02409752.

[87] E. M. Poolman, E. H. Elbasha, and A. P. Galvani. Vaccination and the evolutionary ecology of human papillomavirus. *Vaccine*, 26:C25–C30, 2008. https://doi.org/10.1016/j.vaccine.2008.04.010.

[88] D. P. Hughes, S. B. Andersen, N. L. Hywel-Jones, W. Himaman, J. Billen, and J. J. Boomsma. Behavioral mechanisms and morphological symptoms of zombie ants dying from fungal infection. *BMC Ecol.*, 11, 2011. https://doi.org/10.1186/1472-6785-11-13.

[89] Ø. Øverli, M. Páll, B. Borg, M. Jobling, and S. Winberg. Effects of *Schistocephalus solidus* infection on brain monoaminergic activity in female three-spined sticklebacks *Gasterosteus aculeatus*. *Proc. R. Soc. B*, 268(1474):1411–1415, 2001. https://doi.org/10.1098/rspb.2001.1668.

[90] W. Wesołowska and T. Wesołowska. Do *Leucochloridium* sporocysts manipulate the behaviour of their snail hosts? *J. Zool.*, 292(3):151–155, 2014. https://doi.org/10.1111/jzo.12094.

[91] H. W. Hethcote, M. A. Lewis, and P. van den Driessche. An epidemiological model with a delay and a nonlinear incidence rate. *J. Math. Biol.*, 27(1):49–64, 1989. https://doi.org/10.1007/BF00276080.

[92] K. L. Cooke and P. van den Driessche. Analysis of an SEIRS epidemic model with two delays. *J. Math. Biol.*, 35:240–260, 1996. https://doi.org/10.1007/s002850050051.

[93] S. Gao, L. Chen, J. J. Nieto, and A. Torres. Analysis of a delayed epidemic model with pulse vaccination and saturation incidence. *Vaccine*, 24:6037–6045, 2006. https://doi.org/10.1016/j.vaccine.2006.05.018.

[94] R. Pastor-Satorras and A. Vespignani. Epidemic dynamics and endemic states in complex networks. *Phys. Rev. E*, 63(6):066117, 2001. https://doi.org/10.1103/PhysRevE.63.066117.

[95] M. E. J. Newman. Spread of epidemic disease on networks. *Phys. Rev. E*, 66:016128, 2002. https://doi.org/10.1103/PhysRevE.66.016128.

[96] T. Gross, C. J. D. D'Lima, and B. Blasius. Epidemic dynamics on an adaptive network. *Phys. Rev. Lett.*, 96:208701, 2006. https://doi.org/10.1103/PhysRevLett.96.208701.

[97] G. Wild, A. Gardner, and S. A. West. Adaptation and the evolution of parasite virulence in a connected world. *Nature*, 459:983–986, 2009. https://doi.org/10.1038/nature08071.

[98] T. Day and S. Gandon. Insights from Price's equation into evolutionary epidemiology. In Z. Feng, U. Dieckmann, and S. Levin, editors, *Disease Evolution: Models, Concepts, and Data Analyses*, volume 71 of *DIMACS Series in Discrete Mathematics and Theoretical Computer Science*, pages 23–44. American Mathematical Society, 2006. ISBN: 9780821837535.

[99] T. Day, T. Parsons, A. Lambert, and S. Gandon. The Price equation and evolutionary epidemiology. *Philos. Trans. R. Soc. B*, 375(1797), 2020. https://doi.org/10.1098/rstb.2019.0357.

[100] C. D. Meyer. *Matrix Analysis and Applied Linear Algebra*. SIAM, 2000. ISBN: 9780898714548.

[101] W. Mitkowski. Remarks on stability of positive linear systems. *Control Cybern.*, 29(1):295–304, 2000.

[102] H. Cao and Y. Zhou. The discrete age-structured SEIT model with application to tuberculosis transmission in China. *Math. Comput. Model.*, 55:385–395, 2012. https://doi.org/10.1016/j.mcm.2011.08.017.

[103] H. W. Hethcote. An age-structured model for pertussis transmission. *Math. Biosci.*, 145(2):89–136, 1997. https://doi.org/10.1016/S0025-5564(97)00014-X.

[104] R. Iritani, E. Visher, and M. Boots. The evolution of stage-specific virulence: Differential selection of parasites in juveniles. *Evol. Lett.*, 3(2):162–172, 2019. https://doi.org/10.1002/evl3.105.

[105] L. Berec and D. Maxin. Fatal or harmless: extreme bistability induced by sterilizing, sexually transmitted pathogens. *Bull. Math. Biol.*, 75:258–273, 2013. https://doi.org/10.1007/s11538-012-9802-5.

[106] L. Berec, E. Janoušková, and M. Theuer. Sexually transmitted infections and mate-finding Allee effects. *Theor. Popul. Biol.*, 114:59–69, 2017. https://doi.org/10.1016/j.tpb.2016.12.004.

[107] B. Koskella, T. Giraud, and M. E. Hood. Pathogen relatedness affects the prevalence of within-host competition. *Am. Nat.*, 168(1):121–126, 2006. https://doi.org/10.1086/505770https://doi.org/10.1086/505770.

[108] M. López-Villavicencio, F. Courjol, A. K. Gibson, M. E. Hood, O. Jonot, J. A. Shykoff, and T. Giraud. Competition, cooperation among kin, and virulence in multiple infections. *Evolution*, 65(5):1357–1366, 2010. https://doi.org/10.1111/j.1558-5646.2010.01207.x.

[109] G. R. Price. Selection and covariance. *Nature*, 227:520–520, 1970. http://dx.doi.org/10.1038/227520a0.

[110] G. R. Price. Extension of covariance selection mathematics. *Ann. Hum. Genet.*, 35:485–490, 1972.

[111] S. Levin and D. Pimentel. Selection of intermediate rates of increase in parasite-host systems. *Am. Nat.*, 117(3):308–315, 1981. https://doi.org/10.1086/283708.

Appendix A

Chapter 2 - Evolutionary Analysis for Simple Cases

This appendix provides more details on the evolutionary analysis conducted in the absence of sex-specific differences, as discussed in the Results of the main text.

For the first case, where all sex differences are stripped away, we start our evolutionary analysis by introducing a rare mutant-type pathogen with disease-induced mortality $\tilde{\alpha}$. Transmission from hosts infected with this mutant pathogen strain to susceptible hosts occurs at a rate $\tilde{\beta}$, so the total number $\tilde{I}$ of hosts infected by the mutant strain changes according to

$$\frac{d\tilde{I}}{dt} = \bar{S}\tilde{\beta}\tilde{I} - (\gamma + \tilde{\alpha} + \mu)\tilde{I} = [\tilde{\beta}\bar{S} - (\gamma + \tilde{\alpha} + \mu)]\tilde{I}, \tag{A.1}$$

where $\bar{S}$ represents the equilibrium level of susceptible hosts in (2.15). From (A.1), we see that the mutant pathogen population grows if $\tilde{\beta}\bar{S} - (\gamma + \tilde{\alpha} + \mu) > 0$ and shrinks otherwise. This allows us to define a fitness function for the mutant pathogen strain:

$$W_\alpha(\tilde{\alpha}, \alpha) = \frac{\tilde{\beta}\bar{S}}{\gamma + \tilde{\alpha} + \mu} = \frac{\tilde{\beta}(\gamma + \alpha + \mu)}{\beta(\gamma + \tilde{\alpha} + \mu)}. \tag{A.2}$$

We can recognize $\beta/(\gamma + \alpha + \mu)$ as the resident pathogen's basic reproductive number, $\mathcal{R}_0$ [3]

and similarly for the mutant pathogen. This allows us to interpret W_α as

$$W_\alpha(\tilde{\alpha}, \alpha) = \frac{\tilde{\mathcal{R}}_0}{\mathcal{R}_0}, \tag{A.3}$$

and so maximizing the mutant pathogen's fitness equates to maximizing its basic reproductive number, $\tilde{\mathcal{R}}_0$, as is a common theme in previous pathogen evolution literature (e.g., [10, 13]). If we substitute in $\beta = \beta_{\max}\tilde{\alpha}/(\tilde{\alpha} + d)$, then $\tilde{\mathcal{R}}_0$ is maximized when

$$\tilde{\alpha} = \sqrt{d(\gamma + \mu)}. \tag{A.4}$$

To study the evolution of hosts' immune investment, we then introduce a rare mutant-type host with recovery $\hat{\gamma}$. If new mutant hosts are born at a rate $\hat{b} = b_{\max} - c(\hat{\gamma} + \gamma)$, then the total numbers $\hat{S}$ and $\hat{I}$ of susceptible and infective mutant hosts, respectively, will change according to

$$\frac{d\hat{S}}{dt} = \frac{\hat{b}}{2}(\hat{S} + \hat{I}) + \hat{\gamma}\hat{I} - \hat{S}\beta I - \mu\hat{S} \tag{A.5a}$$

$$\frac{d\hat{I}}{dt} = \hat{S}\beta\bar{I} - (\hat{\gamma} + \alpha + \mu)\hat{I}, \tag{A.5b}$$

where $\bar{I}$ represents the equilibrium level of infective resident hosts given in (2.15). The Jacobian matrix of this subsystem, evaluated at the mutant-free equilibrium $\hat{S} = \hat{I} = 0$, is

$$J = \begin{bmatrix} \frac{\hat{b}}{2} - \beta\bar{I} - \mu & \frac{\hat{b}}{2} + \hat{\gamma} \\ \beta\bar{I} & -(\hat{\gamma} + \alpha + \mu) \end{bmatrix}. \tag{A.6}$$

If we then write $J = F - V$, where

$$F = \begin{bmatrix} \frac{\hat{b}}{2} & \frac{\hat{b}}{2} \\ 0 & 0 \end{bmatrix} \quad \text{and} \quad V = \begin{bmatrix} \beta\bar{I} + \mu & -\hat{\gamma} \\ -\beta\bar{I} & \hat{\gamma} + \alpha + \mu \end{bmatrix}, \tag{A.7}$$

we can use a next-generation matrix approach [30] to define a fitness function W_γ for the mutant-type host as the dominant eigenvalue of the matrix FV^{-1}. Computing this eigenvalue gives us the following fitness function:

$$W_\gamma(\hat{\gamma}, \gamma) = \frac{\hat{b}[(b - 2\mu)(\gamma - \hat{\gamma}) + 2\alpha(\hat{\gamma} + \alpha + \mu)]}{2\mu[b - 2(\alpha + \mu)](\gamma - \hat{\gamma}) + 2b\alpha(\gamma + \alpha + \mu)}. \tag{A.8}$$

From this, we can find the selection gradient $(\partial W_\gamma / \partial \hat{\gamma})|_{\hat{\gamma}=\gamma}$ and substitute in the expression (A.4) for the evolutionarily stable level of pathogen disease-induced mortality.

We next consider the case where there are sex-specific levels of host recovery and pathogen disease-induced mortality, but no inherent asymmetry between host sexes (i.e., no vertical transmission, and female and male hosts incur the same reproductive cost to immune investment). As before, we start by introducing a rare mutant-type pathogen with disease-induced mortality $\tilde{\alpha}_f$ in female hosts and $\tilde{\alpha}_m$ in male hosts. If $\tilde{\beta}_{ij}$ represents the rate of transmission from a sex-j host infected with the mutant strain to a susceptible sex-i host, then the number of female hosts infected with the mutant strain, $\tilde{I}_f$, and the number of male hosts infected with the mutant strain, $\tilde{I}_m$, change according to

$$\frac{d\tilde{I}_f}{dt} = S_f\tilde{\beta}_{ff}\tilde{I}_f + S_f\tilde{\beta}_{fm}\tilde{I}_m - (\gamma_f + \tilde{\alpha}_f + \mu)\tilde{I}_f \tag{A.9a}$$

$$\frac{d\tilde{I}_m}{dt} = S_m\tilde{\beta}_{mf}\tilde{I}_f + S_m\tilde{\beta}_{mm}\tilde{I}_m - (\gamma_m + \tilde{\alpha}_m + \mu)\tilde{I}_m. \tag{A.9b}$$

We can then evaluate the Jacobian matrix of this subsystem at the mutant-free equilibrium (i.e., when $\tilde{I}_f = \tilde{I}_m = 0$) to find

$$J = \begin{bmatrix} S_f\tilde{\beta}_{ff} - \gamma_f - \tilde{\alpha}_f - \mu & S_f\tilde{\beta}_{fm} \\ S_m\tilde{\beta}_{mf} & S_m\tilde{\beta}_{mm} - \gamma_m - \tilde{\alpha}_m - \mu \end{bmatrix}. \tag{A.10}$$

Again using a next-generation matrix approach [30], we write (A.10) as $J = F - V$ where

$$F = \begin{bmatrix} S_f\tilde{\beta}_{ff} & S_f\tilde{\beta}_{fm} \\ S_m\tilde{\beta}_{mf} & S_m\tilde{\beta}_{mm} \end{bmatrix} \quad \text{and} \quad V = \begin{bmatrix} \gamma_f + \tilde{\alpha}_f + \mu & 0 \\ 0 & \gamma_m + \tilde{\alpha}_m + \mu \end{bmatrix}. \tag{A.11}$$

A fitness function W_α for the mutant pathogen strain can then be defined as the dominant eigenvalue of the matrix FV^{-1}. To find the evolutionarily stable levels of disease-induced mortality in female and male hosts, we look for roots of the selection gradients $(\partial W_\alpha/\partial\tilde{\alpha}_f)|_{\tilde{\alpha}_f=\alpha_f}$ and $(\partial W_\alpha/\partial\tilde{\alpha}_m)|_{\tilde{\alpha}_m=\alpha_m}$. While unwieldy to write out in their entirety, these selection gradients do possess a simple structure. In particular,

$$\left.\frac{\partial W_\alpha}{\partial\tilde{\alpha}_f}\right|_{\tilde{\alpha}_f=\alpha_f} = \frac{A(\alpha_f^2 - d(\gamma_f + \mu))}{B} \tag{A.12}$$

and

$$\left.\frac{\partial W_\alpha}{\partial\tilde{\alpha}_m}\right|_{\tilde{\alpha}_m=\alpha_m} = \frac{C(\alpha_m^2 - d(\gamma_m + \mu))}{D}, \tag{A.13}$$

for positive constants A, B, C, and D. This allows us to find the evolutionarily stable levels of pathogen disease-induced mortality to be $\alpha_f = \sqrt{d(\gamma_f + \mu)}$ in female hosts and $\alpha_m = \sqrt{d(\gamma_m + \mu)}$ in male hosts, which are of a similar form to the evolutionarily stable level of pathogen disease-induced mortality (A.4) found in the absence of any sex differences.

Next, we introduce a rare mutant-type host with recovery levels $\hat{\gamma}_f$ in females and $\hat{\gamma}_m$ in males. As discussed in the main text, new mutant hosts are born when a host heterozygous for the mutation mates with a resident (homozygous) host. System (2.11) describes how the numbers of susceptible and infective mutant female hosts, $\hat{S}_f$ and $\hat{I}_f$, change over time. Under the simplifying assumptions made here of no vertical transmission and no sex-specific reproductive costs to immune investment, this system reduces to

$$\frac{d\hat{S}_f}{dt} = \frac{\frac{\hat{b}_f}{2}(\hat{S}_f + \hat{I}_f)(S_m + I_m) + \frac{\hat{b}_m}{2}(S_f + I_f)(\hat{S}_m + \hat{I}_m)}{N} + \hat{\gamma}_f \hat{I}_f - \hat{S}_f \beta_{ff} I_f - \hat{S}_f \beta_{fm} I_m - \mu \hat{S}_f \tag{A.14a}$$

$$\frac{d\hat{I}_f}{dt} = \hat{S}_f \beta_{ff} I_f + \hat{S}_f \beta_{fm} I_m - (\hat{\gamma}_f + \alpha_f + \mu)\hat{I}_f, \tag{A.14b}$$

where $\hat{b}_f = b_{\max} - c(\hat{\gamma}_f + \gamma_m)$ and $\hat{b}_m = b_{\max} - c(\gamma_f + \hat{\gamma}_m)$. An analogous set of equations governs the dynamics of the numbers of susceptible and infective mutant male hosts, $\hat{S}_m$ and $\hat{I}_m$. The Jacobian matrix of this four-dimensional subsystem, evaluated at the mutant-free equilibrium $\hat{S}_f = \hat{S}_m = \hat{I}_f = \hat{I}_m = 0$, can be written as $J = F - V$ where

$$F = \begin{bmatrix} \frac{\frac{\hat{b}_f}{2}(S_m+I_m)}{N} & \frac{\frac{\hat{b}_m}{2}(S_f+I_f)}{N} & \frac{\frac{\hat{b}_f}{2}(S_m+I_m)}{N} & \frac{\frac{\hat{b}_m}{2}(S_f+I_f)}{N} \\ \frac{\frac{\hat{b}_f}{2}(S_m+I_m)}{N} & \frac{\frac{\hat{b}_m}{2}(S_f+I_f)}{N} & \frac{\frac{\hat{b}_f}{2}(S_m+I_m)}{N} & \frac{\frac{\hat{b}_m}{2}(S_f+I_f)}{N} \\ 0 & 0 & 0 & 0 \\ 0 & 0 & 0 & 0 \end{bmatrix} \tag{A.15}$$

and

$$V = \begin{bmatrix} \beta_{ff} I_f + \beta_{fm} I_m + \mu & 0 & -\hat{\gamma}_f & 0 \\ 0 & \beta_{mf} I_f + \beta_{mm} I_m + \mu & 0 & -\hat{\gamma}_m \\ -\beta_{ff} I_f - \beta_{fm} I_m & 0 & \hat{\gamma}_f + \alpha_f + \mu & 0 \\ 0 & -\beta_{mf} I_f - \beta_{mm} I_m & 0 & \hat{\gamma}_m + \alpha_m + \mu \end{bmatrix}. \tag{A.16}$$

The dominant eigenvalue of the matrix FV^{-1} can then be used as a fitness function W_γ for the mutant host [30]. While this fitness function can be computed analytically, finding the roots of the associated selection gradients to compute the evolutionarily stable level of host immune investment must be done numerically.

Appendix B

Chapter 3 - Details of the Replicator Dynamics

Here, we present the details of the derivation of equations (3.3) and (3.4). The replicator dynamic tells us that an individual's decision to start or stop engaging in prophylaxis is proportional to the utility difference between the focal susceptible (resp. infective) individual and the average susceptible (resp. infective) individual in the population, taking into account the utility cost that the focal individual must pay to engage in the prophylactic behaviour. Specifically, the replicator dynamic equation allows us to replace the τ_{ij} terms in our model with the following:

$$-\tau_{01}x + \tau_{10}(1-x) = kx((U_{\text{foc}} - \chi) - U_{\text{avg}}), \tag{B.1}$$

where U_{foc} represents the utility of the focal susceptible individual, U_{avg} represents the utility of the average susceptible individual in the population, and k is a constant that reflects the rate at which individuals change their behaviour based on the behaviour of others. As described in the main text, we measure utility by the force of infection so that the benefit gained by an individual choosing to engage in prophylaxis is a reduced force of infection relative to the average individual. The utility of a focal susceptible individual engaging in prophylaxis, then, is given by

$$U_{\text{foc}} = -(\beta_{10}(1-y) + \beta_{11}y)v, \tag{B.2}$$

while the utility of the average susceptible individual in the population is given by

$$U_{\text{avg}} = -[x(\beta_{10}(1-y) + \beta_{11}y) + (1-x)(\beta_{00}(1-y) + \beta_{01}y)]v. \tag{B.3}$$

Substituting these into the replicator dynamic equation gives

$$-\tau_{01}x + \tau_{10}(1-x) = kx(1-x)[y(\beta_{01} - \beta_{11}) + (1-y)(\beta_{00} - \beta_{10})]v - k\chi x, \tag{B.4}$$

which is equation (3.3) in the main text.

We can derive equation (3.4) in a similar way. Since there is no force of infection acting on an infective individual, the utility of both a focal infective individual engaging in prophylaxis and an average infective individual in the population is zero. However, an infective individual who decides to engage in prophylaxis must still pay the cost of that behaviour. In this case, then, the replicator dynamic equation gives

$$-\phi_{01}y + \phi_{10}(1-y) = -k\chi y. \tag{B.5}$$

Appendix C

Chapter 3 - Linear Stability Analysis

The full resident system of our model (3.5) in the main text is built on the standard two-dimensional SIR model. This standard two-dimensional model has a Jacobian matrix of

$$J = \begin{bmatrix} -\beta_{00}v - 1 & -\beta_{00}u \\ \beta_{00}v & \beta_{00}u - 1 - \gamma \end{bmatrix}. \tag{C.1}$$

which, when evaluated at the disease-free equilibrium (DFE) $(\bar{u}, \bar{v}) = (1, 0)$, has eigenvalues $\lambda_1 = -1$ and $\lambda_2 = \beta_{00} - 1 - \gamma$. The DFE is stable when both eigenvalues are negative, which leads us to the condition that $\mathcal{R}_0 = \beta_{00}/(1 + \gamma) < 1$ for stability.

When $\mathcal{R}_0$ exceeds this threshold, the DFE becomes unstable and the standard two-dimensional system moves towards an endemic equilibrium $(\bar{u}, \bar{v}) = (1/\mathcal{R}_0, (1-1/\mathcal{R}_0)/(1+\gamma))$. To determine the region in which this equilibrium remains stable after we incorporate the host behavioural dynamics, we need to consider the Jacobian matrix of our four-dimensional system (3.5) evaluated at $(\bar{u}, \bar{v}, \bar{x}, \bar{y}) = (1/\mathcal{R}_0, (1 - 1/\mathcal{R}_0)/(1 + \gamma), 0, 0)$:

$$\begin{bmatrix} -\beta_{00}\bar{v} - 1 & -1 - \gamma & * & * \\ \beta_{00}\bar{v} & 0 & * & * \\ 0 & 0 & k(\chi_c - \chi) & 0 \\ 0 & 0 & \frac{\beta_{10}(1+\gamma)}{\beta_{00}} & -1 - \gamma - k\chi \end{bmatrix}, \tag{C.2}$$

where $\chi_c = \mathcal{R}_0 - \left(\frac{k+1}{k}\right)\left(\frac{\beta_{10}}{\beta_{00}}(\mathcal{R}_0 - 1) + 1\right)$ and asterisks denote entries that are possibly non-zero. Since this matrix is block upper triangular, the eigenvalues are given by the eigenvalues of the 2×2 matrices on the diagonal. The 2×2 matrix in the upper left is the Jacobian matrix of the standard two-dimensional SIR model evaluated at the endemic equilibrium $(\bar{u}, \bar{v}, \bar{x}, \bar{y})$, which we know has negative eigenvalues whenever $\mathcal{R}_0 > 1$. The 2×2 matrix in the bottom right is lower triangular, so its eigenvalues are the entries on the main diagonal. The second of these entries is always negative, while the first is negative as long as $\chi > \chi_c$. This defines a critical cost threshold where for $\chi > \chi_c$ the endemic equilibrium $(\bar{u}, \bar{v}, \bar{x}, \bar{y})$ is stable, while for $\chi < \chi_c$ our system tends towards an endemic equilibrium that contains individuals engaging in prophylaxis in some non-zero quantities.

Appendix D

Chapter 3 - Evolutionary Analysis of Simple Cases

Two simple cases, where evolutionary analysis is possible analytically, were discussed in Chapter 3 of the main text. Here, we outline the details of that analysis.

The first special case is when the cost of prophylaxis exceeds the threshold χ_c. In this case, our linear stability analysis shows that the stable endemic equilibrium is $(\bar{u}, \bar{v}, \bar{x}, \bar{y}) = (1/\mathcal{R}_0, (1 - 1/\mathcal{R}_0)/(1 + \gamma), 0, 0)$, where $\mathcal{R}_0 = \beta_{00}/(1 + \gamma)$. We can then solve equation (3.8b) to find two possible equilibria for y_m: $\bar{y}_m = 0$ or $\bar{y}_m = 1/\varepsilon + (k\chi/(\varepsilon(1 + \xi_m))$. Since $\varepsilon \leq 1$, the second of these values is always larger than one and so is not biologically sensible, as y_m is defined to be a proportion. Checking the sign of $d/dy_m(dy_m/dt)$ at the first of these equilibrium values shows that $\bar{y}_m = 0$ is the stable equilibrium. From this, the fitness function in equation (3.9) reduces to

$$W(\xi_m, \xi) = \frac{\beta_{00}(\xi_m)\bar{u}(\xi)}{1 + \gamma(\xi_m)} = \frac{\mathcal{R}_0(\xi_m)}{\mathcal{R}_0(\xi)}, \tag{D.1}$$

and so to find the CSS we need to solve the equation

$$\left.\frac{\partial W}{\partial \xi_m}\right|_{\xi_m=\xi=\bar{\xi}} = \left.\frac{d\mathcal{R}_0(\xi_m)}{d\xi_m}\right|_{\xi_m=\bar{\xi}} = 0. \tag{D.2}$$

This results in a CSS value of $\bar{\xi} = \sqrt{\kappa}$.

The second special case is when the prophylactic measures are cost-free, i.e., $\chi = 0$. As noted in the main text, the system moves towards an endemic equilibrium where some non-zero proportions of susceptible and infective individuals are engaging in prophylaxis. While we do not have exact analytic expressions for these equilibrium values, we can still solve for $\bar{y}_m$ analytically. Under the assumption of zero cost, solving equation (3.8b) gives two possible equilibrium values for y_m: $\bar{y}_m = 1/\varepsilon$ and $\bar{y}_m = (\varepsilon\bar{x} - \bar{x})/(\varepsilon\bar{x} - 1)$. Since $\varepsilon \leq 1$ and $\bar{x} \leq 1$, the first of these is always larger than one and the second is always on the interval $[0, 1]$. Substituting the second of these values into $(d/dy_m)(dy_m/dt)$ shows that $\bar{y}_m = (\varepsilon\bar{x} - \bar{x})/(\varepsilon\bar{x} - 1)$ is the stable equilibrium. Notably, this equilibrium value is independent of the mutant exploitation ξ_m and so the fitness function has the form

$$W(\xi_m, \xi) = \frac{\xi_m}{(\kappa + \xi_m)(1 + \gamma(\xi_m))} B(\xi)\bar{u}(\xi), \tag{D.3}$$

where $B(\xi)$ represents what remains from $\beta_{\text{avg}}(\xi_m, \xi)$ after factoring out the terms involving ξ_m. To find the CSS value, we then solve

$$\left.\frac{\partial W}{\partial \xi_m}\right|_{\xi_m=\xi=\bar{\xi}} = \frac{\kappa - \bar{\xi}^2}{(\kappa + \bar{\xi})^2(1 + \bar{\xi})^2} B(\bar{\xi})\bar{u}(\bar{\xi}) = 0. \tag{D.4}$$

This results in a CSS value of $\bar{\xi} = \sqrt{\kappa}$.

Appendix E

Chapter 3 - Evolutionary Analysis in the Case of Arbitrary Cost

While a full evolutionary analysis of the model in the case of an arbitrary cost value is possible only numerically, we expand here on some analytical details of this case discussed in the main text. In particular, we show that there is a unique stable equilibrium value of y_m on the interval $[0, 1]$, and that the derivative $d\bar{y}_m/d\xi_m$ evaluated at $\xi_m = \xi$ is always positive and discuss the implications of this on the fitness function.

In order to numerically perform the evolutionary invasion analysis, we first need to know that there is a unique equilibrium value of y_m on the interval of $[0, 1]$ and that this value is stable. To find the equilibrium values of y_m, we need to solve equation (3.8b). The right-hand side of this equation is a quadratic polynomial in y_m, so we know there are two possible equilibrium values for y_m. Evaluating (3.8b) at $y_m = 0$ gives

$$\frac{dy_m}{dt} = \frac{\beta_{\max}(1-\varepsilon)\xi_m\bar{x}\bar{u}}{\kappa+\xi_m}, \tag{E.1}$$

which is positive since $\varepsilon \in [0, 1]$. If we then evaluate (3.8b) at $y_m = 1$, we find that

$$\frac{dy_m}{dt} = -\frac{\bar{u}(1-\varepsilon)(1-\bar{x})\beta_{\max}\xi_m + k\chi\xi_m + k\chi\kappa}{\kappa+\xi_m}, \tag{E.2}$$

which is negative since $\varepsilon \in [0,1]$ and $\bar{x} \in [0,1]$. By the Intermediate Value Theorem and the fact that the right-hand side of (3.8b) is quadratic in y_m, this then shows that there is a unique equilibrium value of y_m in the interval $[0,1]$. Moreover, since the derivative dy_m/dt is positive at $y_m = 0$ and negative at $y_m = 1$, this equilibrium value is stable.

With this knowledge, we are able to solve (3.8b) and get an explicit expression for the equilibrium value $\bar{y}_m$. To understand how this value interacts with the fitness function (3.9), we need to understand how $\bar{y}_m$ changes with ξ_m. Differentiating with respect to ξ_m, we are able to get an explicit expression for $d\bar{y}_m/d\xi_m$ and evaluate when $\xi_m = \xi$. Doing so results in an expression of the form

$$\left.\frac{d\bar{y}_m}{d\xi_m}\right|_{\xi_m=\xi} = \frac{a - \sqrt{a^2 - b}}{c}, \tag{E.3}$$

where $a = k\chi(\kappa + \xi) + \beta_{\max}(1 - \varepsilon^2\bar{x})\bar{u}$, $b = 4\beta_{\max}^2\varepsilon(1-\varepsilon)(1-\varepsilon\bar{x})\xi^2\bar{u}^2\bar{x}$, and $c = 2\beta_{\max}\varepsilon(1 - \varepsilon\bar{x})\xi^2\bar{u}\sqrt{a^2-b}/k\chi\kappa$. The fact that $\varepsilon \in [0,1]$ and $\bar{x} \in [0,1]$ allows us to conclude that a, b, and c are all positive. Some simplification of the radicand also shows that $a^2 - b \geq 0$, so we are guaranteed that equation (E.3) is real-valued. This proves that $\sqrt{a^2-b} \leq a$ and, thus, $(d\bar{y}_m/d\xi_m)|_{\xi_m=\xi} \geq 0$.

To see how this affects the evolution of pathogen exploitation, we need to pull apart the fitness function in equation (3.9). Finding a potential CSS value of ξ involves first solving $(\partial W/\partial\xi_m)|_{\xi_m=\xi=\bar{\xi}} = 0$. Using equation (3.9), this gives

$$0 = \left.\frac{\partial W}{\partial \xi_m}\right|_{\xi_m=\xi=\bar{\xi}} = \frac{(\beta_{\text{avg}}'(1+\gamma) - \beta_{\text{avg}}\gamma')\bar{u}}{(1+\gamma)^2}, \tag{E.4}$$

where primes denote derivatives with respect to ξ_m evaluated when $\xi_m = \xi = \bar{\xi}$. This further reduces to solving the equality

$$\frac{\beta_{\text{avg}}'}{\beta_{\text{avg}}} = \frac{\gamma'}{1+\gamma} = \frac{(1+\gamma)'}{1+\gamma}. \tag{E.5}$$

In the absence of individuals engaging in prophylaxis, $\beta_{\text{avg}} = \beta_{00}$ and so solving for the CSS value $\bar{\xi}$ amounts to balancing the standard trade-off between transmission and recovery. However, when individuals take prophylactic measures, β_{avg} becomes more complicated. To understand how β_{avg} responds to changes in exploitation in this case, we take a closer look at β'_{avg}. Using the definition of β_{avg} given in the main text, we have that

$$\beta'_{\text{avg}} = \begin{bmatrix} 1-\bar{x} & \bar{x} \end{bmatrix} \left(\underbrace{\begin{bmatrix} \beta'_{00} & \beta'_{01} \\ \beta'_{10} & \beta'_{11} \end{bmatrix} \begin{bmatrix} 1-\bar{y}_m \\ \bar{y}_m \end{bmatrix}}_{\text{I}} - \bar{y}'_m \underbrace{\begin{bmatrix} \beta_{00}-\beta_{01} \\ \beta_{10}-\beta_{11} \end{bmatrix}}_{\text{II}} \right). \tag{E.6}$$

It follows from the fact that $\beta_{00} \geq \beta_{01} = \beta_{10} \geq \beta_{11}$ and the above proof that $\bar{y}'_m \geq 0$ that terms I and II in equation (E.6) are non-negative. Accounting for individuals engaging in prophylaxis—in particular, infective individuals engaging in prophylaxis—reduces β'_{avg} below the level we would expect in the absence of those measures. If the pathogen increases its exploitation, it leads to an increase in the proportion of infective individuals engaging in prophylactic measures due to the fact that $\bar{y}'_m \geq 0$. This increases the likelihood that the rate of transmission between a susceptible individual and an infective individual will be one of β_{01} or β_{11}, instead of β_{00} or β_{10}. Since β_{01} and β_{11} are always smaller than β_{00} and β_{10}, this leads to a reduction in the rate of change of the average transmission rate in the population. This influence on the rate of change of transmission intertwines with the more standard trade-off between transmission and recovery, and reduces the evolutionarily stable level of pathogen exploitation below what we would expect in the absence of prophylaxis.

Appendix F

Chapter 3 - Perturbation Analysis

Letting $\mathbf{r} = (u, v, x, y)$ and $s = \xi$, we can express the four equations governing the epidemiological dynamics of our system as the vector-valued function $\mathbf{F}(\mathbf{r}, s; \chi)$ and the equation describing the evolutionary dynamics of pathogen exploitation as the scalar-valued function $G(\mathbf{r}, s; \chi)$. We know that below the critical cost threshold χ_c the endemic equilibrium $(\hat{\mathbf{r}}, \hat{s}) = (\hat{u}, \hat{v}, \hat{x}, \hat{y}, \hat{\xi})$ is stable, while above this threshold our system tends towards the endemic equilibrium $(\bar{\mathbf{r}}, \bar{s}) = (\bar{u}, \bar{v}, 0, 0, \bar{\xi})$ where individuals engaging in prophylaxis are absent. The critical cost level represents a bifurcation point where these two equilibria coincide and undergo an exchange of stability. To study how our system reacts as we decrease the cost away from this threshold, we introduce a perturbation parameter $\delta = \chi - \chi_c$ and take a first-order approximation to our new equilibrium point $(\hat{\mathbf{r}}, \hat{s}) = (\bar{u} + \rho_1\delta, \bar{v} + \rho_2\delta, \rho_3\delta, \rho_4\delta, \bar{\xi} + \sigma\delta)$. Knowing that this equilibrium point must satisfy $\mathbf{F}(\hat{\mathbf{r}}, \hat{s}; \chi) = 0$ and $G(\hat{\mathbf{r}}, \hat{s}; \chi) = 0$, our goal is to find expressions for the perturbation coefficients $\rho_1, \rho_2, \rho_3, \rho_4$, and σ.

If we treat $(\hat{\mathbf{r}}, \hat{s})$ as a function of χ, we can make a first-order Taylor series approximation centred around χ_c:

$$\mathbf{F}(\bar{\mathbf{r}}, \bar{s}; \chi_c) + \delta[D_{\hat{\mathbf{r}}}\mathbf{F}(\bar{\mathbf{r}}, \bar{s}; \chi_c)d\hat{\mathbf{r}} + \mathbf{F}_{\hat{s}}(\bar{\mathbf{r}}, \bar{s}; \chi_c)d\hat{s} + \mathbf{F}_{\chi}(\bar{\mathbf{r}}, \bar{s}; \chi_c)] = 0 \tag{F.1a}$$

$$G(\bar{\mathbf{r}}, \bar{s}; \chi_c) + \delta[G_{\hat{\mathbf{r}}}(\bar{\mathbf{r}}, \bar{s}; \chi_c)d\hat{\mathbf{r}} + G_{\hat{s}}(\bar{\mathbf{r}}, \bar{s}; \chi_c)d\hat{s} + G_{\chi}(\bar{\mathbf{r}}, \bar{s}; \chi_c)] = 0, \tag{F.1b}$$

where subscripts denote partial derivatives and $d\hat{\mathbf{r}} = (\rho_1, \rho_2, \rho_3, \rho_4)$ and $d\hat{s} = \sigma$ are the derivatives with respect to χ of $\hat{\mathbf{r}}$ and $\hat{s}$, respectively. We know that $(\bar{\mathbf{r}}, \bar{s})$ is an equilibrium point, so the first term in equations (F.1a) and (F.1b) evaluates to zero. We also observe that every term in $\mathbf{F}$ and G involving χ is multiplied by at least one of x or y, and so the partial derivatives with respect to χ vanish when we evaluate at $(\bar{\mathbf{r}}, \bar{s})$. This simplifies (F.1) to:

$$D_{\hat{\mathbf{r}}}\mathbf{F}(\bar{\mathbf{r}}, \bar{s}; \chi_c)d\hat{\mathbf{r}} + \mathbf{F}_{\hat{s}}(\bar{\mathbf{r}}, \bar{s}; \chi_c)d\hat{s} = 0 \tag{F.2a}$$

$$G_{\hat{\mathbf{r}}}(\bar{\mathbf{r}}, \bar{s}; \chi_c)d\hat{\mathbf{r}} + G_{\hat{s}}(\bar{\mathbf{r}}, \bar{s}; \chi_c)d\hat{s} = 0. \tag{F.2b}$$

We can write (F.2) more succinctly as $J\left[\begin{smallmatrix} d\hat{\mathbf{r}} \\ d\hat{s} \end{smallmatrix}\right] = 0$ where the matrix J has the following structure:

$$J = \begin{bmatrix} * & * & * & * & * \\ * & * & * & * & 0 \\ 0 & 0 & 0 & 0 & 0 \\ 0 & 0 & * & * & 0 \\ 0 & 0 & \frac{\partial}{\partial \bar{x}}\left[\frac{\partial W}{\partial \xi_m}\bigg|_{\xi_m = \xi}\right]_{\chi = \chi_c,\ \xi = \sqrt{\kappa}} & 0 & \frac{\partial}{\partial \xi}\left[\frac{\partial W}{\partial \xi_m}\bigg|_{\xi_m = \xi}\right]_{\chi = \chi_c,\ \xi = \sqrt{\kappa}} \end{bmatrix}, \tag{F.3}$$

with asterisks denoting entries that are possibly non-zero. Since J is a block triangular matrix, the eigenvalues are given by the eigenvalues of the matrices on the main diagonal. The 2×2 matrix in the upper left is the Jacobian matrix arising from the linearization of the standard SIR model around the endemic equilibrium $(\bar{\mathbf{r}}, \bar{s})$. Since the lower-right 3×3 block is lower triangular and has a zero entry on its main diagonal, we can see that zero is an eigenvalue of J. This allows us to interpret $\left[\begin{smallmatrix} d\hat{\mathbf{r}} \\ d\hat{s} \end{smallmatrix}\right]$ as the eigenvector of J associated with the zero eigenvalue, and so shows that there is a non-trivial solution for our perturbation coefficients.

While an analytic expression for this eigenvector can be found, it is unwieldy. Of more interest is the sign of the perturbation coefficient σ, as this tells us in which direction $\bar{\xi}$ moves as we decrease the cost below its critical value. The third row of (F.3) tells us that $\bar{x}$ is a free variable, and the last row tells us that there is a simple relationship between this free variable and $\bar{\xi}$. In particular, if we consider finding the eigenvector $\left[\frac{d\hat{\mathbf{r}}}{d\hat{s}}\right]$ by solving the expression $J\left[\frac{d\hat{\mathbf{r}}}{d\hat{s}}\right] = 0$, then the last row of (F.3) tells us that

$$\sigma = -\frac{\frac{\partial}{\partial \bar{x}}\left[\left.\frac{\partial W}{\partial \xi_m}\right|_{\xi_m=\xi}\right]_{\chi = \chi_c,\ \xi = \sqrt{\kappa}}}{\frac{\partial}{\partial \xi}\left[\left.\frac{\partial W}{\partial \xi_m}\right|_{\xi_m=\xi}\right]_{\chi = \chi_c,\ \xi = \sqrt{\kappa}}}\rho_3. \tag{F.4}$$

We know that the denominator of (F.4) is always negative since $\bar{\xi} = \sqrt{\kappa}$ is convergence stable (see (3.11)). Furthermore, the proportion of susceptible individuals engaging in prophylaxis increases as the cost is decreased below its critical value and $\delta = \chi - \chi_c < 0$ below this cost threshold, so we must have that $\rho_3 < 0$. It follows, then, that the sign of σ is controlled only by the numerator of (F.4) and so we arrive at equation (3.14) in the main text.

Appendix G

Chapter 3 - Maple Code

Here, we present the Maple code, described in Chapter 3 of the main text, used to check the sign of the perturbation coefficient σ for a range of parameter values near the critical cost threshold. Using $\delta = \chi - \chi_c$ as our perturbation parameter, we first define the differential equation for y_m in (3.8b) and solve for the equilibrium value:

```
restart:
with(LinearAlgebra): with(VectorCalculus): with(plots):
dymdt := -(y[m]*(beta[max]*(1 - epsilon)*xi[m]*(1 - x)*
y[m]/(kappa + xi[m]) - beta[max]*(1 - epsilon)^2*xi[m]*
x*(1 - y[m])/(kappa + xi[m])) + (1 - y[m])*(beta[max]*
xi[m]*(1 - x)*y[m]/(kappa + xi[m]) - beta[max]*
(1 - epsilon)*xi[m]*x*(1 - y[m])/(kappa + xi[m])))*u
- k*(chi[c] + delta)*y[m]:
```

Solving this equation returns two possible equilibrium values:

```
ym := solve(dymdt, y[m]):
simplify(subs(delta = chi - chi[c], ym[1])):
simplify(subs(delta = chi - chi[c], ym[2])):
```

These equilibrium values are of the form $(a \pm \sqrt{b})/c$. Knowing that $0 \leq \varepsilon \leq 1$ and $0 \leq \bar{x} \leq 1$

allows us to conclude that $a \leq 0$, $b \geq 0$, and $c \leq 0$. Furthermore, some algebra shows that $b \leq a^2$ and so $\sqrt{b} \leq |a|$. This allows us to conclude that $0 \leq$ ym[1] $\leq$ ym[2]. We now check the derivative of the differential equation to find the stable equilibrium:

```
simplify(subs(y[m] = ym[1], diff(dymdt, y[m]))):
simplify(subs(y[m] = ym[2], diff(dymdt, y[m]))):
```

Since the first of these quantities is negative and the second is positive, this shows that the first root ym[1] is the stable equilibrium. The proof in Appendix E shows that there is a unique stable equilibrium on the interval [0, 1], and so we are guaranteed that ym[1] is on [0, 1]. Thus, we define this as the equilibrium value of y_m:

```
ym := ym[1]:
```

We now define the differential equations for u, v, x, and y in (3.5), as well as the partial derivative of the fitness function with respect to the mutant pathogen exploitation level ξ_m:

```
dudt := 1 - (beta[max]*xi*(1 - x)*(1 - y)/(kappa + xi)
+ beta[max]*(1 - epsilon)*xi*(1 - x)*y/(kappa + xi)
+ beta[max]*(1 - epsilon)*xi*x*(1 - y)/(kappa + xi)
+ beta[max]*(1 - epsilon)^2*xi*x*y/(kappa + xi))*u*v - u:
dvdt := (beta[max]*xi*(1 - x)*(1 - y)/(kappa + xi)
+ beta[max]*(1 - epsilon)*xi*(1 - x)*y/(kappa + xi)
+ beta[max]*(1 - epsilon)*xi*x*(1 - y)/(kappa + xi)
+ beta[max]*(1 - epsilon)^2*xi*x*y/(kappa + xi))*u*v - (1 + xi)*v:
dxdt := -x/u + (k + 1)*x*(1 - x)*(y*(beta[max]*(1 - epsilon)*
xi/(kappa + xi) - beta[max]*(1 - epsilon)^2*xi/(kappa + xi))
+ (1 - y)*(beta[max]*xi/(kappa + xi) - beta[max]*(1 - epsilon)*
xi/(kappa + xi)))*v - k*(chi[c] + delta)*x:
dydt := -(beta[max]*xi*(1 - x)*y*(1 - y)/(kappa + xi)
+ beta[max]*(1 - epsilon)*xi*(1 - x)*y^2/(kappa + xi)
- beta[max]*(1 - epsilon)*xi*x*(1 - y)^2/(kappa + xi)
- beta[max]*(1 - epsilon)^2*xi*x*y*(1 - y)/(kappa + xi))*u
- k*(chi[c] + delta)*y:
W := (beta[max]*xi[m]*(1 - x)*(1 - ym)/(kappa + xi[m]) + beta[max]*
(1 - epsilon)*xi[m]*(1 - x)*ym/(kappa + xi[m]) + beta[max]*
(1 - epsilon)*xi[m]*x*(1 - ym)/(kappa + xi[m]) + beta[max]*
(1 - epsilon)^2*xi[m]*x*ym/(kappa + xi[m]))*u/(1 + xi[m]):
dWdxi := subs(xi[m] = xi, diff(W, xi[m])):
```

Using this, we put together the matrix *J* described in Appendix F:

```
J1 := Jacobian([dudt, dvdt, dxdt, dydt], [u, v, x, y] =
[(1 + sqrt(kappa))*(kappa + sqrt(kappa))/(beta[max]*sqrt(kappa)),
(1 - (1 + sqrt(kappa))*(kappa + sqrt(kappa))/(beta[max]*
sqrt(kappa)))/(1 + sqrt(kappa)), 0, 0]):
J2 := <0, 0, subs(u = (1 + sqrt(kappa))*
(kappa + sqrt(kappa))/(beta[max]*sqrt(kappa)),
x = 0, delta = 0, diff(dWdxi, x)), 0>^%T:
J3 := subs(u = (1 + sqrt(kappa))*(kappa + sqrt(kappa))/
(beta[max]*sqrt(kappa)), v = (1 - (1 + sqrt(kappa))*(kappa
+ sqrt(kappa))/(beta[max]*sqrt(kappa)))/(1 + sqrt(kappa)),
x = 0, y = 0, delta = 0, Jacobian([dudt, dvdt, dxdt, dydt, dWdxi],
[xi] = [sqrt(kappa)])):
J4 := <J1, J2>:
J5 := <J4 | J3>:
J := subs(chi[c] = beta[max]*sqrt(kappa)/((1 + sqrt(kappa))*(kappa
+ sqrt(kappa))) - (k + 1)*((1 - epsilon)*(beta[max]*sqrt(kappa)/((1
+ sqrt(kappa))*(kappa + sqrt(kappa))) - 1) + 1)/k, xi = sqrt(kappa),
delta = 0, J5):
```

We then extract the entry of *J* corresponding to the partial derivative in (3.14). We also define the critical cost threshold χ_c in (3.6):

```
sigmanum := simplify(J[5, 3]):
costthresh := beta[max]*sqrt(kappa)/((1 + sqrt(kappa))*(kappa
+ sqrt(kappa))) - (k + 1)*((1 - epsilon)*(beta[max]*
sqrt(kappa)/((1 + sqrt(kappa))*(kappa + sqrt(kappa))) - 1) + 1)/k:
```

If we choose $\beta_{\max}$ and κ values so that $\mathcal{R}_0 > 1$, we get the following curve (where above the curve $\mathcal{R}_0 > 1$ and below the curve $\mathcal{R}_0 < 1$):

```
R0plot := plot((1 + sqrt(kappa))^2, kappa = 0 .. 5,
color = BLACK, thickness = 3, view = [0 .. 5, 0 .. 10],
labels = [kappa, beta[max]]):
```

If we also choose ε values so that $\chi_c > 0$ and k values so that $\varepsilon < 1$, we can generate a series of $\beta_{\max}$-κ curves and plot them together with the previous curve for $\mathcal{R}_0$:

```
expressions := [seq(seq(subs([epsilon = beta[max]/(((1
+ sqrt(kappa))^2/(beta[max] - (1 + sqrt(kappa))^2) + 10^n
+ 1)*(beta[max] - (1 + sqrt(kappa))^2)) + m*(((1
+ sqrt(kappa))^2/(beta[max] - (1 + sqrt(kappa))^2) + 10^n)
- (1 + sqrt(kappa))^2/(beta[max] - (1 + sqrt(kappa))^2))/
(10*((1 + sqrt(kappa))^2/(beta[max] - (1 + sqrt(kappa))^2)
+ 10^n + 1)), k = (1 + sqrt(kappa))^2/(beta[max]
- (1 + sqrt(kappa))^2) + 10^n], costthresh), m = 1 .. 9),
n = -2 .. 2)]:
for i to 45 do
    p[i] := plot({solve(expressions[i], beta[max])},
    kappa = 0 .. 5, color = GREY, linestyle = DASH):
end do:
display({R0plot, seq(p[i], i = 1 .. 45)},
view = [0 .. 5, 0 .. 10], labels = [kappa, beta[max]]):
```

This generates the plot in panel A of figure 3.2 and suggests that all of the $\chi_c = 0$ curves overlap with the $\mathcal{R}_0 = 1$ curve, meaning that the region in which $\mathcal{R}_0 > 1$ coincides with the region in which $\chi_c > 0$. We can confirm this by looking at the difference between these two curves; running the following line of code will show that this difference is always exactly zero:

```
for i to 45 do
    simplify((1 + sqrt(kappa))^2 - solve(expressions[i],
    beta[max])[2]):
end do:
```

If we use the ε and k values chosen above, we can also look at the value of the partial derivative in equation (3.14). This gives a second set of $\beta_{\max}$-κ expressions that we can plot over top of the expressions for χ_c and $\mathcal{R}_0$ above:

```
expressions2 := [seq(seq(subs([epsilon = beta[max]/(((1
+ sqrt(kappa))^2/(beta[max] - (1 + sqrt(kappa))^2) + 10^n
+ 1)*(beta[max] - (1 + sqrt(kappa))^2)) + m*(((1
+ sqrt(kappa))^2/(beta[max] - (1 + sqrt(kappa))^2) + 10^n)
- (1 + sqrt(kappa))^2/(beta[max] - (1 + sqrt(kappa))^2))/(10*
((1 + sqrt(kappa))^2/(beta[max] - (1 + sqrt(kappa))^2)
+ 10^n + 1)), k = (1 + sqrt(kappa))^2/(beta[max] - (1
+ sqrt(kappa))^2) + 10^n], sigmanum), m = 1 .. 9),
n = -2 .. 2)]:
for i to 45 do
    p2[i] := plot({solve(expressions2[i], beta[max])},
    kappa = 0 .. 5, color = GREY, linestyle = DOT):
end do:
display({R0plot, seq(p[i], i = 1 .. 45), seq(p2[i], i = 1 .. 45)},
view = [0 .. 5, 0 .. 10], labels = [kappa, beta[max]]):
```

This produces the plot shown in panel B of figure 3.2 and shows that all of these curves that represent the roots of the partial derivative in (3.14) lay below the curve for $\mathcal{R}_0 = 1$. So for all sensible sets of parameter values (i.e., all parameter values that satisfy $\chi_c > 0$ and $\mathcal{R}_0 > 1$), (3.14) has the same sign. We can take a test point in this region of parameter space to show that this sign is always positive, meaning that in a neighbourhood below the critical cost value the CSS pathogen exploitation level will decrease below its benchmark value.

Curriculum Vitae

Name:	Evan Mitchell
Post-Secondary Education and Degrees:	University of Western Ontario London, ON 2017 - present Ph.D. McMaster University Hamilton, ON 2015 - 2017 M.Sc. McMaster University Hamilton, ON 2011 - 2015 B.Arts Sc. (Honours)
Honours and Awards:	NSERC USRA 2015
Related Work Experience:	Teaching Assistant University of Western Ontario 2017 - 2021 Teaching Assistant McMaster University 2014 - 2017

Publications:

E. Mitchell and G. Wild. (2020). Prophylactic host behaviour discourages pathogen exploitation. *J. Theor. Biol.*, 503(110388). `https://doi.org/10.1016/j.jtbi.2020.110388`.